Dissertation

Molecular mechanisms of lipotoxicity in endothelial cells

submitted by

Muhammad Jadoon Khan

MSc

for the Academic Degree of

Doctor of Philosophy

(PhD)

at the

Medical University of Graz

Institute of Molecular Biology and Biochemistry

under the supervision of

Univ.-Prof. Dr. Wolfgang F. GRAIER

2013

DECLARATION

I hereby declare that this dissertation is my original work and that I have fully acknowledged by name all those individuals and organizations that have contributed to the research for this dissertation. Due acknowledgement has been made in the text to all other materials used. Throughout this dissertation and in all related publications I followed the guidelines of "Good Scientific Practice".

Graz ---------- ----------

Dedicated to

The man behind all my success,

My Uncle

Taj Gul

ACKNOWLEDGEMENTS

I have no words to express my feelings for the love support and sacrifices made by my parent and my dearest wife to enable me to achieve what I wasn't able otherwise.

I pay my special thanks Prof. Dr. Wolfgang Graier for his guidance and patience he has shown during my stay in the lab. It's just because of his encouragement and pushing me forward both intellectually and practically that I am able to complete this piece of work.

I really enjoyed my time with Dr. Roland from whom I actually learned making hypothesis and converting them into experiments and results.

I am thankful to the members of my thesis committee Prof. Klaus Groschner and ao.-Uni.-Prof Sasa Frank for their useful guidance during my research work.

My colleagues and lab fellows deserve my deep emotions of thanks for their support, assistance and love during my stay in the lab. It is only because of them that I have always felt my working group as a family and I consider the mutual trust I have practiced in this lab is one of unmatchable asset of my life.

Gratitude is due to my Pakistani friends in Graz and other parts of Austria and in different parts of Europe. It is because of all these guys that I have always felt home-like here and have found them around me in times of stress and sorrows and have always shared their happy moments.

Muhammad Jadoon Khan
Graz, Austria

TABLE OF CONTENTS

ABBREVIATIONS

FFA	Free Fatty Acids
DAG	Diacylegylcerols
ZDF	Zucker diabetic fatty
NASH	non-alcoholic steatohepatitis
GLUT	glucose transporter
ER	Endoplasmic reticulum
T2DM	type 2 diabetes mellitus
ROS	reactive oxygen species
SERCA	sarco/endoplasmic reticulum calcium ATPase
UPR	unfolded protein response
SPT	serine palmitoyltransferase
NO	Nitric oxide
CYLD	Cylindromatosis
RIPK	Receptor interacting protein kinase
PA	Palmitic acid
DMEM	Dulbecco's Modified Eagle Medium
HAT	Hypoxanthin, Aminopterin and Thymidine
PBS	Phosphate buffered saline
OA	Oleic acid
BAPTA-AM	N,N,N',N'-tetraacetic acid-(acetoxymethyl) ester
VPS34	vacuolar protein sorting 34

ATG7	autophagy-related protein 7
Ca^{2+}	Calcium ion
BSA	Bovine Serum albumin
siRNAs	Small interfaring
RNA	Ribonucleic acid
DNA	Deoxyribonucleic acid
MTT	3-(4,5-Dimethylthiazol-2-yl)-2,5-diphenyltetrazolium bromide
HCl	Hydrochloric acid
PI	Propidium Iodide
GFP	Green fluorescent protein
DAPI	4'-6-Diamidino-2-phenylindole
STS	staurosporine
FRET	Förster resonance energy transfer
RFP	red fluorescent protein
PCR	Polymerase Chain Reaction
ORF	open reading frame
MCS	multiple cloning sites
TAE	Tris- Acetate- EDTA
RISC	RNA induced silencing complex
ATP	Adenosine triphosphate
ADP	Adinosine diphosphate
RIPA	Radioimmunoprecipitation assay

ACLSM	Array Confocal Laser Scanning Microscopy

ABSTRACT

Accumulation of palmitic acid (PA) in cells from non-adipose tissues is known to induce lipotoxicity resulting in cellular dysfunction and death. A number of different molecular pathways have been proposed to mediate the process of cellular dysfunction and death in different tissues which mainly focus on apoptosis as a major cell death pathway. Recent developments have provided strong evidence on the contribution of necrosis as a programmed cell death pathway (necroptosis) which was otherwise considered as a random or accidental phenomenon. The exact molecular pathways of PA-induced cell death are still mysterious and one or a combination of different signaling cascades may be involved. Here, we show that PA triggers autophagy and lysosomal dysfunction simultaneously leading to endothelial cell death. The PA-induced cell death was predominantly necrotic as indicated by annexin V and propidium iodide (PI) staining, absence of caspase activity, low levels of DNA hypoploidy, and an early ATP depletion. In addition PA induced a strong elevation of mRNA levels of ubiquitin carboxyl-terminal hydrolase (CYLD), a known mediator of necroptosis. Moreover, siRNA-mediated knockdown of CYLD significantly antagonized PA-induced necrosis of endothelial cells. In contrast, inhibition and knockdown of receptor interacting protein kinase 1 (RIPK1) had no effect on PA-induced necrosis, indicating the induction of a CYLD-dependent but RIPK1-independent cell death pathway. PA was recognized as a strong and early inducer of autophagy. The inhibition of autophagy by both pharmacological inhibitors and genetic knockdown of the autophagy-specific genes, vacuolar protein sorting 34 (VPS34), and autophagy-related protein 7 (ATG7), could rescue the PA-induced death of endothelial cells. Moreover, the initiation of autophagy and cell death by PA was reduced in endothelial cells loaded with the Ca(2+) chelator 1,2-bis(o-aminophenoxy)ethane-N,N,N',N'-tetraacetic acid-(acetoxymethyl) ester (BAPTA-AM), indicating that Ca(2+) triggered the fatal signaling of PA. At the same time PA was found to activate calpain 1 and induces lysosomal dysfunction. A siRNA-mediated knock down of calpain 1 inhibited the PA-induced cell death significantly. To summarize PA induces autophagy and lysosomal dysfunction simultaneously leading to ATP depletion which further activates necroptosis in endothelial cells.

ZUSAMMENFASSUNG

Die Anhäufung von Palmitinsäure (PA) in Zellen außerhalb des Fettgewebes ruft bekanntermaßen Lipotoxizität hervor und führt so zu Störungen zellulärer Funktion und zum Zelltod. Eine Vielzahl an molekularen Signalwegen wurde bisher in Verbindung mit diesem Prozess gebracht, die sich allesamt auf Apoptose als vorherrschende Art des Zelltodes konzentrieren. Neuere Ergebnisse zeigen jedoch, dass in diesem Zusammenhang auch Nekrose (Nekroptose) eine bedeutende Rolle spielt und keineswegs, wie bisher angenommen, ein unkontrolliertes und zufälliges Phänomen darstellt. Die genauen molekularen Mechanismen des PA-induzierten Zelltodes sind immer noch ungeklärt und könnten sowohl eine einzige, oder aber eine Kombination aus verschiedenen Signalkaskaden beinhalten.

In dieser Arbeit wird veranschaulicht, dass PA sowohl Autophagie, als auch lysosomale Dysfunktion auslöst, was den Zelltod von Endothelzellen zur Folge hat. Diese Art des PA-induzierten Zelltodes war vorwiegend den Signalwegen der Nekrose zuzuordnen, wie durch Annexin V und Propidiumiodid (PI)-Färbungen gezeigt werden konnte. Auch das Fehlen von Caspase-Aktivität, das geringe Vorkommen von DNA-Hypoploidie und eine frühe Abnahme der ATP-Konzentration weisen auf einen nekrotischen Zelltod hin. Darüber hinaus rief PA eine ausgeprägte Zunahme des Auftretens von mRNA für ubiquitin carboxyl-terminal hydrolase (CYLD) hervor, welche als Vermittler von Nekroptose gilt. Durch siRNA-vermittelten Knockdown von CYLD konnte das Auftreten des PA-induzierten Endothelzelltodes signifikant verringert werden. Hemmung bzw. Kockdown von receptor interacting protein kinase 1 (RIPK1) hingegen hatten keinen Effekt auf die PA-induzierte Nekrose, was auf die Aktivierung eines CYLD-abhängigen aber RIPK1-unabhängigen Weg des Zelltodes hindeutet. PA stellte sich zudem als potenter und rascher Auslöser von Autophagie dar. Das Unterdrücken der Autophagie, sowohl durch pharmakologische Hemmstoffe, als auch über Knockdown der Autophagie-spezifischen Gene vacuolar protein sorting 34 (VPS34) und autophagy-related protein 7 (ATG7) verhinderten den PA-verursachten Tod von Endothelzellen. Die Effekte von PA auf Endothelzellen waren nur in abgeschwächter Form zu beobachten, wenn die Zellen zuvor mit dem Ca^{2+}-Chelator 1,2-bis(o-aminophenoxy)ethane N,N,N',N'-tetraacetic acid-(acetoxymethyl) ester (BAPTA-AM) beladen wurden, was veranschaulicht, dass Ca^{2+} am Auslösen der zum Zelltod führenden PA-

Signalkaskade beteiligt ist. Außerdem wurde PA als Aktivator von calpain 1 und damit als Auslöser lysosomaler Dysfunktion identifiziert. Über siRNA-vermittelten Knockdown von calpain 1 konnte der PA-induzierten Zelltod signifikant vermindert werden. Zusammenfassend löst PA zeitgleich sowohl Autophagie als auch lysosomale Dysfunktion aus, was zu einem Abfall der zellulären ATP-Konzentration führt und somit die Nekroptose von Enothelzellen weiter vorantreibt.

1. INTRODUCTION

1.1 Lipotoxicity

Accumulation of excess lipids in non-adipose tissues leads to cell dysfunction or cell death. This phenomenon, known as lipotoxicity is responsible for a number of pathogenesis in humans. The term lipotoxicity was first coined by Dr Unger referring to the deteriorating effect of triglyceride accumulation in pancreatic β-cells on glucose stimulated insulin secretion (1).

Free fatty acids are synthesized through *de novo* synthesis pathways utilizing the common building blocks (2) and are used by hydrolyzing them trough cellular lipases and burning them through beta-oxidation to generate energy (3,4). Free Fatty Acids (FFA's) can also be imported into cells by both protein-mediated transport (5) and free movement across the cell membrane (6). This transport of FFA's depends on cellular demands or extracellular concentrations of FFA (7). FFA's delivered into the cell are utilized for a number of important biological processes such as membrane biosynthesis (8), energy production (9), lipid signaling (10), post-translational protein modification (11) and regulation of transcription (12). Excess lipids are esterified and stored in the form of triglyceride in lipid droplets and serves as a life saving energy reservoir in the time of famine and starvation (13). A balance is always maintained between lipid supply and demand through the storage of lipids in the form of lipid droplets in lipid storage tissues like adipose tissue (14). These lipid droplets are then mobilized in the form of free fatty acids (FFA), diacylegylcerols (DAG) and other fatty acid derivatives through a well orchestrated enzymatic system of the cell which is controlled by a hormonal system and droplet-associated proteins in mammals (4). A proper functioning of this enzymatic and hormonal system and a balanced between supply and demand of lipids is necessary for the normal tissue metabolism and function, as is shown by the genetic knock out mice to study the effect of different enzymes involved in lipid metabolism (15,16).

Only adipose tissue has this unique capacity to store large amounts of excess FFAs in the form of cytosolic lipid droplets (14) while cells of non-adipose tissues have only a limited capacity for lipid storage. An excess of lipids above this limited capacity results in cellular dysfunction or cell death which is termed as lipotoxicity. Hence, broadly, an accumulation of excess lipids in non

adipose tissue resulting in a number of different complications is known as lipotoxicity. A generalized representation of lipotoxicity is given in figure 1-1.

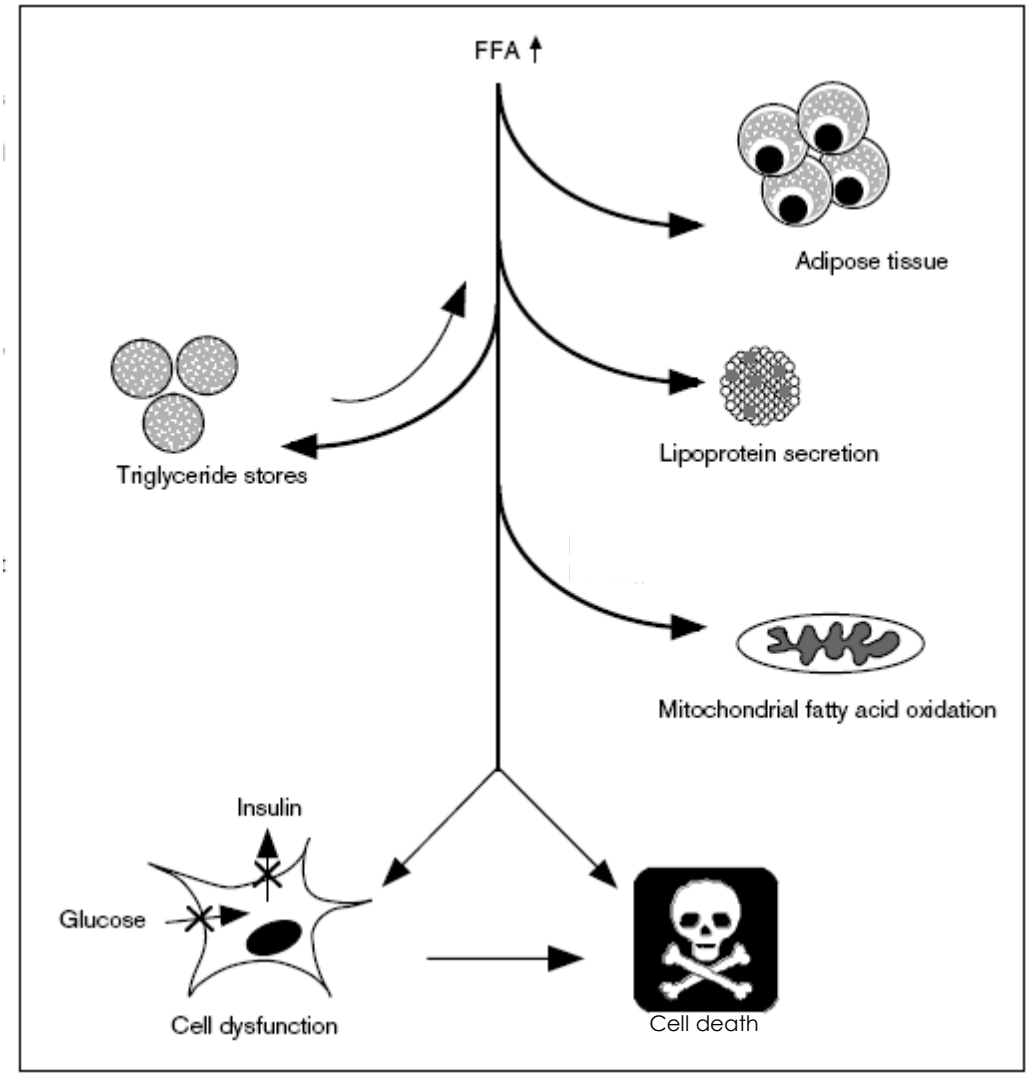

Figure 1-1: *a generalized schematic representation of lipotoxicity. Elevated FFA's are stored in adipose tissue or secreted the form on lipoproteins. FFA's are stored in triglyceride stores and are mobilized back to FFA on demand. Fatty acids are metabolized in mitochondria through β-oxibation and excess of FFA can lead to cellular dysfunction and cell death. (Modified from Schaffer JE, 2003)*

1.2 Lipotoxic complications

Some of the most common complications caused by lipotoxicity are obesity (17), insulin resistance (18), cardiovascular complications (19), atherosclerosis (20) and diabetes (21,22). In addition, a number of neurodegenerative disorders are caused by an altered lipid homeostasis (23). Almost all major tissues and organs are reported to be affected by the excess lipids. These include kidneys (24), pancreas (25), liver (26), heart (27) and brain (23). A defect in the mitochondrial fatty acid oxidation pathway results in cardiac overload of lipids and is associated with heart failure and sudden death (28). Similarly, other metabolic alterations that lead to the accumulation of lipids in cardiac tissue are known to be associated with cardiomyopathy (29). Mice lacking long-chain acyl-coenzyme A (CoA) dehydrogenase are known to develop fibrosis which may lead to arrhythmias (30). In Zucker diabetic fatty (ZDF) rats with elevated serum FFA and triglyceride levels results in apoptotic cardiomyocyte death and a decrease in systolic function (31). In skeletal muscles accumulation of excess lipids lead to the generation of insulin resistance and type 2 diabetes by reducing insulin receptor substrate 1 phosphorylation and phosphatidylinositol 3-kinase (PI3K) activity which fails to promote translocation of the GLUT4 glucose transporter to the plasma (32). In pancreatic β-cells accumulation of FFA alters insulin secretion and leads to β-cell apoptosis (33). In humans, non-alcoholic steatohepatitis (NASH) is the most prominent condition associated with triglyceride and FFA accumulation in the liver which leads to hepatocyte damage and fibrosis ultimately resulting in liver cirrhosis (34). A study in rats suggests that FFAs carried by albumin plays a role in the pathogenesis of tubulointerstitial injury in kidneys (35). In hypothalamus lipotoxicity induce ER stress which can lead to metabolic syndrome (36). Figure 1-2 represents a few complications related to lipotoxicity while brief mechanisms of lipotoxicity in different cell and tissue types is shown in Table 1-1.

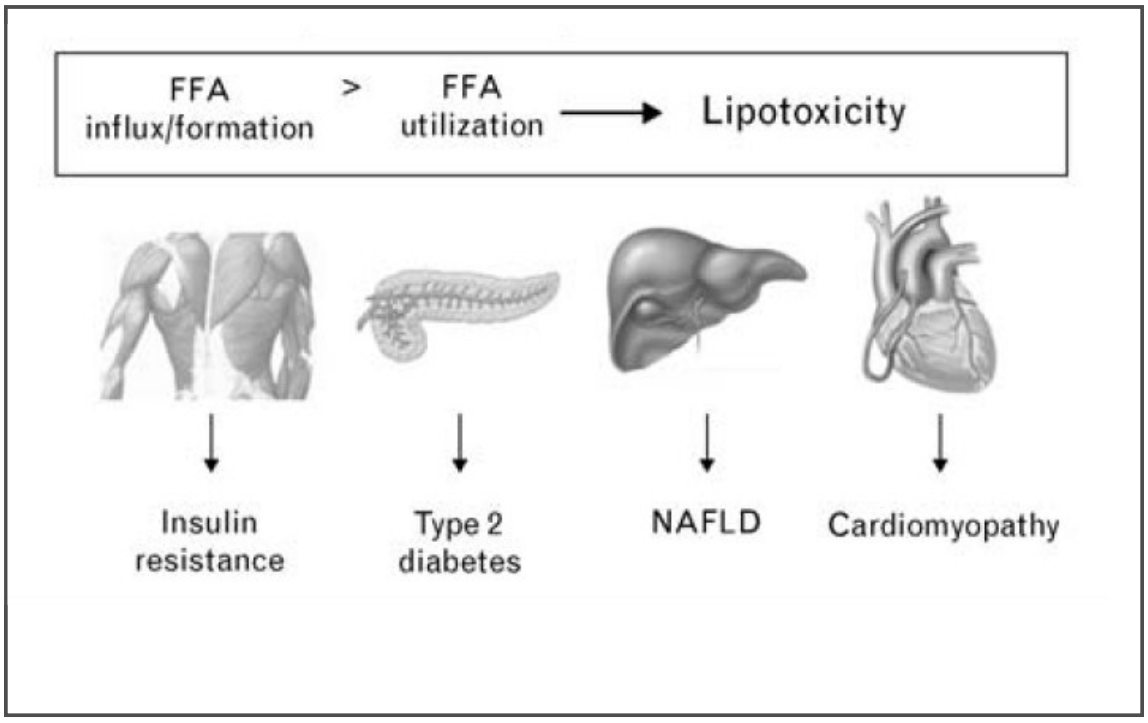

Figure 1-2: *Simplified scheme of lipotoxic complications (Modified from Garbarino and Sturley 2009)*

1.3 Lipotoxicity and endothelial dysfunction

A thin layer of cells that lines the interior surface of blood vessels and lymphatic vessels is called Endothelium. It works as an interface between blood or lymph in the lumen and the rest of the vessel wall. The cells that form the endothelium are called endothelial cells. Endothelial cells in direct contact with blood are called vascular endothelial cells (38).

The major functions of endothelium includes fluid filtration, blood vessel tone, hemostasis, neutrophil recruitment, and hormone trafficking. Figure 1-3 shows a general structure of a blood vessel wall and endothelial cells.

Table 1: The mechanisms of lipotoxicity are cell type and lipid-species dependent. Table is taken from Garbarino *et al.*, 2009 (37).

Lipid species	Cell type	Mechanism
Unsaturated fatty acid (UFA)	Neuronal cells, HUVECs	Activation of protein phosphatase type 2C (PP2Ca/b); leads to BAD dephosphorylation
	Huh7, HepG2	JNK-dependent upregulation of TNF-related apoptosis inducing ligand (TRAIL) receptor death receptor 5 (DR5); caspase 3/7 activation
	Huh7, HepG2	Transcriptional alterations within apoptotic, proliferation, and redox balance cascades; induction of oxidative stress and TGFb dependent apoptotic cascades
	Lymphocytes, Jurkat and Raji cells	Activation of PPAR, Caspases 3, 6, TNF-a production
	18 rat b-cells, INS-1(E) cells	Induction of C/EBP homology protein (CHOP) and the UPR (ATF4, eIF2-a phosphorylation, splicing of XBP1)
	McArdle Cells	UPR induction (eIF2a phosphorylation, XBP1 splicing)
	Dgat1_/_ Fibroblasts	Not determined
	dga1D plh1D (S. pombe)	DAG accumulation; ROS production
	are1D are2D dga1D lro1D (S. cerevisiae)	ROS accumulation; UPR induction
Saturated fatty acid (SFA)	HepG2	JNK activation (activation of Bax); cytochrome c release; induction of caspases 3, 7.
	Microvascular mesangial cells	Caspase 9 activation; release of cytochrome c and endonuclease G
	b-cells	Induction of C/EBP homologous protein and the UPR (ATF4, eIF2-a phosphorylation, and splicing of XBP1)
	INS-1(E), 18 rat b-cells	IRE1, ATF6 and PERK activation; ER Caþ2 depletion; JNK activation and subsequent induction of AP-1
	hCAECs	p38 MAPK dependent degradation of inhibitor of NF-kB

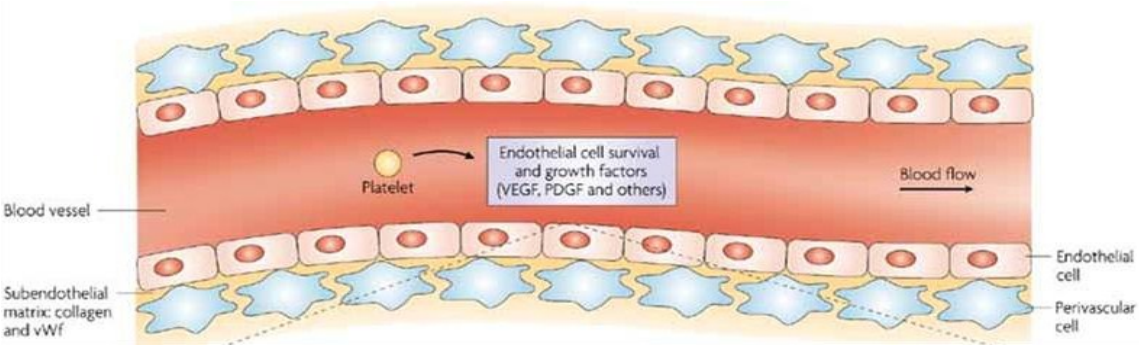

Figure 1-3: A schematic representation of endothelial cell lining (Modified from (39)*)*

Endothelium is in direct contact with the blood and hence is the first target of deleterious effects of fatty acids. Therefore, a number of complications have been known to be associated with elevated fatty acid levels worldwide. The major risk factors for the development of cardiovascular diseases are Obesity and type 2 diabetes mellitus (T2DM) which have attained an epidemic level (40).

1.4 Mechanisms of Lipotoxicity

There are a number of ways through which lipid overload leads to cellular dysfunction or cell death which are discussed following.

1.4.1 Lipotoxicity and mitochondrial dysfunction

Mitochondria being central to energy production are the key targets of substrate overload. Fatty acids are oxidized in mitochondria through beta-oxidation (41) and an overload will cause mitochondrial dysfunction which can be both changes in mitochondrial number and morphology (42). Although both saturated and unsaturated fatty acids are directed to mitochondria for β-oxidation, only long chain saturated fatty acyl CoAs serves as a substrate for de novo synthesis of ceramide. This specificity is achieved by the enzymes serine palmitoyl transferase and ceramide synthase as suggested by Brookheart *et al*. (43) mitochondrial number is inversely proportional to the activity of mitochondria as found in *ob/ob* and *db/db* mice. Its was shown that although the number of mitochondria(44) were

increased in these models the mitochondrial activity was decreased (45,46) which is suggestive of increased uncoupling by the fatty acids.

In addition FFA can directly affect mitochondria by inducing the opening of permeability transition pore and cytochrome C release which initiates apoptosis finally (47). Also saturated fatty acids are found to be poor substrate for the synthesis of cardiolipin thus leading to decreased cardiolipin concentration in mitochondria (48). Mitochondria with a decreased cardiolipin concentration are more prone to the opening of permeability transition pore releasing cytochrome C and thus more susceptible to apoptotic cell death (49). Saturated fatty acids are also suggested to affect the mitochondrial membrane phospholipids and produce reactive oxygen species (ROS) and thus alter mitochondrial physiology (43).

1.4.2 Lipotoxicity and ER stress

In primary cells bulk membrane biogenesis mainly occurs in ER and Golgi apparatus which together constitute endomembrane compartment in the cytosol. The major lipid content synthesized in the ER is glycolipids and sphingolipids. Both saturated and unsaturated FFA's are directed to ER for complex lipid synthesis (43). ER contains all the major enzymes responsible for the synthesis of all these different lipid moieties (50). Proper lipid composition of ER is of utmost importance as any changes in ER lipid composition may have drastic effects on ER physiology. Ca^{2+} storage is one of major function of ER and it is reported that altered ER fatty acid and lipid composition result in the inhibition of sarco/endoplasmic reticulum calcium ATPase (SERCA) activity and ER stress (51). Similarly, Volmer *et al.* reported that membrane lipid saturation activates endoplasmic reticulum unfolded protein response (UPR) transducers through their transmembrane domains (52). *In vitro* supplementation of cultured fibroblasts, myoblasts, and b cells with saturated FFAs alteraters ERstructure and function which precede UPR activation. This suggests that lipid incorporation into ER contributes to initiate ER stress and UPR (53,54). UPR itself leads to the activation of certain genes that are involved in lipid metabolism and try to compensate the situation but in worst case it initiates apoptosis leads to cellular dysfunction (50). Recently it has been shown that reducing palmitate-induced ER stress through a chemical chaperone, tauroursodeoxycholate, prevents apoptosis in pancreatic β-cells (55) while another chemical

chaperon, 4-phenyl butyric acid (4-PBA), ameliorates palmitate-induced inhibition of glucose-stimulated insulin secretion (GSIS) in the same cells (56).

1.4.3 ROS generation

Reactive oxygen species (ROS) play an important role in cellular redox signaling pathways (57) and a very well organized enzymatic scavenging system (e.g dismutase and peroxidase) and other redox-sensitive modulators (e.g., vitamins E and glutathione) are working continuously to keep a check on ROS levels of the cell (58). However, in pathophysiological conditions, ROS generation may surpass the antioxidant scavenging system resulting in a net increase in the ROS levels of the cell. These elevated ROS levels cause oxidative damage to all biomolecules like lipids, protein content and DNA ultimately resulting in impairing membrane integrity, organelle function and gene regulation (59). A disbalance in redox signaling can have deleterious effects on cell leading to cellular dysfunction, mediated by, mitochondrial damage (60,61) and ER stress and in extreme cases to cell death (62).

Under conditions of hyperlipidemia and type 2 diabetese it has been shown that DNA and protein oxidation products, pro-oxidants and cellular glutathione disulphide levels were elevated (43). Similar findings have also been reported in *ob/ob*, *db/db* and AY mice under conditions of lipid overload (63). One of a direct effect of ROS is lipid and protein peroxidation which leads to organelle dysfunction and cell death (64). Lipids induce elevated ROS by fueling and accelerating the respiration machinery (65). It has also been reported that long chain nonesterified fatty acids decrease mitochondrial ROS generation at the reverse electron transport but increase it at the forward transport (66). The effect can be reversed by using chemical scavengers or by over expression of ROS neutralizing enzymes like superoxide dismutase and catalases (67).

1.4.4 Ceramides

Ceramide is an important lipid second messenger known for initiation of apoptosis under some conditions of stress (68,69). It is synthesized by three different pathways: 1*)* hydrolysis of sphingomyelin (SM) by sphingomyelinase, 2*)* palmitoyl CoA condensation with serine by serine palmitoyltransferase (SPT) which is also termed as de novo synthesis (70) and 3) the

sphingolipid salvage pathway (71). It has been shown in *in vitro* studies that under conditions of substrate overload *de novo* ceramide synthesis is increased (72,73) while its role in inducing apoptosis is reported variably (72,74). Fig 1-4 summarizes the involvement of fatty acid metabolites leading to mitochondrial dysfunction and ER stress which can further lead to cell death.

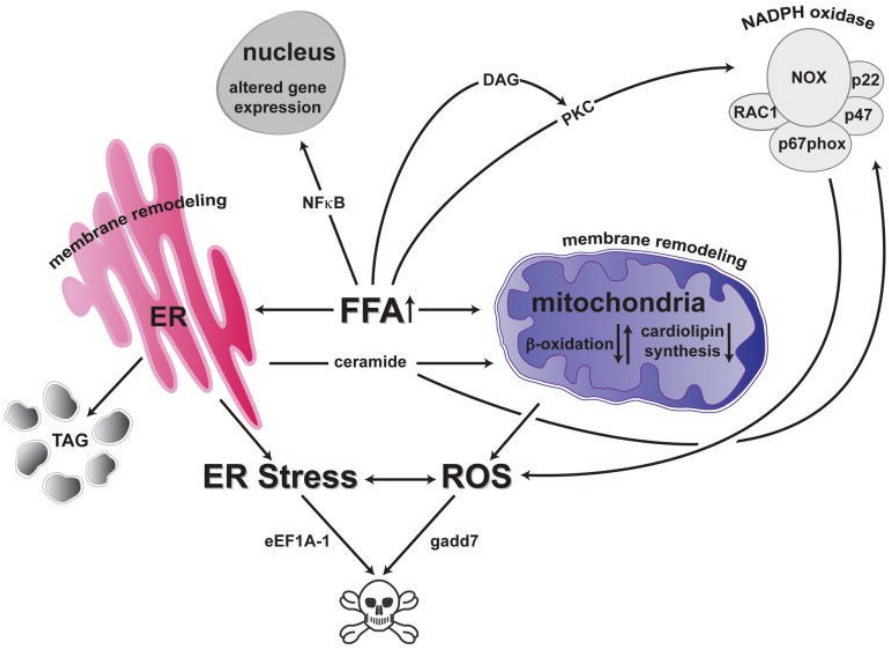

Figure 1-4: a scheme showing how FFA affect different cellular organelle and how the organelle interact with each other either to respond to lipid overload or to compensate the effects of lipid overload finally leading to cellular dysfunction and cell death. (Taken from Brookheart et al., 2009 (43)

1.4.5 Nitric Oxide signaling

Nitric oxide is a signaling molecule which is synthesized by NO synthase as an uncharged diatomic gas having a half life of several seconds at low concentrations in tissues (75). NO is also known as endothelial derived relaxing factor as endothelium of blood vessels uses NO to signal smooth muscle cells to relax, a process known as vasodilation resulting in increased blood flow (76). Thus NO signaling has an important role in regulating blood flow and a dysregulation of NO signaling contributes to a number of different diseases like heart disease, hypertension and stroke, gastrointestinal distress, erectile dysfunction and neurodegeneration

(75). It has been reported that free fatty impairs NO production in endothelial cells through IKK β (77).

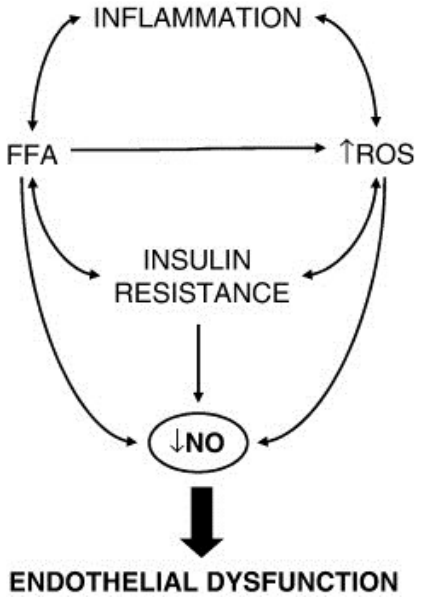

Figure 1-5: a generalized scheme showing how FFA results in endothelial dysfunction medicated by NO bioavailibity. (Taken from Imrie et al., 2010 (78)*)*

1.5 Lipotoxic cell death mechanisms

The above mentioned outcomes of lipid over load ultimately lead to cellular dysfunction or cell death. So far the most studied mechanism of cell death is apoptosis which is mediated by different signaling pathways in different cell types. The involvement of other cell death mechanisms in combination with apoptosis or in isolation have not been studied much. Recently there are some reports which also highlight the involvement of autophagic cell death and necrosis or necroptosis in lipotoxic cell death but there is still much to be explored regarding their molecular mechanism. In the following section difference cell death mechanisms are discussed briefly in context of lipid over load and lipotoxicity.

1.5.1 Apoptosis

Nature has evolved the mechanisms to keep a check on the regular growth of cells and tissues and cells have adopted mechanisms to get rid of unwanted cells. Apoptosis is a programmed cell death mechanism, conserved from yeast to humans (74,79-81), which is regulated by

number of different proteins, factors and enzymes finally leading to death and disintegration of the cell (81). It has been reported by different groups that saturated fatty acids induce apoptosis in different cell types which is mediated by different mechanisms (82-85). Apoptosis is always preceded by other cellular damage like induction of ER stress and mitochondrial dysfunction. A release of Ca^{2+} from ER is one of the key steps in the process leading to mitochondrial swelling and opening of permeability transition pore, release of cytochrome c and activation of activator and effector caspases (86). There are variable reports regarding the FFA intermediate metabolites like ceramide on cellular apoptosis (72,74,87). Similarly role of NO signaling is reported variably, depending on cell and tissue type (88).

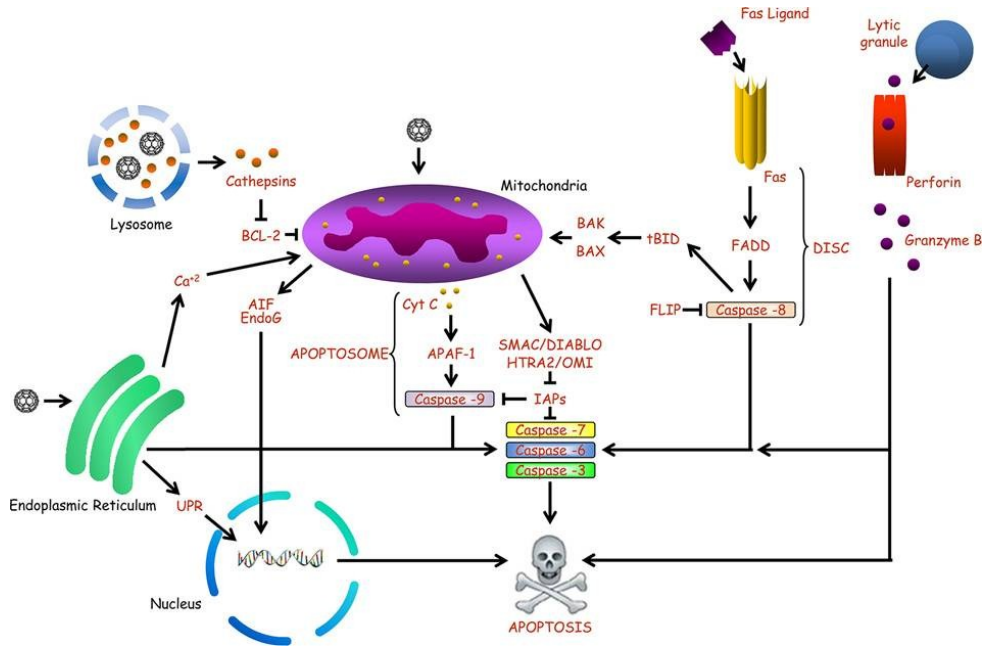

Fig 1-6: a simplified flow chart of apoptosis (taken from Andón et al. (81)

1.5.2 Necrosis and Necroptosis

Necrosis was generally regarded as a sudden and non programmed cell death pathway (89). A number of stimuli were generally attributed with the onset of necrosis including physical damage to the cellular membranes and organelle, a sudden increase in the ROS production above a certain level and energy crisis due to a decrease in ATP levels below a certain level (90). Recently, it has been shown that necrosis is not just a sudden cell death pathway but is also controlled by certain proteins and is programmable (91). Receptor interacting protein

kinases (RIPK's) are among the first proteins which have been identified to participate in the process of programmed necrosis which is also termed as necroptosis (92). Recently CYLD has been identified to play a role in the onset of necroptosis by inhibiting caspase 8 (93). Similarly calpains, the cystiene proteases are also known to execute necrosis once activated by a cytosolic Ca^{2+} overload (94). Figure 1-7 represents some pathways which can end up at programmed necrosis or necroptosis.

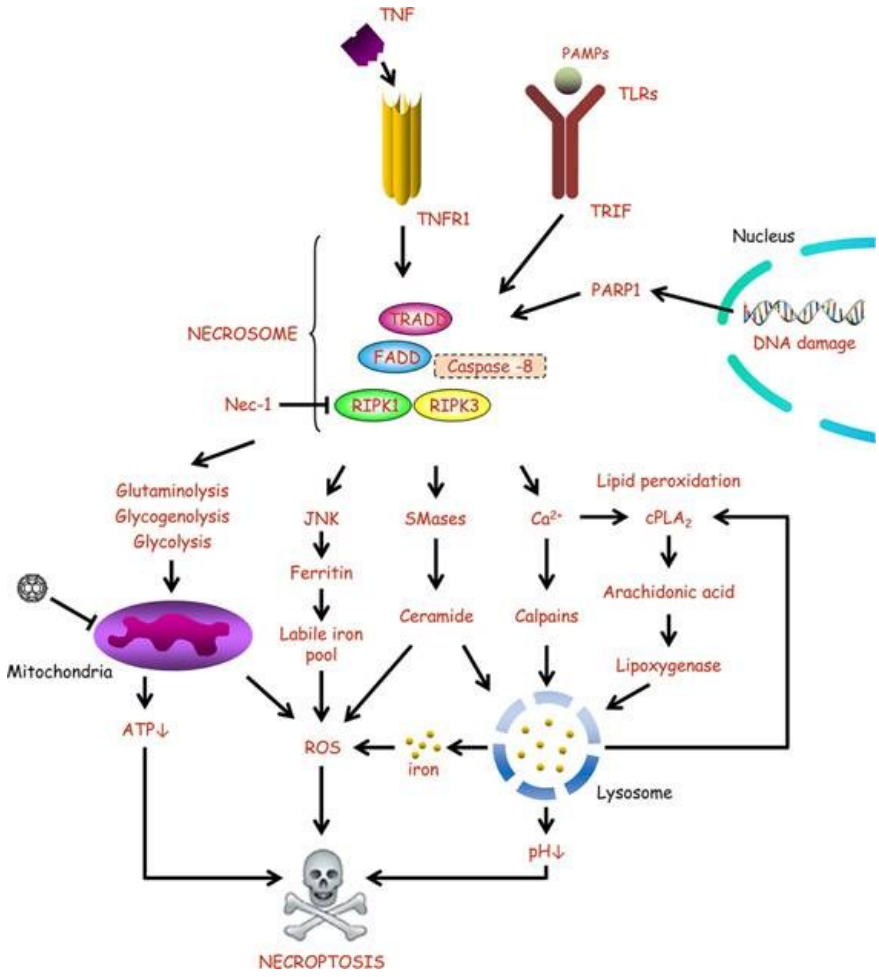

Fig 1-7: a simplified flow chart of necroptosis (taken from Andón et al. (81)

1.5.3 Autophagy and autophagic cell death

Autophagy is an evolutionarily conserved process which combats metabolic hardships (95) and other stresses (96) leading to organelle dysfunction. Autophagy is prosurvival in this regard when it provides nutrients to a starving cell (97) or removing the damaged parts and

leaving functionally fit parts that cell can survive the unusual environmental or internal stressed conditions (98). The process starts with encircling the damaged organelle or the material destined to degradation into a double membrane known as autophagosomes. Autophagosomes are then fused with the lysosomes resulting in an autolysosomes (99). The lysosomes are acidic compartments which contain a number of acid hydrolases (100) and lipases (101). Cellular organelle and macromolecules destined to autolysosmes are degraded by these enzymes and the molecules are supplied back to the energy producing machinery to replenish cellular energy requirements (102). The process is prosurvival if not interrupted (103,104) or exceed the normal limits (105). An interruption to the process or exaggerated autophagy initiates cell death pathways, termed as autophagic cell death (106). Autophagy can lead to cell death either by over-eating of the cellular parts (105) or initiating apoptosis(107) or necrosis (108). Figure 1-8 shows a simplified way how autophagy is initiated and its fate.

Recently it was found that autophagy mobilized lipid droplets in times of starvation (109). Also there are recent reports that palmitic acid can trigger autophagy which slows down apoptosis in βcells (110). In another study palmitic acid was found to harm the lysosomes in neuronal cells (111). Furthermore, it has also been reported that fatty acids decreases autophagic turn over by harming lysosomes leading to energy crisis (112). Molecular pathways are being studied to explore the intermediate players involved in fatty acid triggered autophagy. Protein kinase C has also been demonstrated to be one of the major enzymes that control palmitic acid induced autophagy in β- cells (113).

So far there is very little knowledge about induction of autophagy by palmitic acid. However, a few reports are available (as mentioned in previous paragraph) regarding the molecular pathway responsible for its activation. Similarly the fate of autophagy is variable in different cell types. Until recently, there is no report regarding PA induced autophagy in endothelial cells. Keeping in view the utmost importance of this pathway in endothelial physiology and pathology this study was designed with the following aims.

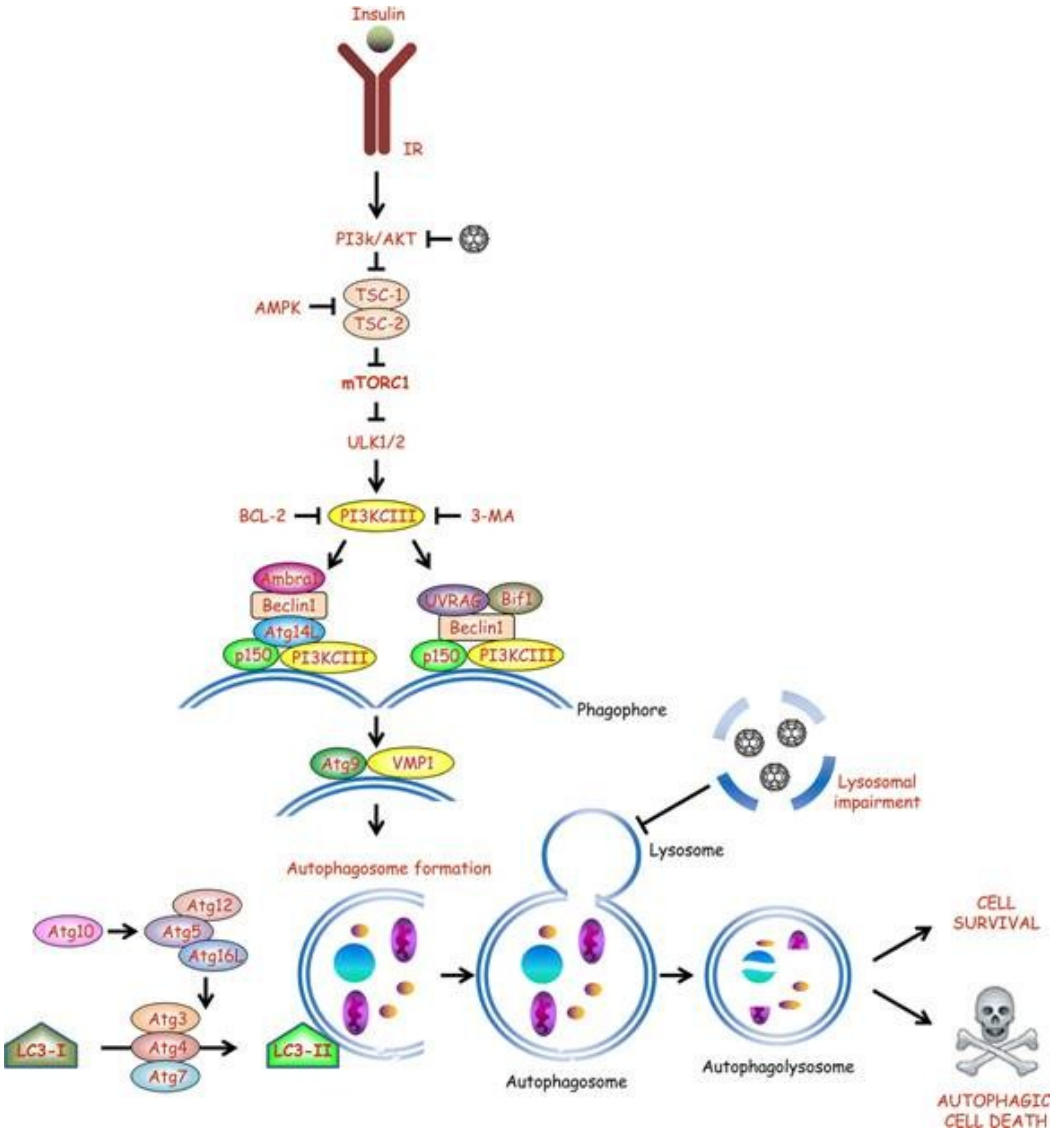

Fig 1-8: A simplified flow chart of mechanism of autophagy and autophagic cell death (taken from Andón et al. (81)*.*

Aims and Objective

Keeping in view the deleterious of effects of PA on different tissues and recent developments in the field of cell death mechanism this study was designed with the following aims.

1. A comparative study of different molecular mechanisms of PA induced cell death
2. To study the induction of PA induced autophagy in endothelial cells
3. Effect of PA on Ca^{2+} homeostasis of endothelial cells and its effect on autophagy and cell death
4. To identify the molecular targets that are controlling PA induced cell death in endothelial cell

2. MATERIALS AND METHODS

2.1 Cell Culture

Human umbilical vein endothelial derived cell line EA.hy926 which is a hybrid with A549 human lung carcinoma epithelial cells (114), were used in this study at passages 45 to 85. Cells were grown in DMEM containing 10% foetal calf serum (FCS), 1% hypoxanthine-aminopterin-thymidine (HAT) medium (5 mM hypoxanthin, 20 µM aminopterin and 0.8 mM thymidine), 50 units/ml penicillin, 50 µg/ml streptomycin, and were maintained at 37 °C in 5% CO_2 atmosphere in a humidified environment. Cells were harvested by trypsinization after washing them briefly with warm PBS (37°C) and were grown directly on plastic in 24 well plates for cell viability assays and in 6 wells or on 10cm dishes for protein, RNA and DNA isolation.while on glass cover slips (ø 30 mm) for confocal and epifluorescence imaging. Cells were used when between 80 and 100% confluence.

2.2 Cell treatment

Cells were treated with saturated free fatty acid palmitic acid (PA) or mono-unsaturated oleic acid (OA) in normal cell culture medium containing 10% FCS. The fatty acids were directly added to the medium. To treat the cells with different pharmacological tools cells were incubated with the given pharmacological agent for 20 minutes before the free fatty acids were added to the medium. Experiments performed with BAPTA loaded cells BAPTA was replenished after every 6 hours as it was found to lose its efficiency after 6 hours.

2.3 PA:BSA complex preparation

Palmitic and oleic acid was complexed to BSA in a 6:1 ratio. Both fatty acids were dissolved in 0.1N NaOH and was heated at 70°C for 30 minutes to make a soup. The soup was then added drop wise to 5.7% BSA and continuous stirring. The complex was filtered through a 0.2 µm filter to sterilize it. The complex was aliquot and stored at -20°C and was thawed to room temperature just before use.

Caution: The complex should be clear and any turbid or milky appearance is an indication of clumping of the fatty acids which is not complexed to the BSA and such solution must not be used.

2.4 Cell Transfection protocol for over expression

Cells were grown as mentioned in section 3.1. At a confluence of approximately 80 %, the cells were transiently transfected with 2 µg of purified plasmid DNA using TransFast™ Transfection Reagent (Promega, Mannheim, Germany). 2 µg of DNA was diluted in 1ml DMEM medium without any supplements and 4 µl of TransFast ™ reagent was added in a sterile tube. The mixture was vortexed immediately and was incubated at room temperature for 15 minutes to allow liposome formation. Growth medium was gently aspirated from the cells and the medium containing DNA and TransFast ™ reagent was added to the cells. the cells were incubated for 1 hour at 37°C under the normal cell culture conditions and 1 ml of normal culture medium containing all the supplements, FCS and antibiotics was added to the cells for another 4 hours. After that this Transfection medium was replaced with normal cell culture medium and the cells were allowed to grow and express the transfected DNA for at least 16 hours and then they were examined accordingly. This general procedure was for the cells growing in a 6 well plate and the quantities mentioned are for 1 well of 6 well plate.

2.5 Transfection protocol for siRNA mediated knock-down

Small interfering RNA (siRNA) is a widely used tool to knock down the expression of a particular target protein by targeting the mRNA which is then degraded by the cellular RNA degradation machinery.

These siRNAs were co-transfected with some modifications to the transfection protocol previously described (section 3.4):

The Transfection mixture was formulated as follows:

Transfection reagent per;

1 well of a 6 well plate:	1 well of a 24 well plate
500 µL serum-free DMEM	130 µL serum-free DMEM
2.0 µL of 40µM siRNA	0.5 µL of 40µM siRNA
4 µL TransFast™ transfection reagent	1 µL TransFast™ transfection reagent

Transfection mixture was vortexed and incuabated at room temperature for 15 minutes. Cellular medium was aspirated and Transfection mixture was added to the cells. Cells were incubated with transfection mixture for 1 hour and equal volume of DMEM without serum was added to the cells and incubated for 18 hours, after which it was replaced with normal serum containing cell culture medium. After 44 to 48 hours of Transfection cells were used for further experiments.

2.6 Cell death Assays

2.6.1 Cell viability assay

2.6.1.1 MTT Assay

Cellular viability was measured using 3-(4,5-Dimethylthiazol-2-yl)-2,5-diphenyltetrazolium bromide (MTT). The MTT assay is a colorimetric assay for measuring the activity of enzymes that reduce MTT to formazan dye, giving a purple color. A main application allows assessing the viability. It is also used to determine cytotoxicity of potential medicinal agents and toxic materials, since those agents would stimulate or inhibit cell viability. For the assay, endothelial cells were plated in a 24 well plate. After each treatment cells were washed with warm PBS and incubated for 3 hours with normal cell culture medium containing 0.5 mg/ml MTT (Sigma-Aldrich, Vienna, Austria). Cells of each well were washed twice with ice cold PBS and were lysed with 200 µl of a lysis buffer composed of 0.04 M HCl in absolute isopropanol. 24 well plate was then continuously shaken at room temperature for 15 minutes on a microplate shaker. The absorbance was subsequently measured at 530 nm on a Wallace Perkin Elmer Victor 1420-004 multi-label plate reader. Data were normalized to respective controls and represented as percent viability of the controls.

2.6.1.2 Phase contrast microscopy

Morphological changes are one of the hallmarks of cell death and this property has been used to monitor cell death (115) previously. For this purpose Endothelial cells were grown on small polystyrene dishes (35 X 10 mm, Corning B.V. Life Sciences, Amsterdam, The Netherlands) until 80 % confluency in under normal culture conditions. During image acquisition a HEPES-bufferd medium was used instead that was composed of (in mM): 135 NaCl, 5 KCl, 2 CaCl2, 1 MgCl2, 10 Hepes acid, 2.6 NaHCO3, 0.44 KH2PO4, 0.34 Na2HPO4, 10 D-glucose, 0.1% vitamins, 0.2% essential amino acids and 1% penicillin/streptomycin; pH was adjusted to 7.4 with NaOH. 2 dishes were stably mounted on the motorized xy-table of an inverted microscope (Axio Observer.Z1 from Zeiss, Göttingen, Germany), and bright-field images were taken every 5 minutes alternately from the 2 dishes using a 10x objective (Plan-Neofluar 10x/0.3 Ph1 M27, Zeiss). During the experiments cells were kept at 37 °C using a closed incubator system (Visitron Systems, Puchheim, Germany), which was installed on the microscope. To avoid loss of medium by evaporation dishes were covered with respective caps (Corning B.V. Life Sciences). This arrangement allowed us to observe cells for more than 20 h alternatively in the presence of BSA alone (Control) or PA (500 μM) complexed to BSA. VisiView® software (Visitron Systems) was used for imaging while the images were then binarized and quantitatively analyzed by using MetaMorph® software (Visitron Systems).

2.6.2 AnnexinV/PI staining

AnnexinV/PI staining is used to differentiate between apoptotic and non-apoptotic (necrotic) cells (116). The assay is based on the differential symmetry of plasma membrane during apoptosis. Under normal physiological conditions, a cell has an asymmetric distribution of phospholipids in the two leaflets of the cell membranes with phosphatidylserine (PS) facing the cytosolic side (Devaux, 1991, Connor et al., 1992, Higgens, 1994). However, during early apoptosis this membrane asymmetry is rapidly lost without losing membrane integrity (Koopman et al., 1994; Homburg et al., 1995; van Engeland et al., 1996, 1997, 1998). This property of the cell is utilized to differentiate between apoptotic and necrotic cells by staining the cells for PS with a fluorescence labeled annexin V which specifically binds to PS in a Ca^{2+} dependent manner. On the other hand cell loses plasma membrane integrity during necrosis which can be detected by propidium iodide staining as it's not cell permeable and enters the

cell only when cell membrane is compromised. Thus a cell positive for annexin V staining but not PI is apoptotic and the cells which are also positive for PI staining are grouped as necrotic cells.

In this assay Annexin-V-Fluos staining kit from Roche Biodiagnostics (Roche Diagnostics GmbH, Vienna, Austria) was used. According to the manufactures' protocol 20 µl of Annexin-V-Fluos was diluted in 1ml incubation buffer and 20 µl of propidium iodide was added. Cells were washed with warm PBS and 100 µl of this mixture were added directly to the cells. After 20 minutes of incubation 500 µL of incubation buffer was added to the glyass cover slip in a perfusion chamber and were analyzed on a Zeiss Axioskop microscope. Images were obtained at RT using a Cy3 optical filter set for PI staining, an enhanced GFP optical filter set for Annexin V staining, and a differential interference contrast filter set for transmitted light images. Cells positive for annexin V and/or PI were counted manually and are were plotted graphically.

2.6.3 DNA laddering

Cleavage and fragmentation of chromosomal DNA into oligonucleosomal size fragments is an integral part of apoptosis (117). During apoptosis endonucleases are activated which degrades the genomic DNA specifically at internucleosomal linker region and produces 180- to 185-base pairs DNA fragments. These fragments can be separated and visualized on agarose gel and are a known marker for apoptosis. To observe any DNA laddering cells were treated for 24 h with 0.5 mM PA and BSA as a control and Genomic DNA was isolated by Wizard® Genomic DNA purification kit (Promega, Madison, USA) according to the manufacturer's protocol. The purified DNA was then run on a 0.7 % agarose gel and was documented by Genosmart gel documentation system (VWR, Vienna, Austria).

2.6.4 Quantification of DNA hypoploidy by flow cytometry:

DNA hypoploidy is the term used for the accumulation of fragmented DNA and a decrease in haploid or diploid DNA content as a consequence of the activation of endonucleases during apoptosis (118). Different stages of DNA content during a cell cycle can be analyzed by staining the DNA different staining dyes e.g propidium iodidem (PI), ethidium bromide or 4'-

6-Diamidino-2-phenylindole (DAPI) and can be quantified by flow cytometry (119). Endothelial cells were grown to 90% confluence and were treated with BSA, 0.5 mM palmitic acid (PA) and 300 nM staurosporine (STS) for 16 h. Cells were washed twice with warm PBS and trypsinized. Cells were pelleted by centrifugation and fixed by incubation with 70% ethanol on ice for 15 min. Cells were pelleted and resuspended in 500 µl propidium iodide (PI) solution (in PBS: 50 µg/ml PI, 0.1 mg/ml RNase A, 0.05% Triton X-100) and incubated at 37 °C for 40 minutes. The PI solution was diluted further by adding 3 ml of PBS and cells were pelleted by centrifugation. Cells were resuspended in 500 µl PBS for analysis by flow cytometry (FACSCalibur, Becton Dickinson, Mountain View, CA). Individual cells were distinguished from cell debris and aggregated cells by means of forward-scatter/side-scatter gating, and PI fluorescence intensity was measured in 10,000 cells.

2.6.5 Detection of caspase-3 activity using Casper3-GR

Caspases are a family of cystine aspartate proteases which play a central role in apoptosis. Caspase can be divided into apoptosis activator and apoptosis executioners. Caspase 2, 8, 9 and 10 are known to be apoptosis activators while caspase 3, 6 and 7 are apoptosis executioners (120). A number of assays have been developed to monitor the activation of these proteases. We used a a Förster resonance energy transfer (FRET) based sensor Casper3-GR (24), (Casper3-GR vector DNA was purchased from BioCat GmbH, Heidelberg, Germany) for caspase-3 activity, in order to monitor apoptosis in our model of cell death. The sensor consists of a green (GFP) and a red fluorescent protein (RFP) connected by a linker with the caspase-3 cleavage sequence DEVD. In the absence of caspase-3 activity the two fluorescent proteins show highly effective FRET. The activation of caspase-3 during apoptosis leads to cleavage of DEVD sequence, which causes the separation of the FPs yielding a reduction of the respective FRET signal, while the GFP signal increases.

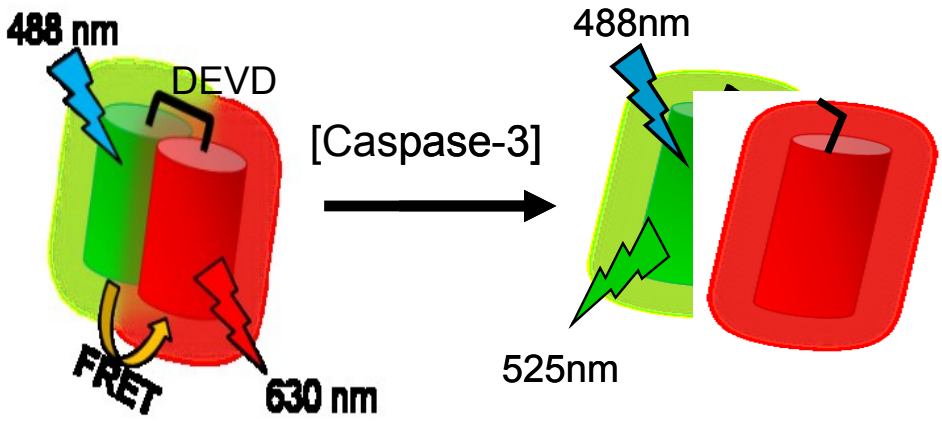

Figure 2-1: Schematic illustration of Casper3-GR

Cells were transfected with the Casper3-GR and after 24 hours of transfection cells were treated with BSA or PA for 16-18 h. Staurosporin was used as a positive control Images were taken on the ACLSM using a 40x objective (Zeiss). The following 3 channels for imaging the red fluorescence protein (RFP), the green fluorescence protein (GFP) and the FRET signal between GFP and RFP were used to determine the cleavage of the sensor by caspase-3: RFP-channel: excitation 561 nm laser line, emission was collected at 630/75 nm; GFP-channel: excitation 488 nm laser line, emission was measured at 525/40 nm; FRET between GFP and RFP: excitation 488 nm laser line, emitted light was imaged at 630/75 nm. The 3 channels were imaged consecutively using the same exposure times (500 ms). Caspase-3 activity was expressed as the ratio of GFP/FRET.

2.7 Molecular Biology Methods:

2.7.1 Isolation of Total RNA from Animal Cells using peqGOLD total RNA kit

To isolate RNA the peqGOLD total RNA extraction kit was used. RNA was isolated from cell grown in a confluent monolayer according to manufacturer's Protocol for Animal Cells. Cells were harvested after washing two times with PBS.

Cells were lysed by adding 400 µl of RNA Lysis Buffer T directly to 1 well of a 6 well plate. The lysate was transferred into a DNA removing column placed in a 2.0 ml collection tube and was centrifuged at 12.000 x g for 1 min at room temperature. The flow-through lysate was

transferred into a new 1.5 ml tube. An equal volume (400 µl) of 70 % Ethanol was added to the lysate and mixed thoroughly by vortexing. PerfectBind RNA Column was placed in a new 2.0 ml collection tube (supplied) and the lysate was added directly to the membrane and centrifuged at 10.000 x g for 1 min. The flow-through liquid was discarded and the membrane was washed by adding 500 µl of RNA Wash Buffer I to the PerfectBind RNA Column and centrifuge for 15 sec at 10.000 x g. The flow-through was discarded and the membrane was washed again with 600 µl RNA Wash Buffer II by centrifugation at 10.000 x g for 15 sec. The flow-through liquid was discarded and the column was dried by centrifugation for 1 min at 10.000 x. PerfectBind RNA Column was placed into a fresh 1.5 ml microcentrifuge tube and 50 - 100 µl sterile RNAse-free dH2O was added directly to the binding matrix in the PerfectBind RNA Column and centrifuged for 1 min at 5.000 x g to elute RNA. The RNA was stored at -70°C before further use.

2.7.2 Measuring the concentration of nucleic acids

The concentration of RNA and DNA samples were either determined using UviLine 9400 spectrophotometer or the Peqlab ND-1000 spectrophotometer.

2.7.2.1 UviLine 9400 spectrophotometer

The concentration of nucleic acid samples were measured using a Hellma TrayCell in a UviLine 9400 spectrophotometer by UV light absorption wavelengths. TrayCell is a fibre-optic Micro cell designed for measurements of DNA/RNA samples and enables highly accurate analysis of extremely small samples with remarkable reproducibility. Nucleic acid free water was used for the reference (blank Absorption at 260 nm and 280 nm of sample(s) were read. The concentration as well as the purity of the sample(s) was calculated using the acquired values:

Purity:

abs260/abs280RNA	=	1.7-1.9
DNA	=	0.5-1.7

Calculation of Nucleic Acid Concentration: abs260 x 4 = RNA in µg/µl

abs260 x 5 = DNA in µg/µl

2.7.2.2 Peqlab ND-1000 spectrophotometer

2 µl of a nucleic acid sample was directly applied onto the measurement spot of the Nanodrop (ND) instrument. RNA or DNA concentrations were immediately measured and calculated by the system.

2.7.3 cDNA Synthesis using High Capacity cDNA Reverse Transcription Kit

the success of an accurate quantitative Real Time PCR experiments depend on the accurate quantities of cDNA taken. Therefore, it is important to ensure complete reverse transcription of RNA samples into cDNA samples. For this purpose High-Capacity cDNA Reverse Transcription Kit from Applied Biosystems was used which contains random primers, which warrant that the first strand synthesis occurs efficiently with all species of RNA molecules present, including mRNA and rRNA. It also contains of a 10x RT buffer, a 25x dNTP Mix (100 mM) and the MultiScribe™ Reverse Transcriptase. In order to avoid RNA digestion the RNasin® RNase Inhibitor (Promega) was used in the reaction mixture as well.

The kit components were allowed to thaw on ice and the RT master mix was prepared on ice.

The 2X reaction mixture was made on ice as follows:

10x RT buffer	2.0 µl
25x dNTP mix (100 mM)	0.8 µl
10x RT Random Primers	2.0 µl
MultiScribe™ Reverse Transcriptase	1.0 µl
RNase Inhibitor	1.0 µl
Nuclease-free H_2O	3.2 µl
Total per reaction	10.0 µl

All the components were mixed gently and placed on ice.

2µg of RNA was taken and was diluted to 10µl with Nuclease-free H_2O and was mixed then with the 2X reaction mixture. The tubes were sealed and were briefly centrifuged to spin down the contents and to eliminate any air bubbles.

The tubes were place on ice until the thermal cycler is ready to use.

To program the thermal cycling conditions were as follows:

Table 2-1: Thermal Cycling Conditions for RT-PCR

	Step 1	**Step 2**	**Step 3**	**Step 4**
Temperature	25°C	37°C	85°C	4°C
Time	10 min	120 min	5 sec	Forever

2.7.4 Specific Polymerase Chain Reaction (PCR)

The polymerase chain reaction (PCR), developed in 1983 by Kary Mullis, is a scientific technique in molecular biology to amplify a single or a few copies of a piece of DNA to generate thousands to millions of copies of a particular DNA sequence using site specific primers. PCR is one of the most important techniques in the molecular biology and has its applications in biological and medical research. In 1993, Mullis was awarded the Nobel Prize in Chemistry along with Michael Smith for developing the technique which revolutionized the field.

GoTaq Green master mix from Promega® was used to amplify the target DNA using a site specific pair of primers. Following standard PCR reaction was used:

GoTaq Green master mix 2x	10 µl
Gene specific forward primer (10µM)	1µl
Gene specific reverse primer (10µM)	1µl

cDNA or 5-50 ng of plasmid DNA	2 µl
ddH_2O	6 µl

Following thermal cycling conditions were used generally:

Standard PCR Conditions:

95°C	15 min (Initial denaturating step)	
94-95°C	1 min (denaturating)	
50-65°C	1 min (primer annealing	30-40 cycles
72°C	1 min (extension)	
72°C	10 min (final extension s	
4°C	Forever	

2.7.4.1 Primer Design

The specificity of PCR depends primarily on the designing of an optimal primer with which only a specific sequence is amplified and all the non-specific and non target regions from of the DNA or cDNA are excluded. Certain parameter should always be taken into account while designing a primer which includes length of primer, GC content, primer dimmers and hairpin formation. These parameters should be taken into account while designing a primer for cloning. In designing the real time primers we should take some more parameters into account in order to avoid the amplification of the traces of the genomic DNA. A primer designed at the exon-intron junction flanking two consecutive exons is considered to be a better primer.

We used *MS Dos Program Primer Designer – Version 2.0* to design the primers for cloning purpose while the primers for real time PCR were designed by using web based primer designing Scitools from Integrated DNA technology.

2.7.4.1.1 Primer designing for cloning

The sequences of diverse genes (ORF = open reading frame) were obtained from the *National Center for Biotechnological Information (NCBI)* and in FASTA format and saved in *.txt format. The sequence was opened into the *Primer Designer* and the parameters were defined according. Furthermore, additional sequences for restriction sites were included in both forward and reverse primers and the primers which satisfy all the parameters optimally were selected.

2.7.4.1.2 Primers designing for real time PCR

Primers for the real time PCR was designed by web based primer designing tool of integrated DNA technology. Either a refseq accession number from the NCBI data base or the sequence in FASTA format defining exons in uppercase and intron in lowercase can be used for designing the primers.

Table 2-2: List of Primers used for real time PCR

VPS34-F	5'-GGGATTAGTGCTGAGGTCATG-3'
VPS34-R	5'-AGTCTATGTGGAAGAGTTTGCC-3'
CYLD-F	5'-TGGGATGGAAGATTTGATGGAG-3'
CYLD-R	5'-CATAAAGGCAAGTTTGGGAGG-3'
RIPK1-F	5'-CATGGAAAAGGCGTGATACAC-3'
RIPK1-R	5'-ACTTCCCTCAGCTCATTGTG-3'
ATG7-F	5'-TTTTGCTATCCTGCCCTCTG-3'
ATG7-R	5'-GCTGTGACTCCTTCTGTTTGAC-3'

2.7.4.2 Dilution of Primers

The primers were dissolved with sterile double deionized water (ddH_2O) according to the provided data sheet to a concentration of 100 µM (stock, stored at –20°C). Stock solutions were diluted 1:10 with ddH_2O to 10 µM (working solution).

2.7.4.3 Real time PCR

Real time polymerase chain reaction is a method to quantiate the differential levels of expression of a given gene. It's a widely used technique to analyze the absolute and relative gene expression at the level of transcription. The method is also used for the evaluation of siRNA knock-down efficiency. A number of different variations to technique are available.

LightCycler 480 Instrument (Roche) was used for real time PCR. The LightCycler instrument basically consists of two different components: a cycler component and a fluorimeter component. The thermal chamber is directly connected to the optical system of the fluorimeter. The homogeneous, 470 nm light beam (excitation) is subsequently focused onto the individual wells of a 96 well plate and hence onto the samples to be measured. The detection channel within the LightCycler fluorimeter is equipped with a filter. This permit analyzes at certain emission wavelengths, which allow exact measurements of emission from a distinct fluorophore.

QuantiFast™ SYBR Green PCR Master Mix was used to detect the copy number of RNA in the sample. SYBR Green I is a dye that binds specifically to double-stranded DNA. Its inherent fluorescence is enhanced when it binds to the minor groove of double-stranded DNA. During PCR, SYBR Green I binds to DNA products as soon as they are synthesized. Thus, the increase in SYBR Green I fluorescence, when measured at the end of each elongation cycle, indicates the amount of PCR product formed during that cycle. Dye staining can detect from approximately 1 to 10^9 copies of a target sequence. The maximum excitation of SYBR Green I dye occurs at 497 nm. Maximal emission of DNA stained with SYBR Green I occurs at 521 nm.

The components of QuantiFast™ SYBR Green PCR Master Mix include HotStartTaq *Plus* DNA Polymerase, QuantiFast SYBR Green PCR Buffer, SYBR Green I, and ROX passive reference dye.

The following reaction set up was used.

cDNA sample	2 µl
QuantiFast™ SYBR Green PCR Master Mix	5 µl
Forward Primer	1µl
Reverse Primer	1µl
RNase free water	1µl

After a brief centrifugation step at 1,000 rpm for 10 sec the LightCycler instrument was loaded with a 96 well plate.

The following cycling conditions were used:

Table 2-3: Real-Time PCR Cycling Conditions

Step	**Time**	**Temperature**
PCR initial activation step	15 min	95°C
Two-step cycling		
Denaturation	10 sec	95°C
Combined annealing/extension	30 sec	60°C
Number of cycles	40	

2.7.4.4 Analysis of quantitative RT-PCR

The out coming crossing points of the particular PCR-reactions were analyzed by the REST software version 384® (Relative Expression Software Tool), which was downloaded from http://rest.gene-quantification.info/.

Accordingly, the downregulation of the gene in its siRNA samples was calculated and plotted in percentage to their negative controls.

2.7.5 Cloning of Venus-LC3

LC3 was amplified from human cDNA with site specific primers and was run on agarose gel in order to get a single band of correct size as compared to the DNA molecular weight marker. The PCR product was purified from the gel using Wizard® SV Gel and Clean-Up System (Promega Corp.) according to manufacturer's protocol. This purified DNA and the vector DNA was then digested with appropriate restriction enzymes. Venus-LC3 was cloned in multiple cloning site of pcDNA 3.1 cloning vector (Invitrogen, Austria) using the BamHI and EcoRI restriction sites followed by sub-cloning of Venus using restriction sites KpnI and BamHI. Chemically competent Top10 bacterial strain was transformed through heat shock for 1 min at 42°C. The positively transformed cells were selected through ampicillin resistance by growing the bacteria on lauria bertaini (LB) (10g trypton + 10g NaCl + 5 g yeast extract, in 1 liter, pH= 7.0-7.5) plates containing 15% agar and 100µg/ml ampicillin. Individual colonies were selected and were further grown in liquid LB broth containing 100µg/ml ampicillin. The plasmid DNA was isolated with Wizard® Plus SV Minipreps DNA Purification Systems (Promega Corp.) and control digestion was made by using a set of restriction enzymes from multiple cloning sites (MCS) of the vector. The restricted plasmid DNA was run on 1.5% agarose gel in 1X Tris- Acetate- EDTA (TAE) buffer at a voltage of 70V under constant current to separate the DNA bands. Bacteria containing the correctly ligated vector containing LC3 were stored in 20% glycerol containing LB medium and were stored at -70°C.

For large scale DNA preparation positively transformed bacterial cells were grown in 200ml of LB medium containing 100µg/ml ampicillin overnight and DNA was isolated by PureYield™ Plasmid Maxiprep System (Promega Corp.) as per manufacturer's protocol.

2.7.6 siRNA Design

RNA interference (RNAi) is an evolutionarily conserved mechanism for silencing gene expression in eukaryotes ranging from plants to humans (121). The first reports about the successful use of double stranded RNA based specific gene silencing was described by Fire and Mello in 1998 (122). After that the technique has been used tremendously for gene silencing in a wide variety of organisms ranging from plants to humans (121). The technique utilizes the natural RNA silencing machinery of the cell comprising of RNA induced silencing complex (RISC) and DICER an endoribonuclease a member of RNAase III family.

Thermodynamic properties, local structure of target RNA and the availability of free ends of the siRNA antisense strand have been described to be relevant for the efficient siRNA knock downso far (123). The efficiency of different siRNA is different and need a proper optimization with respect to time and quantity of siRNA used. Usually an siRNA for which the efficiency of knock down is already reported is preferred. Efficiency of knock down is usually measured by real time PCR to quantiate the target RNA or with western blot to quantitate the the target protein. The proteins having a longer half life are hard to knock down than the one with a shorter half life.

The following siRNA were selected from the literature already reporting their functional knock down efficiently.)

Table 2-4: List of siRNA's

siRNA	Sequence	Reference
ATG7	5′-CAGUGGAUCUAAAUCUCAAACUGAU-3′	Hoyer-Hansen *et al.*(124)
VPS34	5′-GUGUGAUGAUAAGGAAUAU-3	Gao *et al.*(125)
CYLD	5′-CGAAGAGGCTGAATCATAA-3′	Stegmeier *et al.*(126)
RIPK1	5'-CTGGGCGATATTTGCAAATAACC-3'	Self designed
RIPK3	5'-CAGCCTGATGTCGTGCGTCAAGTTAAA-3'	Cho *et al*(127)

2.8 ATP Measurement

Separation of adenine nucleotides was performed on a Hypersil ODS column (5 µm, 250 × 4 mm inner diameter), using a L2200 autosampler, two L-2130 HTA pumps, and a L2450 diode array detector (all from VWR Hitachi). The wavelength for detection of adenine nucleotides was set at 254 nm. EZchrom Elite (VWR) was used for data acquisition and analysis. After trypsinization and mild centrifugation (supernatant discarded) cellular proteins of EA.hy926 cells were precipitated with 250 µl of perchloric acid (0.4 mol/liter). After centrifugation (12,000 × *g*), 100 µl of the supernatant was neutralized with 10–12 µl of potassium carbonate (2 mol/liter, 4 °C). The supernatant obtained after centrifugation was used for HPLC analysis (injection volume: 40 µl). The pellets of the acid extract were dissolved in 0.5 ml of sodium hydroxide (0.1 mol/liter) and used for protein determination (BCA assay, Pierce).

2.9 Western Blotting

Endothelial cells were washed twice with ice-cold PBS and total cellular protein was isolated by lysing the cells with RIPA buffer containing a protease inhibitor mixture (Sigma). The protein concentration was measured using a Thermo Scientific Pierce BCA protein assay kit (Thermo Fisher Scientific Inc.). 30 µg of protein were separated by SDS-PAGE and transferred to a nitrocellulose membrane. The membrane was blocked with 5% BSA solution in PBST for 1 hour and was incubated with the primary antibody at 4 °C overnight. Membrane was washed with PBS containing 0.1% tween 20 for 5-6 times, each washing step was around 10 minutes on a shaker. Primary antigen-antibody complex was detected by incubating the blot with a horseradish peroxidase-conjugated secondary antibody at room temperature for 1 h and the membrane was washed again for 5-6 times with PBS containing 0.1% tween 20. The membrane was further developed with the ECL plus Western blotting detection system (GE Healthcare) and the chemiluminescencel was detected on by Kodak® BioMax Light film. The signal was developed by exposing the film to a developer solution and was further fixed by a fixation solution. ImageJ was used for dencitometric analysis of the intensity of different bands and was normalized to the intensity of the house keeping protein β-actin, as a loading control.

2.10 Cytosolic Ca^{2+} Measurement

For cytosolic Ca^{2+} measurements the Fura-2 technique was used as described previously (128). Cells were loaded with Fura-2/AM and rested prior to experiments in a Hepes-buffered solution containing (in mm): 135 NaCl, 5 KCl, 2 $CaCl_2$, 1 $MgCl_2$, 10 Hepes acid, 2.6 $NaHCO_3$, 0.44 KH_2PO_4, 0.34 Na_2HPO_4, 10 d-glucose, 0.1% vitamins, 0.2% essential amino acids, and 1% penicillin/streptomycin; pH was adjusted to 7.4 with NaOH. For experiments in intact cells Ca^{2+} containing experimental buffer was composed of (in mm): 138 NaCl, 5 KCl, 2 $CaCl_2$, 1 $MgCl_2$, 10 d-glucose, and 10 Hepes acid; pH was adjusted to 7.4 with 1 m NaOH. For experiments in Ca^{2+}-free solution, experimental buffer containing 1 mm EGTA instead of $CaCl_2$ was used.

Experiments were performed on a Nikon inverted microscope (Eclipse 300TE, Nikon, Vienna) equipped with CFI Plan Fluor ×40 oil immersion objective lens (NA 1.3, Nikon, Vienna, Austria), an epifluorescence system (150 W XBO; Optiquip, Highland Mills, NY), a computer-controlled *Z*-stage (Ludl Electronic Products, Haawthrone, NY), and a liquid-cooled charged-coupled device camera (−30 °C; Quantix KAF 1400G2, Roper Scientific, Acton, MA). All devices were controlled by MetaFluor4.0 software (Visitron Systems, Puchheim, Germany). Fura-2/AM was simultaneously excited at 340 nm (340HT15, Omega Optical, Brattleboro, VT) or 380 nm (380HT15, Omega Optical) and emission was monitored at 510 nm (510WB40, Omega Optical). Cytosolic Ca^{2+} was expressed as the ratio of emitted fluorescence at 340 and 380 nm (F_{340}/F_{380}). Cells were perfused using a perfusion system and stimulated in nominal Ca^{2+}-free experimental buffer containing 100 μm histamine and 15 μm BHQ.

2.11 Array Confocal Laser Scanning Microscopy

High resolution imaging of annexin V/PI and Venus-LC3 was performed using an array confocal laser scanning microscope. The array confocal laser scanning microscope was built on an inverse, fully automatic microscope (Axio Observer.Z1 from Zeiss, Göttingen, Germany) that was equipped with a ×100 objective (Plan-Fluor ×100/1.45 Oil, Zeiss), a Nipkow-based confocal scanner unit (CSU-X1, Yokogawa Electric Cooperation, Tokyo, Japan), a motorized filter wheel (CSUX1FW, Yokogawa Electric Cooperation) on the

emission side, and an AOTF-based laser merge module for laser lines 405, 445, 473, 488, 515, and 561 nm (Visitron Systems). Emission was acquired with a charged-coupled device camera (CoolSNAP-HQ, Photometrics, Tucson, AZ). All devices were controlled by VisiView Premier acquisition software (Visitron Systems).

3. RESULTS

3.1 Palmitic acid induce lipotoxicity in endothelial cells but not oleic acid

Different cells and tissue type show differential responses to free fatty acid overload (129-134). Therefore, first susceptibility of the endothelial cell line, EA.hy926, to PA-induced cell death was tested. Palmitic and oleic acid was used as members of saturated and unsaturated fatty acids respectively, as these are the most common free fatty acid found in plasma (135). For this purpose cells were treated with PA or OA complexed to BSA in a 6:1 and cell viability was measured with the MTT assay at different times of incubation (Fig. 3-1). After 12 h of incubation with PA, cell viability was found to be already significantly reduced and further decreased with time. The cell viability declined more than 80% after 28 h of incubation with PA (Fig. 3-1, left panel), pointing to a strong cytotoxic effect of this saturated fatty acid on endothelial cells. The PA-induced cell death was further examined using long-term phase-contrast imaging, which showed an impaired cell proliferation and an accumulation of detached, dying cells upon incubation with PA (Fig. 3-1, right panel).

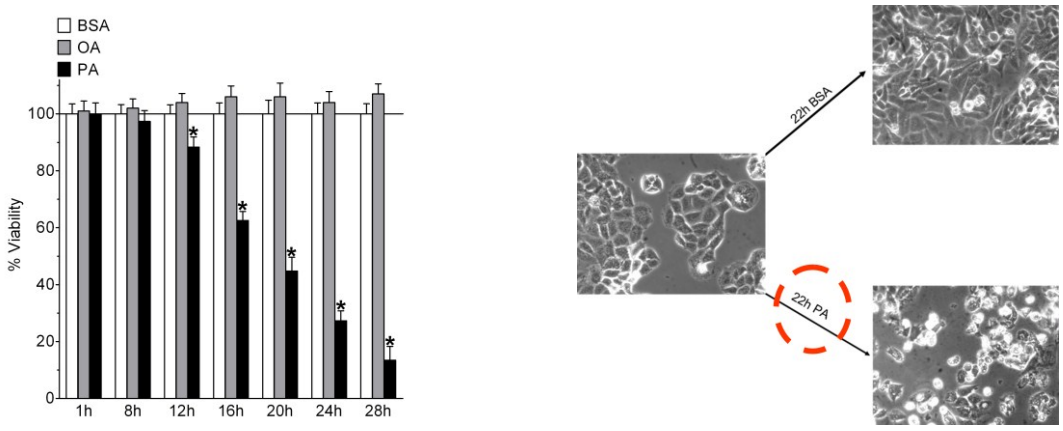

Figure 3-1: *Left panel: cells were treated with BSA alone (white columns, n=3), 0.5mM OA (gray columns, n=3), or 0.5 mM PA (black columns, n = 3) and cell viability was measured with MTT assay at the time points indicated. Fatty acids were complexed to BSA. Data were normalized to BSA as control and represented as percentage viability. *, p<0.05 versus BSA. Right panel: cells were treated with PA or BSA and images were taken after 22 hours of incubation.*

In contrast, cell treatment with OA did not affect the viability of the cells (Fig. 3-1, left panel). These findings are in line with earlier studies using other cell types (129-134) and approved EA.hy926 cells as a suitable model to explore the molecular mechanisms of PA-mediated lipotoxicity.

3.2 Mode of cell death

Mode of cell death is one of the most important determinants in cytotoxicity research. It is always recommended to use a number of different methods in order to determine the mode of cell death.

As first step mode of PA-induced cell death was investigated by annexin V and PI staining. A major proportion of the cells exposed to PA for 12 h were found to be positive both for annexin V and PI (Fig. 1, B and 1C), which is indicative of necrosis. Moreover, the annexin V/PI-positive cells contained round and intact nuclei (Fig. 3-2), pointing to necrotic cell death.

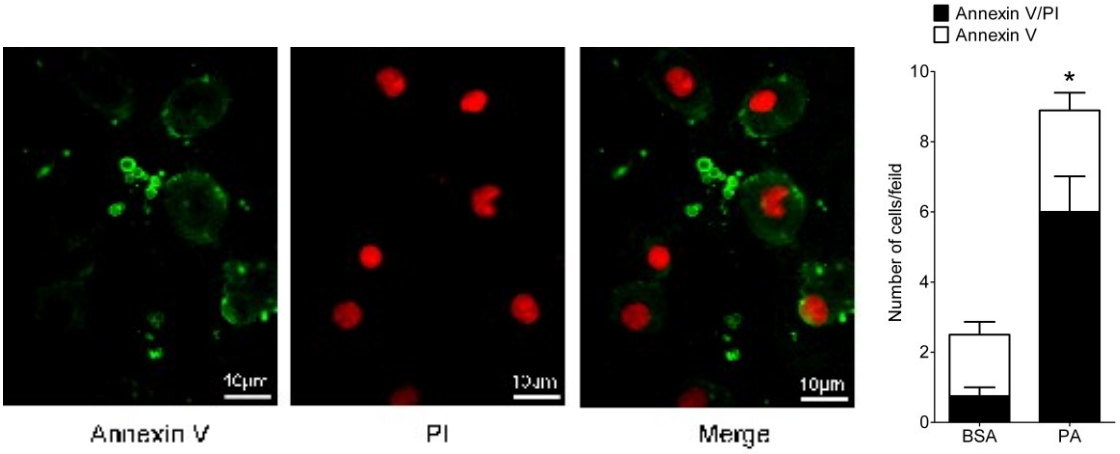

Figure 3-2: *Representative images of Annexin/PI staining of Endothelial cells (left panel). majority of the cells were both positive for annexin and PI which is an indication of necrosis. furthermore the clear round nuclei of the PI positive cells point towards necrosis than apoptosis. Right panel represents the graphical presentation of the annexin V/PI costaining for the cells exposed to 0.5mM PA (n=4) or BSA alone (n=4) (asterisk refers to annexin V/PI). *, p<0.05 versus BSA.*

To further exclude the role of apoptosis in the process of PA-induced death of the endothelial cells, cells were treated with benzyloxycarbonyl-Val-Ala-Asp(OMe)-fluoromethylketone (Z-VAD-fmk), a cell permeable, irreversible pan-caspase inhibitor that hinders apoptosis (136). Z-VAD-fmk failed to exhibit any effect on PA-induced endothelial cell death (Fig. 3-3), thus, further confirming that the mode of PA-induced death of the endothelial cells was necrotic and not apoptotic.

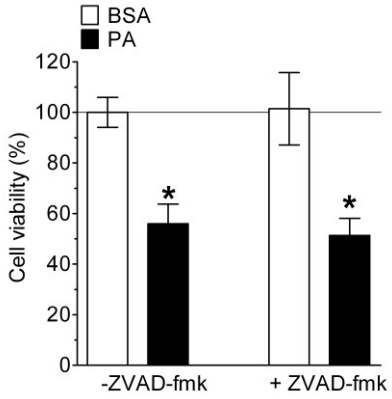

Figure 3-3: *cells were treated with the solvent (DMSO, control, -Z-VAD-fmk, n = 3) or with 20 μM Z-VAD-fmk (+zVAD-fmk, n=3) prior to treatment with 0.5mM PA or BSA alone and cellular viability was measured with MTT assay. *, p<0.05 versus BSA (51.3 ± 6.7% in the Z-VAD-fmk treated as compared with 55.9 ± 7.7% in controls).*

The absence of caspase activation in PA-induced cell death was further documented using the caspase-3 apoptosis sensor Casper3-GR (137). Casper3-GR is a FRET-based sensor for measuring caspase-3 activity, consisting of a green (GFP) and a RFP that are connected by the

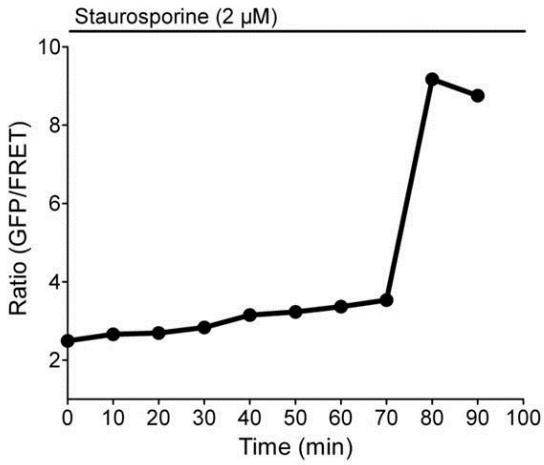

Figure 3-4: *Kinetics of the impact of 2 µM staorosporine on the GFP/FRET ratio of Casper3-GR*

caspase-3 cleavage sequence DEVD (Fig 3-1). As a positive control cells expressing Casper3-GR were treated with staurosporine, which is a strong inducer of apoptosis, revealed an increase of the GFP/FRET ratio after 80 min, indicating the cleavage of the sensor by the activation of caspase-3 (Fig. 3-4).

In contrast, cell treatment with PA for 16 h failed to increase the basal GFP/FRET ratio of Casper3-GR, indicating the absence of caspase-3 activation (Fig. 3-5). This indicate that PA is unable to activate capspase 3 or 7 and thus is not inducing apoptosis in endothelial cells.

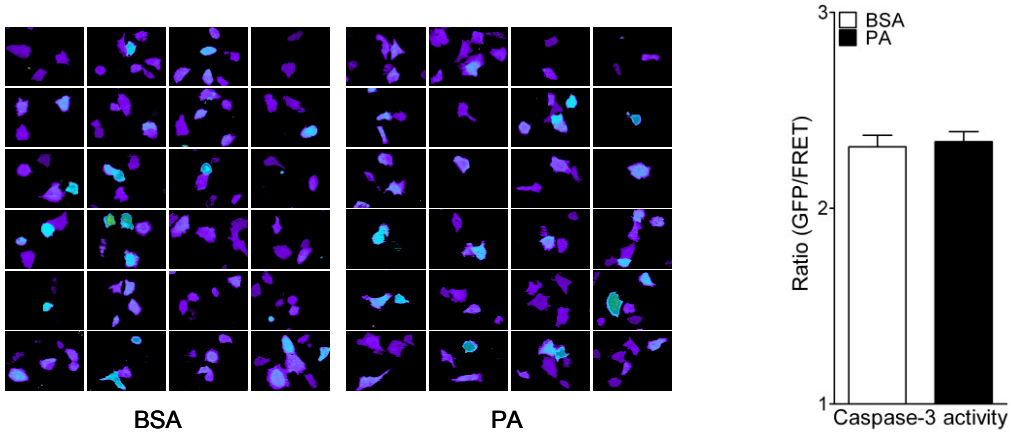

Figure 3-5: *Cells were treated with BSA or 0.5 mM PA for 16-18 h and caspase activity was measure using the FRET based caspase-3 activity sensor, Casper3-GR. Populations of cells*

were imaged randomly (left panel) and the ratio images (GFP/FRET) were calculated. Sum ratio of all images is presented in the right panel.

DNA laddering is one of the hallmarks of apoptosis and is used as a marker for apoptosis (118). Fragmentation of DNA leads to a lowering of the haploid or diploid DNA content. This lowering of the DNA content is known as DNA hypoploidy and is quantified by FACS. Quantitation of DNA hypoploidy showed only a small proportion of cells with reduced DNA content when cells were treated with PA for 18 h (Fig. 3-6).

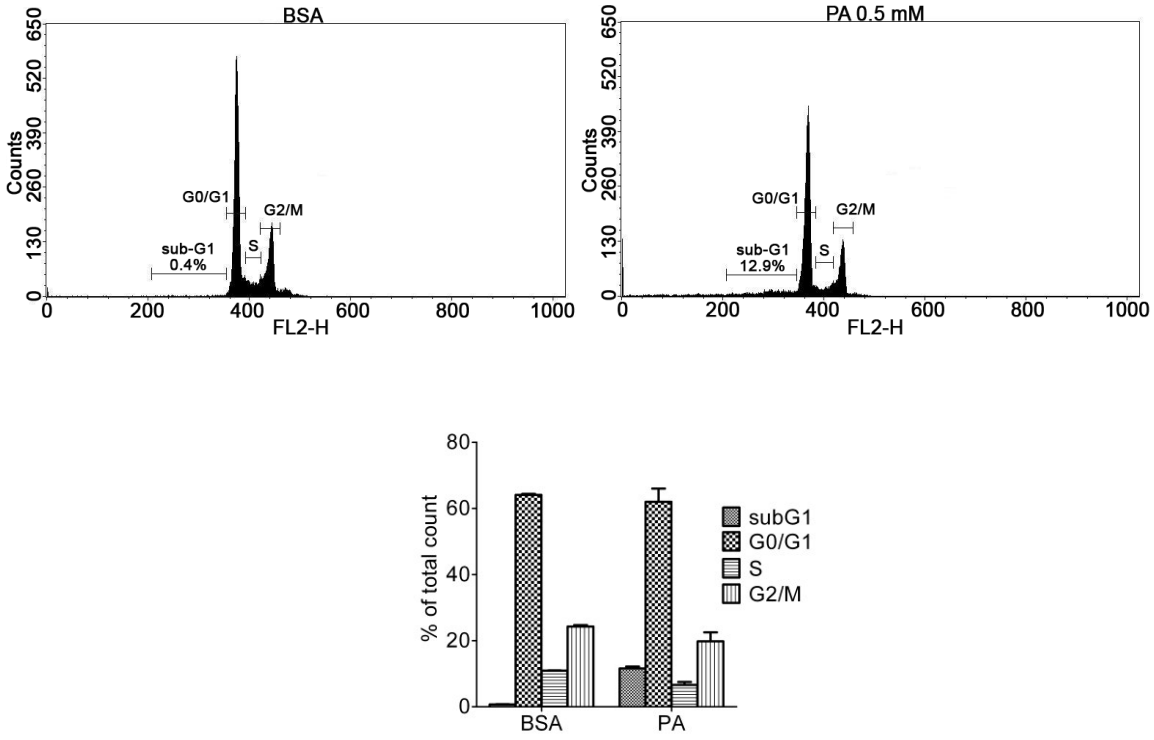

Figure 3-6: *Histograms of cell cycle analysis by flow cytometry for DNA hypoploidy. Cells were treated with BSA (upper left panel) or 0.5mM PA(upper right panel) and were analyzed after 18 h of incubation. Statistical analysis of the histograms is shown in lower panel.*

Also no DNA laddering was observed on the agarose gel even if cells were treated for 24 h with the fatty acid (Fig. 3-7), whereas under these conditions 70% of the cells were found dead with the MTT assay. In summary, these data confirm that the PA-induced cell death is predominantly necrotic.

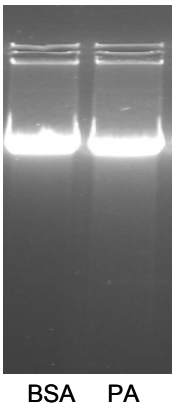

Figure 3-7: *DNA laddering pattern treated with BSA and PA for 24 hours.*

Energetically apoptosis is an active process and need a proper supply of ATP in order to execute the cell death while it is known that cells undergo necrosis in case of energy crisis (138). ATP levels of the cells were measure with HPLC and it revealed revealed a significantly reduced ATP levels in cells that have been exposed to PA already at 8 h and further decreased tremendously until 16 h (Fig. 3-8). This emphasizes necrosis as the terminal point of PA-induced cell damage as energetically the conditions are not favorable for the cells to undergo apoptosis. As the onset of cell death is between the 8- and 16-h time point the drop in ATP levels are earlier than the onset of cell death and more than 40% of the cells were already found dead after 16 h.

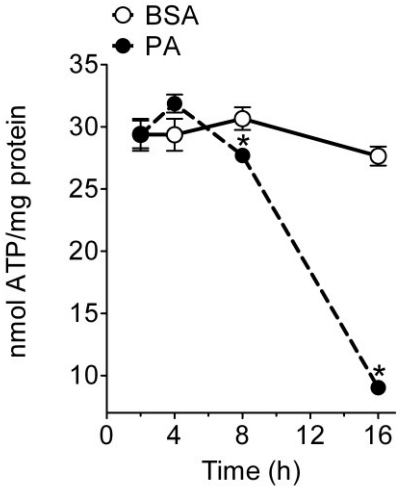

Figure 3-8: *Statistical data representing nmol of ATP/mg of protein in the cells exposed to 0.5mM PA (black circles, dotted line, n=6 for each time point) or BSA alone (white circles, continuous line, n=6 for each time point). *, p<0.05 versus BSA*

These data challenge the dogma that lipotoxicity is exclusively apoptotic and align with our earlier findings that free fatty acids induce necrosis and not apoptosis in yeast (139).

3.3 PA Induces RIPK3 and CYLD-dependent but RIPK1-independent Programmed Necrosis (Necroptosis)

Necrosis was once considered as non programmed and sudden cell death (140,141). But recently, a great deal of evidence has accumulated that the necrotic pathway can also occur in a highly regulated manner (142) and a number of players involved in programmed necrosis or necroptosis has been identified. The kinases, receptor-interacting protein kinase-1 (RIPK1), RIPK3, and the receptor interacting protein (RIP) 1 de-ubiquitin enzyme CYLD are known initiators of programmed necrosis (127,143)

According to the available data, next, the molecular mechanism of PA-induced necrosis in endothelial cells was investigated. Necrostatin-1, a specific inhibitor for RIPK1, was used to inhibit necrosis in endothelial cells but as represented in Fig. 3-9 necrostatin-1 did not affect the PA-induced cell death.

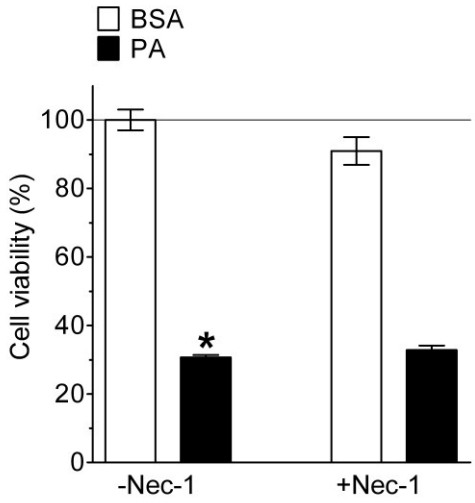

Figure 3-9: *cells were pretreated with solvent (DMSO, control, -Nec-1, n = 4) or 30 µm necrostatin-1 (+Nec-1, n = 4) for 20 min and were incubated for 24 h with BSA or 0.5 mm PA and cellular viability was measured with MTT assay. *, p < 0.05 versus BSA.*

Furthermore, siRNA-mediated knockdown of RIPK1 (Fig. 3-10 left panel) also could not inhibit PA-induced cell death (Fig. 3-10 right panel). This indicate that PA induced necroptosis is independent of RIPK1 activity.

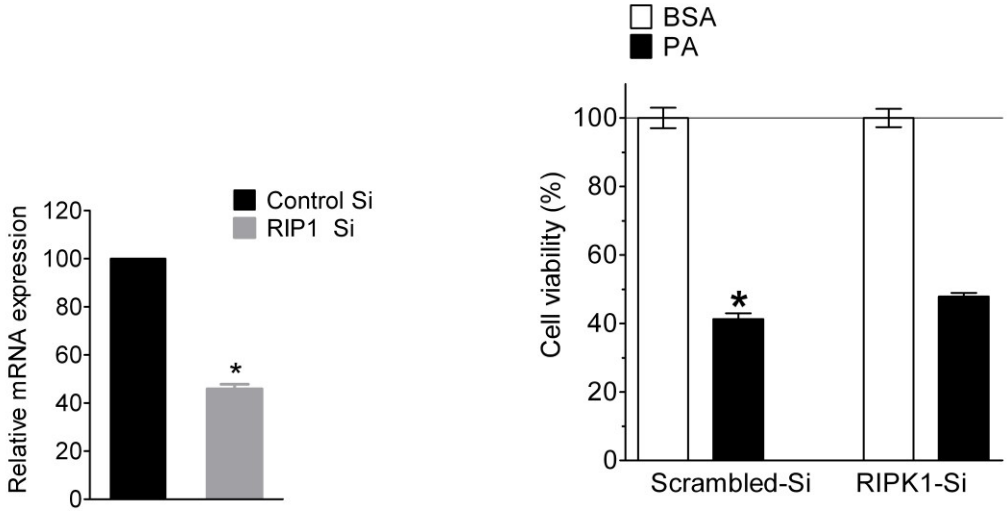

Figure 3-10: *Knockdown efficiency of RIPK1 (RIP1) siRNA in the percentage of mRNA expression compared with scramble siRNA (n = 3 for all columns presented). *, p < 0.05 versus scrambled siRNA is shown in left panel. Right panel represents cell viability 48 h after transfection of cells with either scrambled siRNA (left pair of columns, n = 18 for both conditions) or siRNA against RIPK1 (right pair of columns, n = 18 for both conditions). Cells were incubated for 24 h with BSA alone (white columns) or 0.5 mm PA complexed to BSA (black columns) and cell viability was measured using the MTT assay. Viability is expressed in percentage, whereas the average value of cells treated with scrambled siRNA and BSA alone was defined as 100%. *, p < 0.05 versus BSA, and #, p < 0.05 versus PA with scrambled siRNA (47.8 ± 1.0% dead cells in RIPK1-siRNA as compared with 41.2 ± 1.6% dead cells in scrambled siRNA)*

On the other hand a knockdown of CYLD (Fig. 3-11 left panel) could inhibit the PA-induced cell death significantly (Fig. 3-11, right panel). This data confirms that PA induces a RIPK1 independent but CYLD dependent necroptosis in endothelial cells.

In line with these results it was found that mRNA level of CYLD was strongly elevated of the after 16 h of incubation with PA, whereas no change in the expression pattern of RIPK1 could be observed under these conditions (Fig. 3-12).

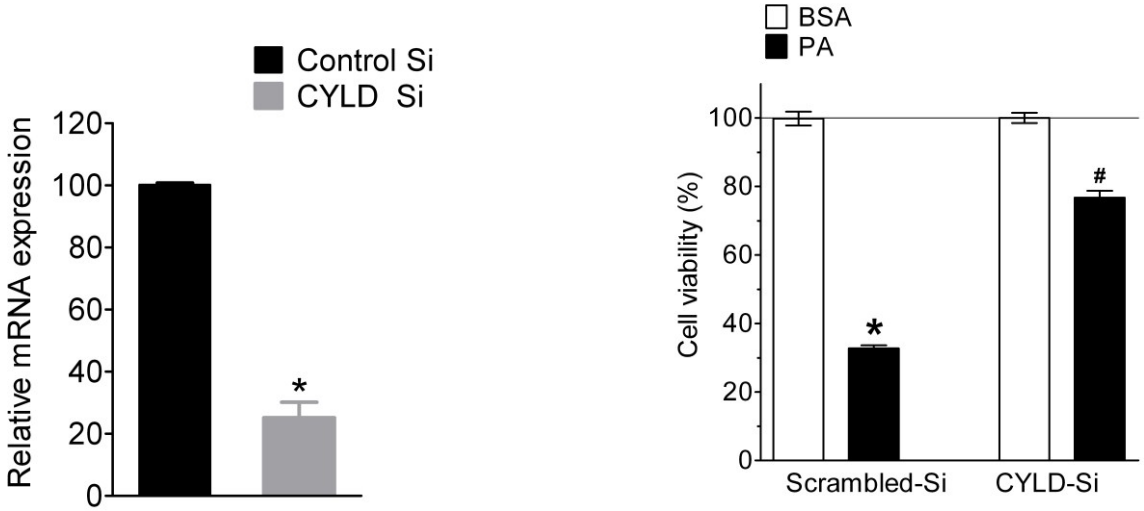

Figure 3-11: *knockdown efficiency of CYLD siRNA in percentage of mRNA expression compared with scramble siRNA (*n = *6). *,* p < *0.05* versus *scrambled siRNA (left panel). Impact of siRNA-mediated knockdown of CYLD on cell viability under analogous conditions described in figure 4:10, right panel, (*n = *18 for each column). *,* p < *0.05* versus *BSA, and #,* p < *0.05* versus *PA with scrambled siRNA.*

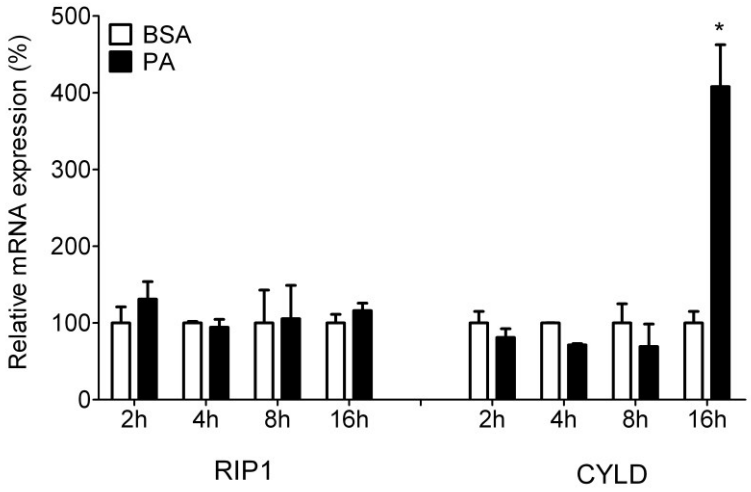

Figure 3-12: *The relative mRNA expression of RIPK1 and CYLD in cells treated with BSA or 0.5 mm PA for 2, 4, 8, and 16 h. The relative expression is presented as a percentage of BSA-treated cells at the given time point. *, $p < 0.05$ versus BSA at the given time point (n = 3).*

We failed to perform respective experiments for RIPK3 expression levels most likely because of too low mRNA levels coding for this protein in the endothelial cells used (supplemental Fig. 4, A and B). Nevertheless, cells treated with a validated siRNA against RIPK3 (127) showed a significantly increased viability if treated with PA for 24 h in four sets of independent experiments (Figure 3-13).

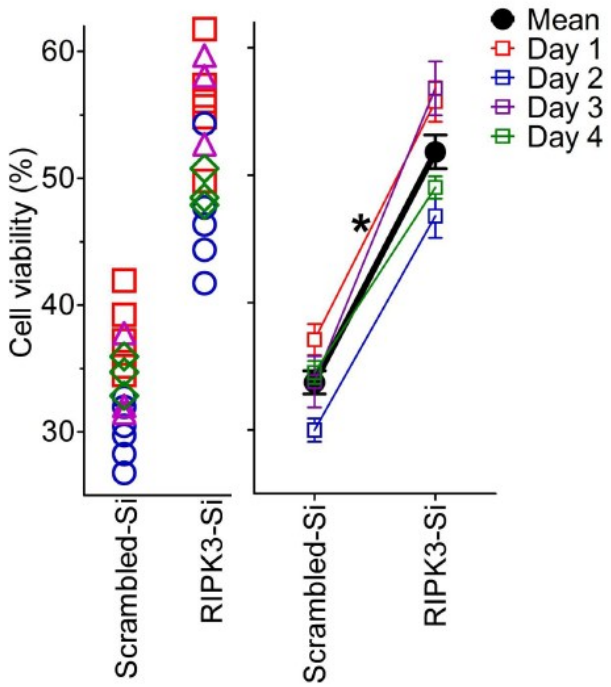

Figure 3-13: *Cell treatment with siRNA against RIPK3 partially rescued PA induced endothelial cell death. Cells were transfected with either scrambled siRNA or siRNA against RIPK3 for 48 hour and were then treated with 0.5 mM PA complexed to BSA or BSA alone as control. 24 h after cell treatment with PA or BSA alone the viability of the cells was quantified using the MTT assay. Data are presented as percentage viability compared to the respective BSA controls. The symbols in the left panel represent all the individual values from four different sets of experiments that were performed on four different days (each color represent one set of experiments). In addition in the right panel the respective mean values + SEM of each of the four independent experiments, and the accumulative mean + SEM of all values are plotted. *P < 0.05 versus scrambled siRNA, all means were significantly different. However, for each individual experiment with siRNAs the cell viability was determined by normalizing to its respective BSA controls.*

Although we could not quantify the RIPK3 knockdown efficiency these findings suggest that PA induces a CYLD- and RIPK3-dependent but RIPK1-independent programmed necrosis.

3.4 PA Triggers Autophagy in Endothelial Cells

Recent data demonstrated the induction of autophagy by PA in beta cells (144). Accordingly, a possible role of autophagy in PA-induced cell death was investigated. For this purpose cleavage of the microtubule-associated protein 1 light chain 3 (LC3), a marker for autophagy (145), was blotted. Considerable cleavage and lipidation of LC3 to LC3-I (not lipidated) and the phosphatidylethanolamine-conjugated LC3-II was detected in cells that were treated with PA, whereas OA did not induce LC3-II formation (Fig. 3-14).

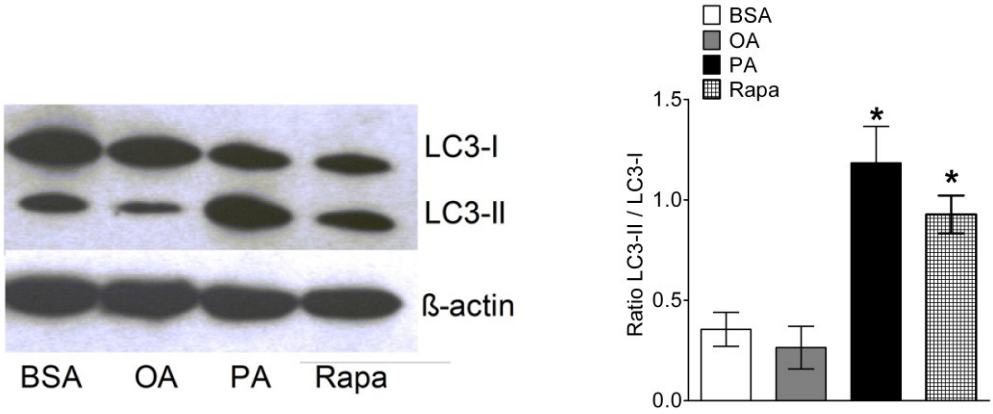

Figure 3-14: *Cells were treated with BSA, OA, PA, and rapamycine (Rapa) for 8 h and the extracted protein was immunoblotted against LC3 antibody. β-Actin was used to normalize the data for equal protein loading (left panel). Right panel represents graphical representation of the average band densities from 3 different experiments. *, $p < 0.05$ versus BSA*

To gauge the magnitude of the induction of autophagy by PA, cells were also treated with 50 nm rapamycin, a well characterized inducer of autophagy (146) As shown in Fig. 3-14 right and left panel, PA was even more effective than rapamycin to stimulate LC3-II lipidation under these conditions. The PA-induced lipidation of LC3-II was dependent on both the time of PA incubation (Fig. 3-15) and the concentration of the fatty acid (Fig. 3-16).

The induction of autophagy by PA was further examined by imaging the cellular distribution of Venus-LC3, a fusion construct of the yellow fluorescent protein Venus with LC3. In control cells that were treated with BSA alone Venus-LC3 was mainly distributed in the cytosol and only a small number of autophagosomes were visible, indicating a low level of autophagy under these conditions (Fig. 3-17 left panel). In

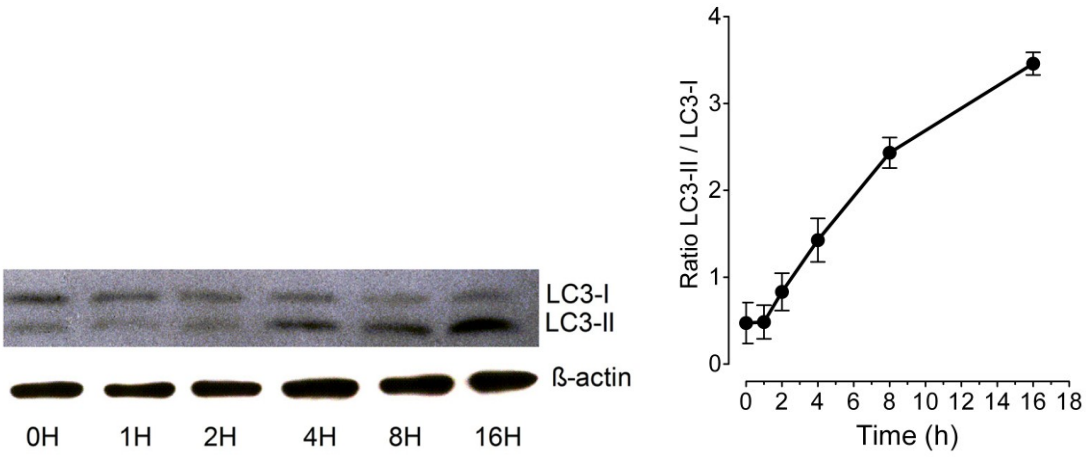

Figure 3-15: *Time dependence of the PA-induced cleavage of LC3 expressed as the LC3-II/LC3-I ratio over time (*n = *3 for each time point)*

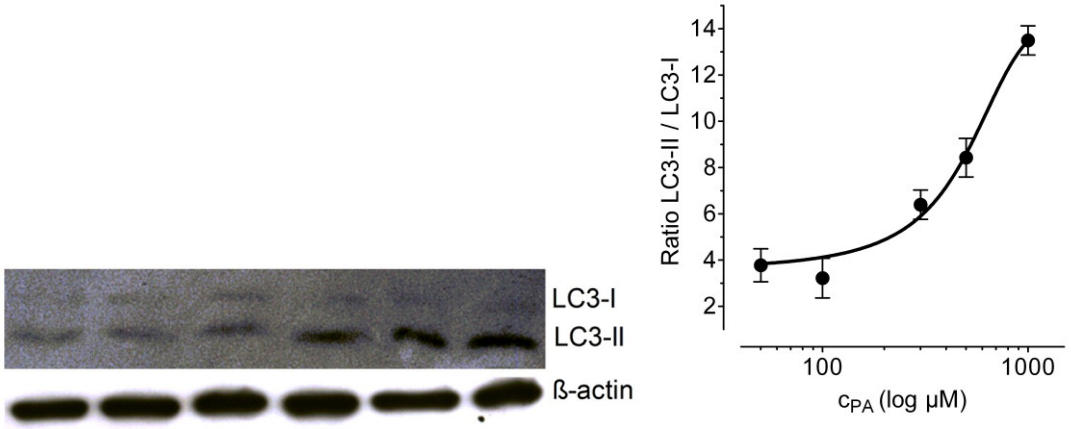

Figure 3-16: *concentration-response curve of PA-induced cleavage of LC3 (n = 3 for each concentration). PA was complexed to BSA.*

contrast, cells incubated with PA for 8 h exhibited a large number of autophagosomes with accumulated Venus-LC3 (presumably as Venus-LC3-II). This confirms the induction of autophagy by PA in the EA.hy926 cells (Fig. 3-17 right panel).

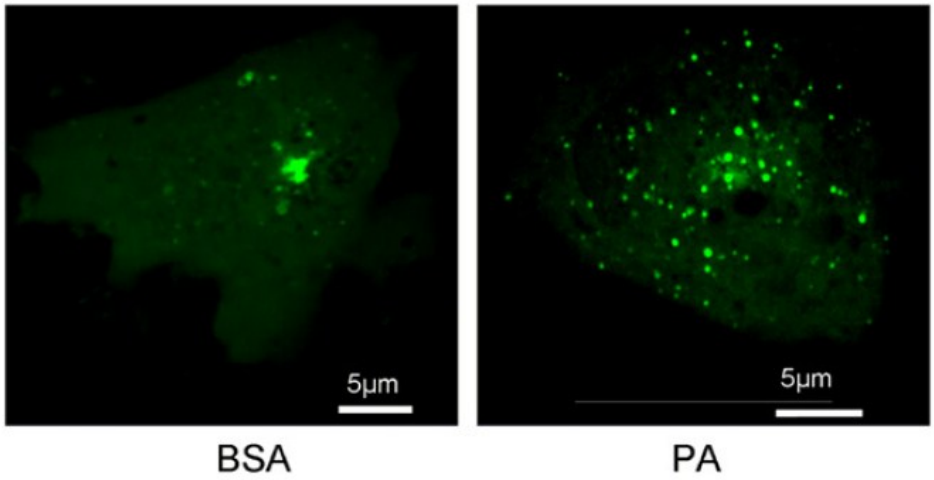

Figure 3-17: *Representative images of cells expressing Venus-LC3. Images show the subcellular distribution of Venus-LC3 in control cells (left image, BSA alone for 8 h after cell transfection) and in cells treated for 8 h with 0.5 mm PA complexed to BSA (right image).*

To verify whether or not the PA-induced autophagy goes to completion, we measured LC3-II also in the presence of bafilomycin A (50 nm), a known inhibitor of the autophagic flux (146). As shown in Fig. 3, H and I, LC3-II was further increased in the presence of bafilomycin A under control conditions and in cells pretreated with PA until 8 h. These findings indicated that PA induces a genuine and strong autophagy in endothelial cells. However, at 16 h of incubation with PA the accumulation of LC3-II was hampered, indicating the onset of incomplete autophagy which is suggestive of the induction of lysosomal dysfunction at that time point as there are some reports of PA induced lysosomal dysfunction in some cell types (147).

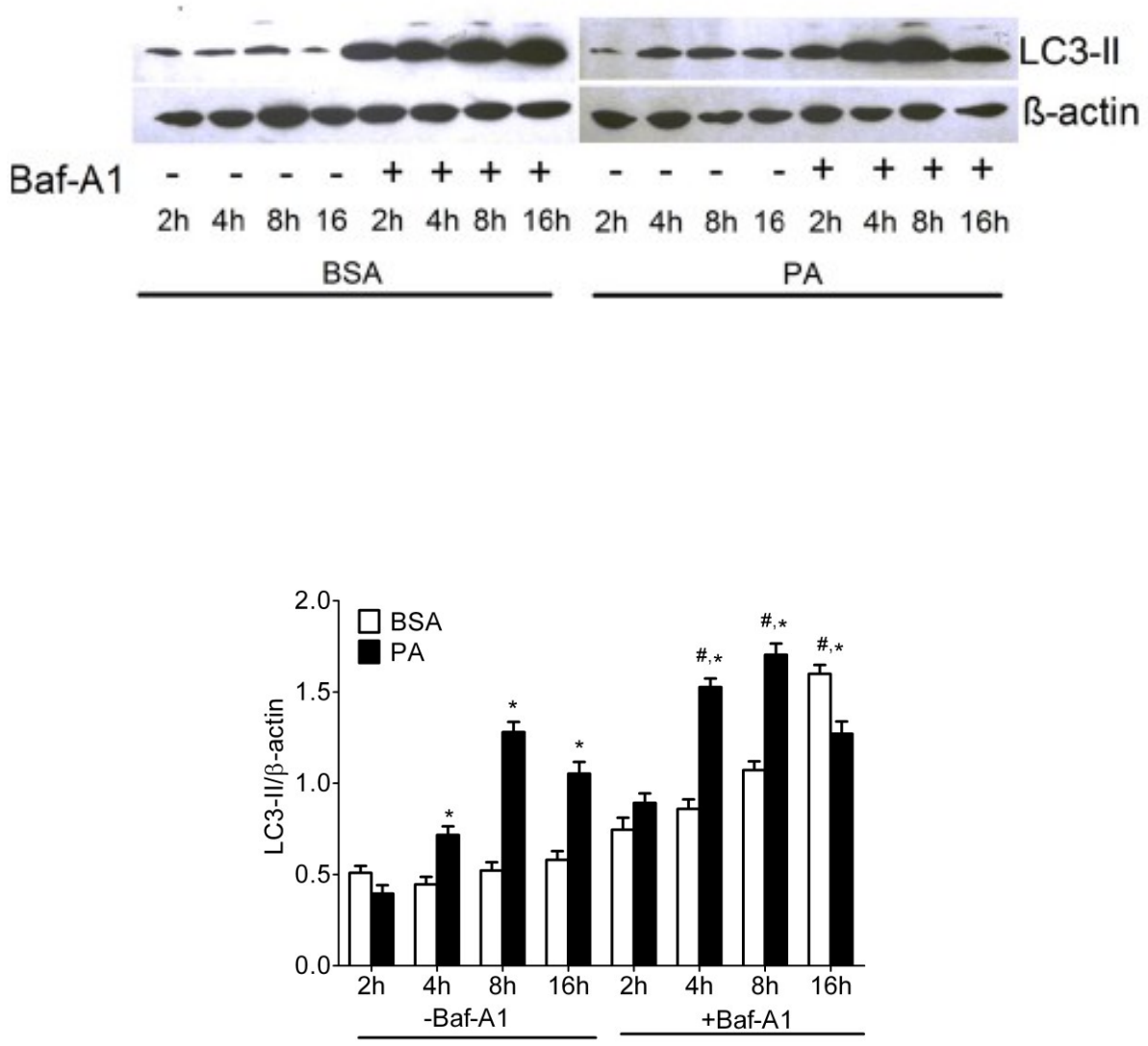

Figure 3-18: *Palmitic acid reduces autophagic flux with time. Cells were treated with BSA or 0.5 mm PA in the presence or absence of bafilomycin A1 (Baf-A1) and the isolated proteins at the given time points were immunoblotted for LC3. Representative image of three independent experiments is presented in upper panel, whereas statistical data of three independent experiments are shown in lower panel. *, p < 0.05 versus BSA at a given time point, and #, p < 0.05 versus PA with treated with DMSO (control, -Baf-A1) at a given time point (n = 3)*

This finding was further supported by the degradation pattern of sequestome 1 (p62), a frequently used marker for the measurement of the autophagic flux (32). Corresponding to the pattern of LC3-II accumulation (Fig. 3, H and I), the levels of p62 gradually decreased in cells

treated with PA until 8 h, whereas a significant accumulation of this protein was observed at 16 h (Fig. 3, J and K).

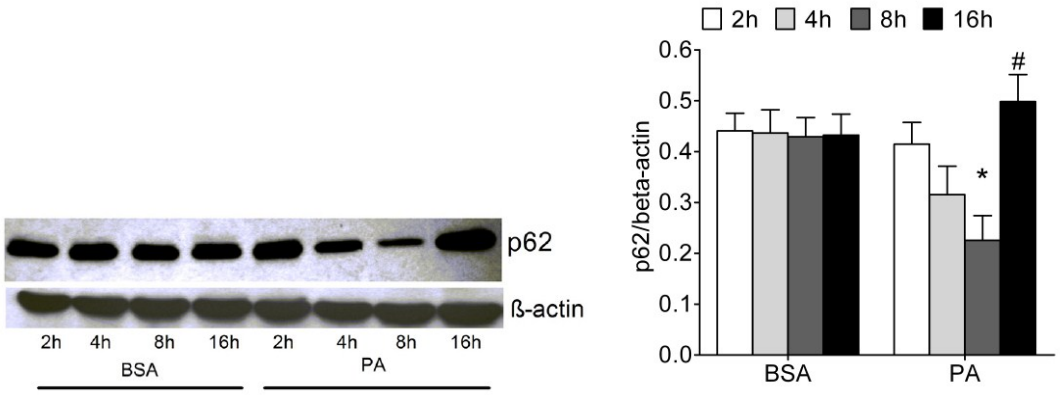

Figure 3-19: *left panel; Representative image of three independent experiments showing the degradation pattern of p62. Cells were treated with BSA or 0.5 mm PA and isolated proteins at the given time points were blotted for p62. Statistical data of three independent experiments are shown in right panel. *, $p < 0.05$ versus BSA at a given time point; #, $p < 0.05$ versus PA at 8-h time point (n = 3).*

This data indicate that PA induce a strong genuine autophagy with a normal autophagic flux in the beginning but at later stages the autophagic flux is hampered at later stages of incubation which is also recently reported by Las *et al.* (148)

3.5 Inhibition of Autophagy Rescues Endothelial Cells from PA-induced Cell Death

To investigate the role of autophagy induction on cell death autophagy was inhibited with wortmannin or 3-MA and measured the effect on lipotoxic cell death. Wortmannin and 3-MA are known to prevent autophagy by their inhibitory effect on VPS34 (33, 34). As expected, inhibition of VPS34 by either wortmannin prevented PA-induced autophagy indicated by a lack of LC3 lipidation in cells pretreated with this inhibitor (Fig. 3-20).

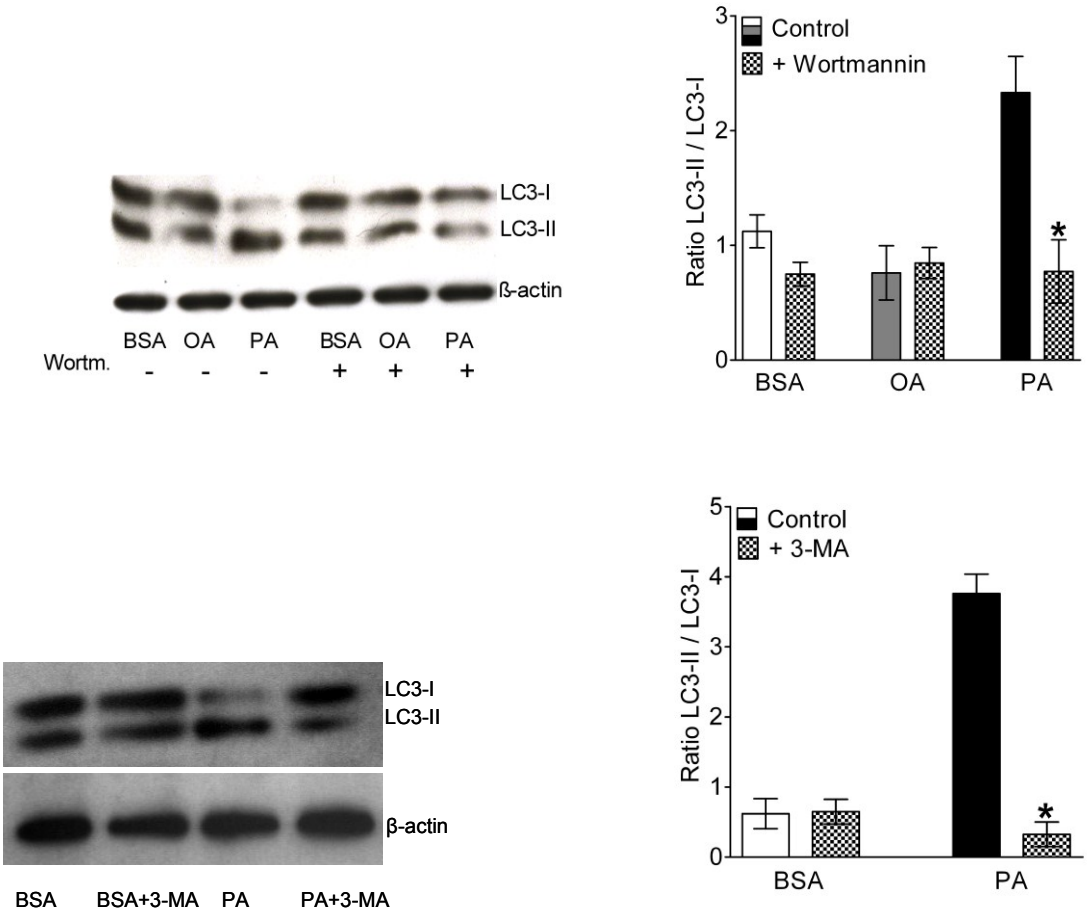

Figure 3-20: *Inhibition of autophagy rescued endothelial cells from PA-induced death. upper left panel, representative Western blot showing LC3 cleavage of cells that were incubated for 8 h with BSA alone, 0.5 mm OA, or 0.5 mm PA in the absence (−) and presence (+) of 10 μm wortmannin. Upper right panel, statistical data of LC3 cleavage from Western blots shown in panel f (n = 3 for all conditions). *, p < 0.05 versus control. lower left panel, representative Western blot showing LC3 cleavage of cells that were incubated for 8 h with BSA alone or 0.5 mm PA in the absence (−) and presence (+) of 10 mm 3-MA. Lower right panel, statistical data of LC3 cleavage from Western blots shown in panel f (n = 3 for all conditions). *, p < 0.05 versus control.*

Hence, we investigated the putative role of autophagy on lipotoxic cell death. We found that the cells pretreated with wortmannin were resistant to PA-induced cell death even after 36 h of

incubation with the fatty acid (Fig 3-21 left panel). As wortmannin inhibits all different classes of PI3Ks, the effect of 3-MA, a highly specific inhibitor of PI3K class III (vesicular protein sorting 34; VPS34) was tested. As shown in Fig. 3-21 right panel, 3-MA was also highly effective in preventing PA-induced cell death.

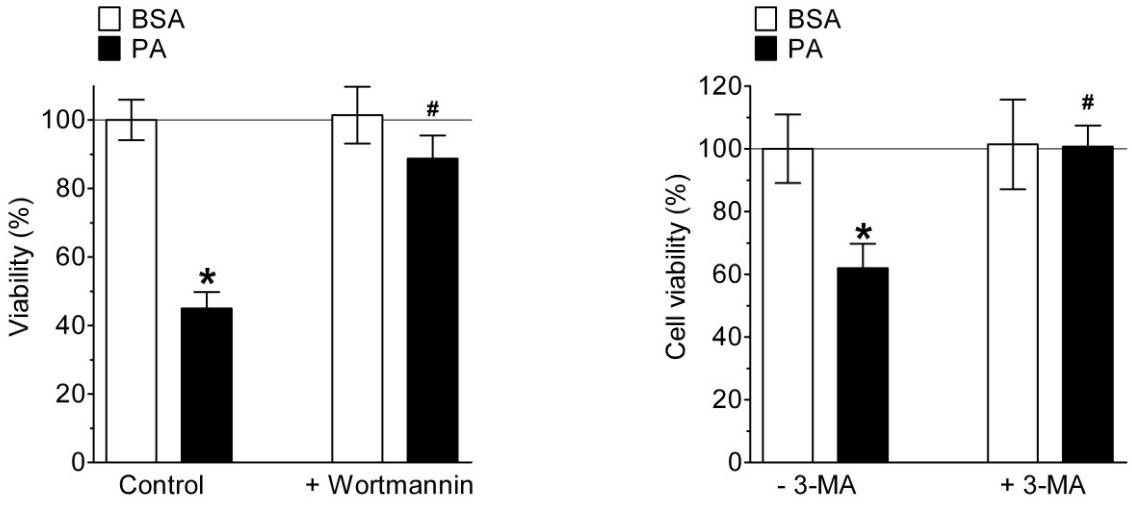

Figure 3-21: *left panel, columns represent average cell viabilities that were determined using the MTT assay of cells not pretreated with wortmannin (left pair of columns, −Wortmannin) that were incubated for 24 h with BSA alone (left white column, n = 3) or with 0.5 mm PA complexed to BSA (left black column, n = 3), and cells pretreated with 10 μm wortmannin (right pair of columns, +Wortmannin) for 20 min prior to an incubation with either BSA alone (right white column, n = 3) or with 0.5 mm PA complexed to BSA (right black column, n = 3). *, p < 0.05 versus BSA, and #, p < 0.05 versus PA without wortmannin. right panel, cells were treated with 10 mm 3-MA, another specific inhibitor of PI3K III and autophagy, and cell death was analyzed by the MTT assay (n = 3 for all conditions). *, p < 0.05 versus BSA, and #, p < 0.05 versus PA without 3-MA.*

The effect of PI3K (class III) inhibitors on PA-induced cell death was further tested using long-term phase-contrast microscopy, which confirmed their potency to rescue endothelial cells from PA-mediated lipotocixity (Fig. 3-22).

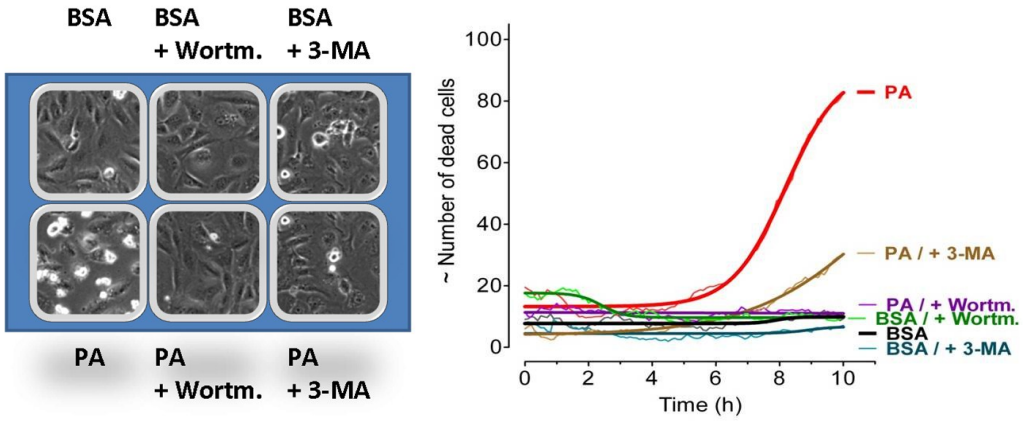

Figure 3-22: *left panel, schematic illustration of endothelial cells grown in an 8 well imaging chamber that allowed long-term phase-contrast imaging of 6 different conditions indicated in sequence. Right panel, the increase in brightness of detached dying cells was used to quantify the number of dying cells over time under respective conditions. Representative curves were fitted using the Bolzmann sigmoidal from.*

3.6 Genetic Knockdown of Autophagy Related Genes Rescues PA-induced Cell Death

Inhibition of autophagy with pharmacological inhibitors is an efficient way to block autophagy but specificity of these inhibitors is always a question mark as any pharmacological inhibitor can have a number of known or unknown off target effects. Therefore, genetic knock down of autophagy specific genes is a recommended approach in order to affirm the role of autophagy in cell death. To confirm the role of autophagy in the cell death two autophagy specific genes was slected for knock down i.e VPS34 and ATG7. The effects thereof on PA-induced cell death were investigated by the knock down of these genes and measuring the cell death with MTT assay. The siRNAs against both VPS34 and ATG7 were found efficient in decreasing respective mRNA levels (Fig. 3-23 upper panel). Both VPS34 and ATG7 were found to efficiently inhibit PA induced endothelial cells death (Fig. 3-23 lower left and right panel). This confirms that PA induced autophagy is required to mediate cell death in endothelial cells.

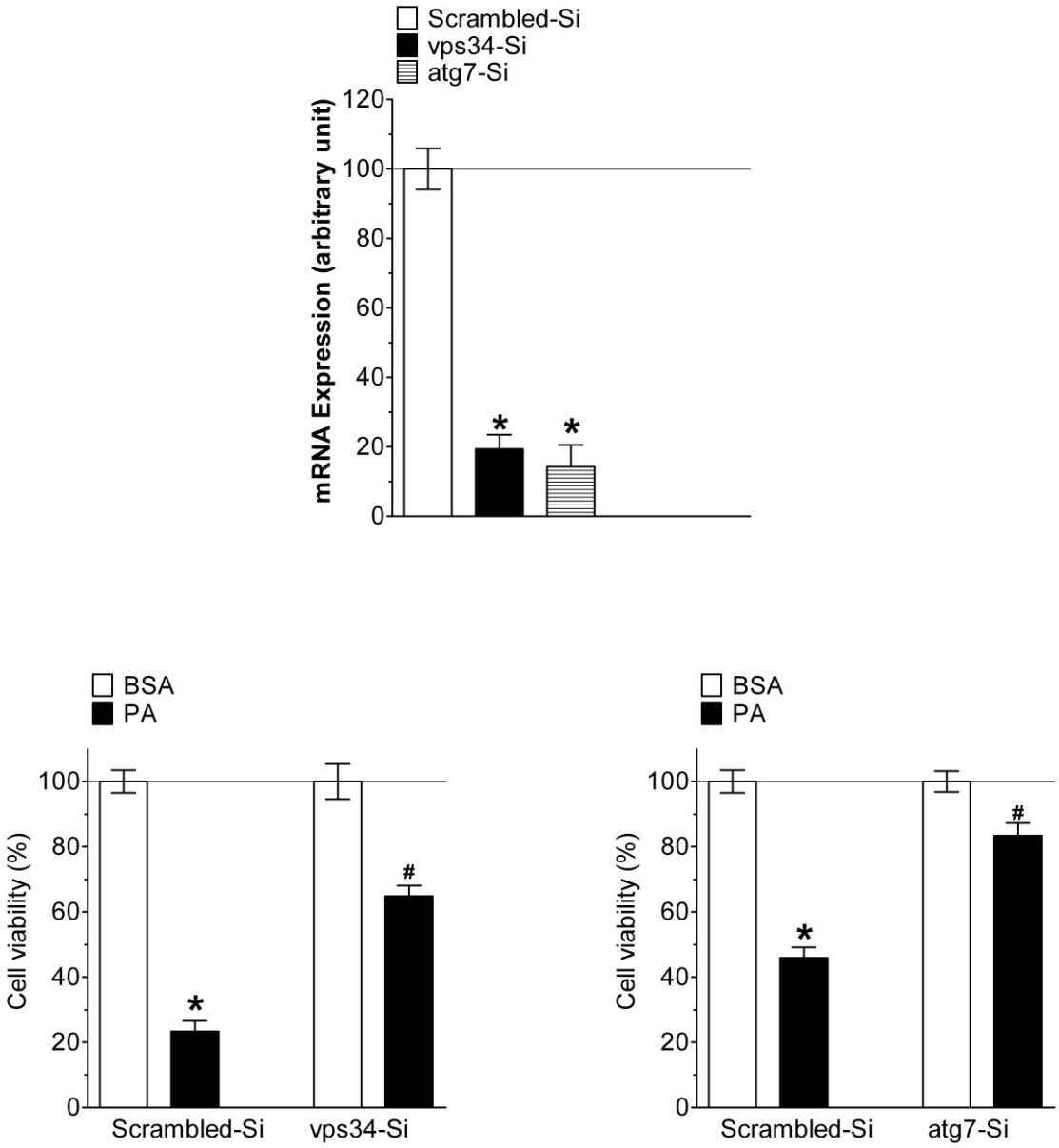

Figure 3-23: *upper panel, knockdown efficiency of individual siRNA in the percentage of mRNA expression compared with scramble siRNA (n = 3 for all columns presented). *, p < 0.05 versus scrambled siRNA. Lower left panel, 48 h after cells transfection with either scrambled siRNA (left pair of columns, n = 9 for both conditions) or siRNA against VPS34 (right pair of columns, n = 9 for both conditions) cells were incubated for 24 h with BSA alone (white columns) or 0.5 mm PA complexed to BSA (black columns) and cell viability was measured using the MTT assay. Viability is expressed in percentage, whereas the average value of cells treated with scrambled siRNA and BSA alone was defined as 100%. *, p < 0.05*

*versus BSA, and #, p < 0.05 versus PA with scrambled siRNA. Lower right panel, impact of siRNA-mediated knockdown of ATG7 on cell viability under analogous conditions described in panel b (n = 9 for each column). *, p < 0.05 versus BSA, and #, p < 0.05 versus PA with scrambled siRNA.*

3.7 PA-induced Ca^{2+} Elevation Triggers Autophagy in Endothelial Cells

Ca^{2+} is a unique 2nd messenger which can control a wide variety of functions. Recently there are some reports about the role of Ca^{2+} in autophagy (149). To verify these finding cytosolic Ca^{2+} was chelated with BAPTA-AM and the lipidation of LC3 was measured by Western blotting. It was found that autophagy was inhibited by BAPTA-AM treatment (Fig. 3-24). This indicated that the induction of autophagy by PA was dependent on cytosolic Ca^{2+} elevation.

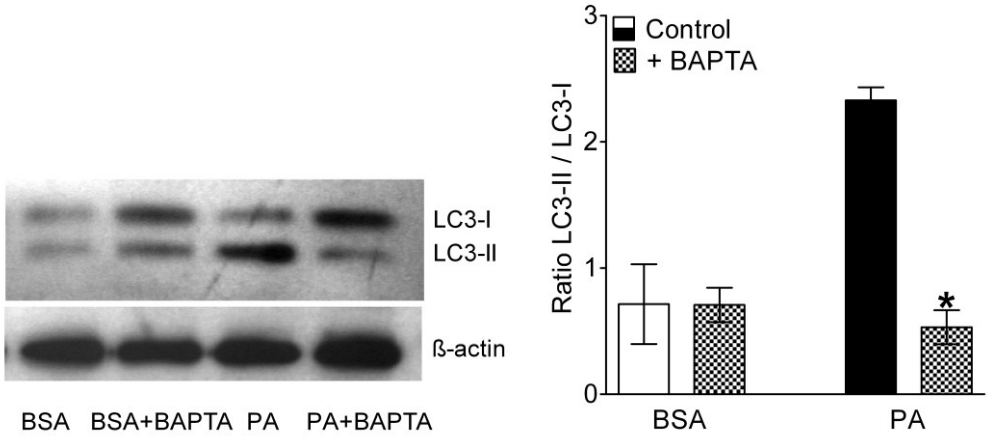

***Figure 3-24**: Left panel, representative Western blot showing LC3 cleavage of BAPTA-AM-loaded cells that were incubated for 8 h with BSA alone or 0.5 mm PA. Right panel, statistical data of LC3 cleavage from Western blots (n = 3 for all conditions). *, p < 0.05 versus control.*

To verify whether or not cell treatment with PA impacts Ca^{2+} signaling of endothelial cells cytosolic Ca^{2+} was measured under the conditions of fatty acid exposure. Basal $[Ca^{2+}]_{cyto}$ was assessed first in the presence and absence of extracellular Ca^{2+} using Fura-2/AM-loaded cells. Subsequently, Ca^{2+} was released from the endoplasmic reticulum (ER) in a Ca^{2+}-free medium by cell stimulation with the IP3-generating agonist histamine and the sarco/endoplasmic reticulum Ca^{2+}-ATPase inhibitor BHQ to assess the ER Ca^{2+} content (Fig. 3-25). In a Ca^{2+}-

containing buffer the treatment with PA caused a significant increase of basal levels of $[Ca^{2+}]_{cyto}$ already after 4 h of incubation, and $[Ca^{2+}]_{cyto}$ remained elevated until 8 and 16 h of incubation (Fig. 3-25). Removal of extracellular Ca^{2+} led to a decrease in basal $[Ca^{2+}]$cyto in cells that were pretreated with PA, indicating that store-operated Ca^{2+} entry was activated (Fig. 3-25, lower left panel). In contrast, cells incubated with OA did not show significant changes of basal Ca^{2+} levels in the cytosol (Fig. 3-25, lower left panel). The amount of releasable Ca^{2+} from the ER was clearly smaller in cells pretreated with PA (Fig. 3-25, lower right panel). Notably, the effect on ER Ca^{2+} mobilization was seen already after 2h of incubation with PA and was more pronounced with time (Fig 3-25). Cells pretreated with OA, however, revealed normal Ca^{2+} signals upon ER Ca^{2+} depletion (Fig 3-25). These data indicate that the accumulation of PA within endothelial cells is associated with a slow, time-dependent leak of Ca^{2+} from the ER. The consequence is a reduced Ca^{2+} content of the ER and elevated basal cytosolic Ca^{2+} levels, possibly due to the stimulation of Ca^{2+} entry via the store-operated Ca^{2+} entry pathway.

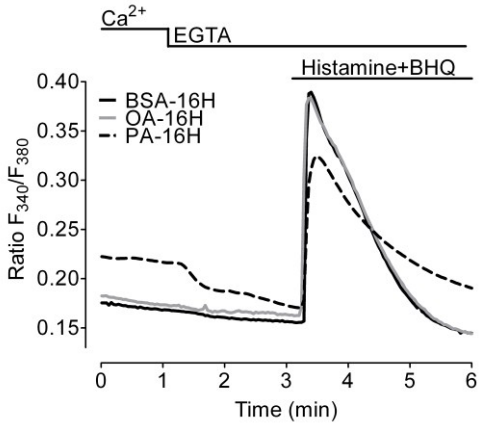

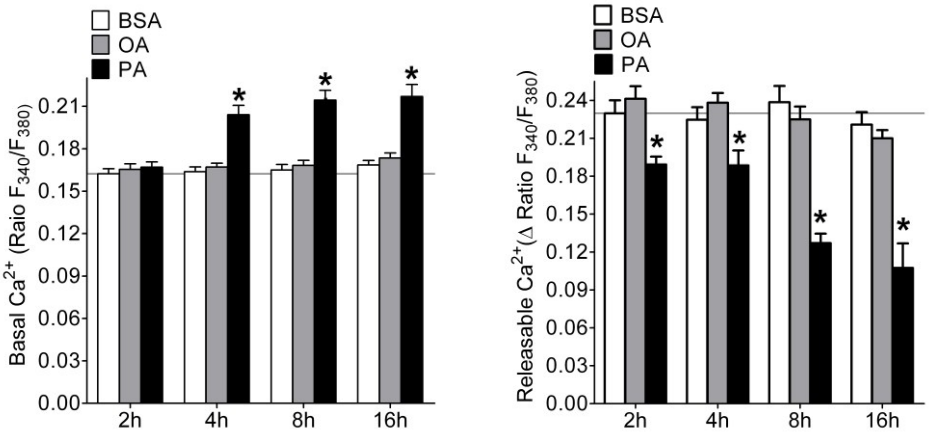

Figure 3-25: *PA induces release of Ca^{2+} from ER and results in cytosolic Ca^{2+} elevation. Upper panel, representative Ca^{2+} signals of Fura-2/AM-loaded cells 16 h after incubation with BSA alone (black continuous line), 0.5 mm OA (gray continuous line), and 0.5 mm PA (black dotted line). The indicated signals were first recorded in Ca^{2+} containing medium (2 mm) and subsequently Ca^{2+} was mobilized from the ER by cell stimulation with 100 µm histamine and 15 µm BHQ in a Ca^{2+}-free medium (1 mm EGTA). Lower left panel, statistics of basal ratio values of Fura-2/AM-loaded cells in the presence of extracellular Ca^{2+} (2 mm), and Lower right panel, average δ values of the maximal Ca^{2+} peaks upon cell stimulation with 100 µm histamine and 15 µm BHQ in the absence of extracellular Ca^{2+} (1 mm EGTA) at different times after incubation with BSA alone (Control, white columns, n = 9, ×118 cells at 2 h, ×127 cells at 4 h, ×130 cells at 8 h, and ×127 cells at 16 h), with 0.5 mm OA (gray columns, n = 9, ×113 cells at 2 h, ×127 cells at 4 h, ×133 cells at 8 h, and ×132 cells at 16 h), and with 0.5 mm PA (black columns, n = 9, ×115 cells at 2 h, ×124 cells at 4 h, ×118 cells at 8 h and ×107 cells at 16 h). *, $p < 0.05$ versus BSA.*

Furthermore, the role of cytosolic Ca^{2+} on cell viability was investigated. Cells were treated with BAPTA-AM for 20 min prior to treatment with PA for 24 h, and cellular viability was measured with the MTT assay. It was found that cell loading with BAPTA-AM inhibited PA-induced cell death significantly (Fig. 3-26).

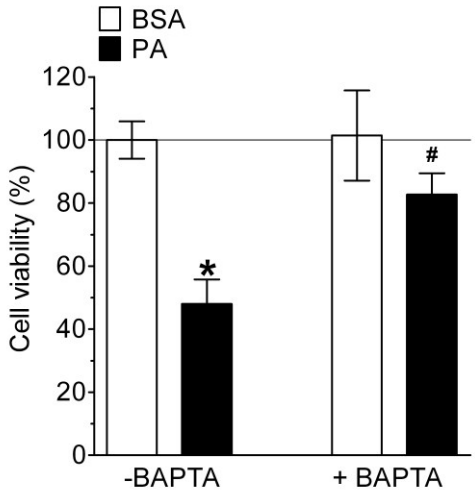

Figure 3-26: *effect of chelating cytosolic Ca^{2+} on cell viability. Cells were pretreated with BAPTA-AM for 20 min and then incubated with 0.5 mm PA or BSA alone for 24 h. Cell viability was measured with the MTT assay and data were normalized to BSA as a control and represented as mean viability (n = 3, for all conditions). *, $p < 0.05$ versus BSA, and #, $p < 0.05$ versus PA without BAPTA-AM-loaded cells.*

3.8 PA induced lysosomal dysfunction in Endothelial cells

Mechanistically autophagy starts with the formation of autophagosomes, which finally fuse with lysosomes to form autolysosomes where the cargo material is degraded by lysosomal hydrolytic enzymes (150). The fusion of autophagosomes with lysosomes can be blocked pharmacologically with bafilomycin A1 (151). Consequently, we tested whether or not such an intervention of the autophagic cycle hinders the completion of autophagy on PA-induced cell death. Accordingly, cells were pretreated with bafilomycin A1 and cell viability was measured without and with PA-exposure. Cells treated with bafilomycin A1 revealed increased cell viability under control conditions (Fig. 3-27). In contrast, the inhibition of the autophagic cycle by bafilomycin A1 strongly enhanced the susceptibility of endothelial cells to PA-induced cell death (Fig. 3-27).

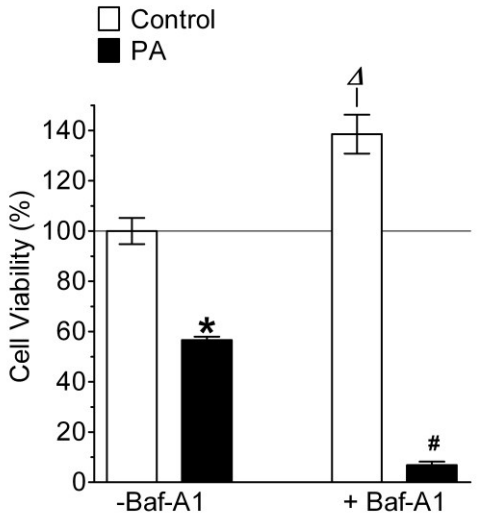

Figure 3-27: *Cells were treated with 100 nM bafilomycin-A1 (+ Baf-A1, right pair of columns) and DMSO (- Baf-A1, left pair of columns) as a control for 20 min and then incubated with 0.5 mM PA (black columns) and BSA (white columns) for 24 h. Cell viability was measured with MTT assay and presented in percentage of BSA without Baf-A1 (n=3 for all conditions). *P < 0.05 vs. BSA, and #P < 0.05 vs. PA without Baf-A1*

Consequently, the possibility of PA-induced lysosomal dysfunction as a putative hallmark of lipotoxic cell damage and death of endothelial cells was investigated. Acridine orange, a fluorescent dye that accumulates specifically in functioning lysosomes of intact cells (152) was used to verify lysosomal (dys)function. Although the number of acridin orange positive lysosomes were roughly the same in endothelial cells exposed for 10 h either to BSA or PA (BSA: 185 ± 24; n = 12 cells and PA: 201±24; n=13) (Fig. 3-28), the average intensity of acridin orange in lysosomes was significantly decreased in PA treated cells (Fig. 3-28) indicating impaired lysosomal acidification.

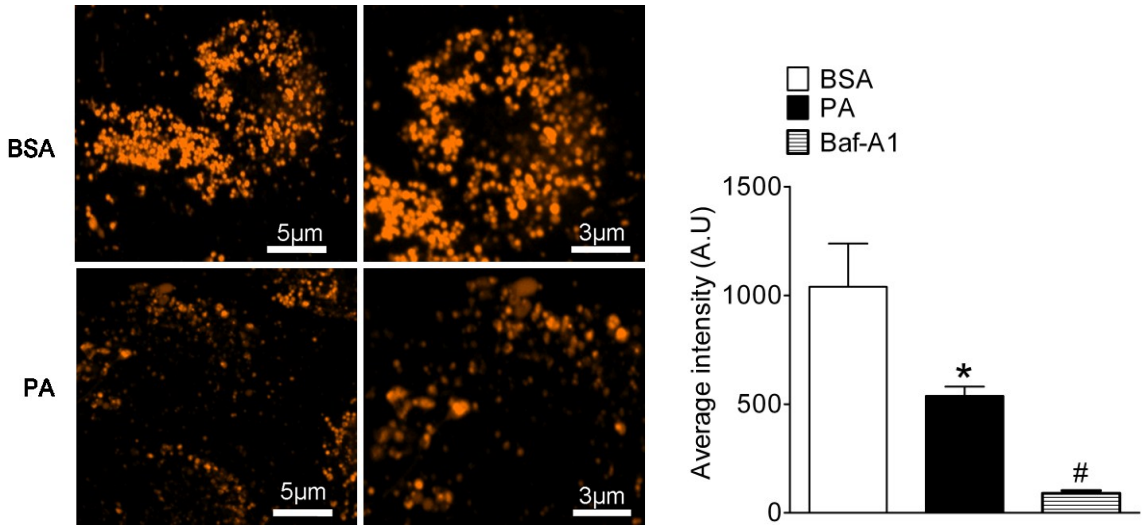

Figure 3-28: *Left panel, representative of cells loaded with acridine orange under control conditions (BSA alone, upper images) and pretreated with 0.5 mM PA for 10 h (lower images). Right panel, average intensity per lysosome of cells incubated for 10 h with BSA alone (white column, n=3), 0.5 mM PA complexed to BSA (black column, n=3), or for 20 min with 100 nM baflomycin A1 (striped column, n=5). *P < 0.05 vs. BSA.*

In agreement with these findings, cells that were incubated with bafilomycin-A1 as positive control of existing lysosomal dysfunction showed minimal lysosomal fluorescent signals (Fig. 3-29). The analysis of the average diameter of single lysosmes revealed that in PA-treated cells lysosomes are enlarged (Fig. 3-29). Moreover, the subcellular distribution of lysosomes was affected by cell treatment with PA (Fig. 3-29) and the distance between individual lysosomes was increased (Fig. 3-29).

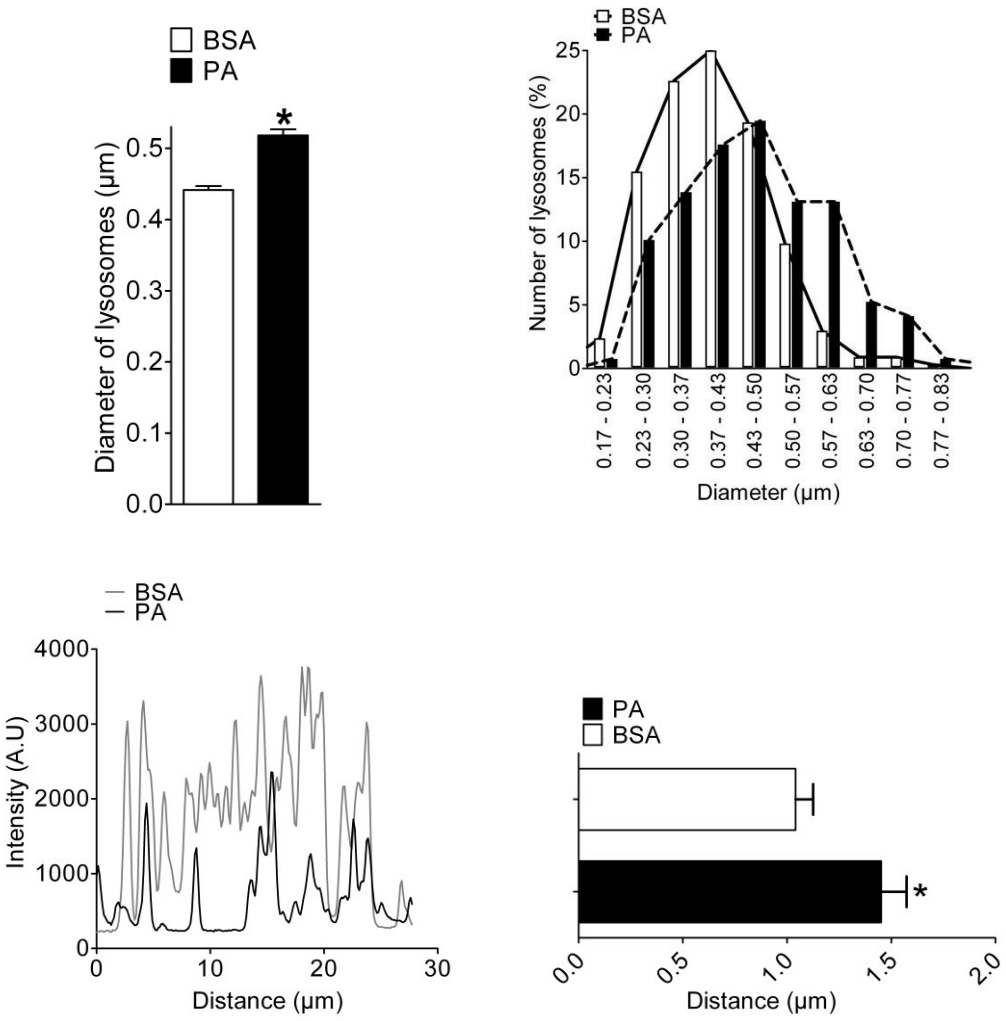

Figure 3-29: *Upper left pane, average diameter of single lysosomes of cells treated for 10 h with BSA alone (white column, n=4, 339 single lysosomes) or 0.5 mM PA complexed to BSA (black column, n=4, 273 single lysosomes). *P < 0.05 vs. BSA. Upper right panel, representative histogram of diameters of lysosomes from cells treated for 10 h with BSA alone (white columns, continuous line) and 0.5 mM PA complexed to BSA (black columns, dotted line). Lower left panel, representative line scans of cells stained with acridin orange. Lines were selected randomly. Peaks indicate the presences of lysosomes on lines in cells incubated with BSA alone (grey line) or 0.5 mM PA (black line) for 10 h. Lower right panel, statistics to line scans presented in panel f. Columns represent the average distance between individual lysosomes on randomly selected lines. Data were obtained using cells treated for 10 h with BSA alone (white column, n=3) or 0.5 mM PA (black column, n=3). *P < 0.05 vs. BSA*

3.9 Calpain 1 a possible instigator of PA induced lysosomal dysfunction

Calpain1 is a Ca^{2+} dependent non lyosomal protease(153) which can cause lysosomal rupture by the degradation of heat shock protein 70.1 (154). We found that PA activates calapin1 efficiently as measured by the self catalytical cleavage of calpain1 on western blot after incubating the cells with PA (figure 3-30). In order to evaluate the role of calpain1 in PA induced endothelial cell necroptosis calapin1 was knocked-down by siRNA and cell death was measured with MTT assay. It was found that knock-down of calpain 1 was able to inhibit PA induced cell death significantly as shown in figure 3-30.

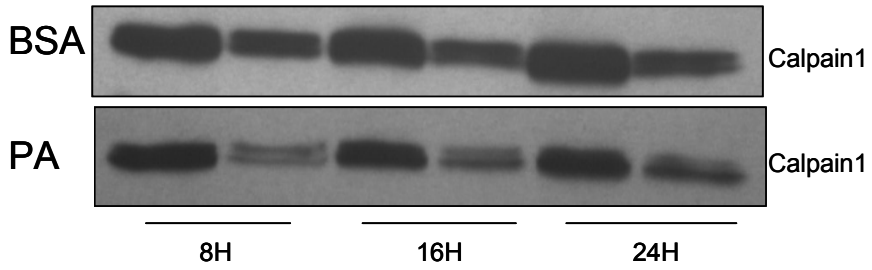

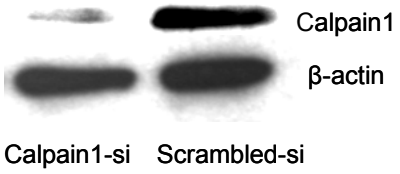

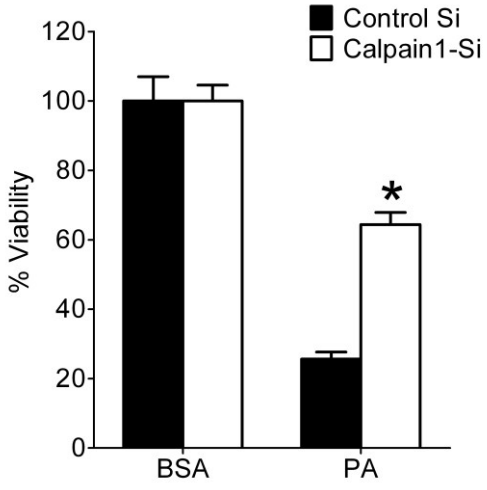

Figure 3-30: *Upper panel, western blot indicatin the activation of calpain1 by self catalytic cleavage upon incubation with PA and isolatin the protein on the time indicated. Lower left panel, wester blot showing the efficiency of siRNA against calpain1 after 48 hours of transfection. Lower right panel, Impact of siRNA-mediated knockdown of calpain1. cell viability 48 h after transfection of cells with either scrambled siRNA (left pair of columns, n = 18 for both conditions) or siRNA against calpain1 (right pair of columns, n = 18 for both conditions). Cells were incubated for 24 h with BSA alone (white columns) or 0.5 mm PA complexed to BSA (black columns) and cell viability was measured using the MTT assay. Viability is expressed in percentage, whereas the average value of cells treated with scrambled siRNA and BSA alone was defined as 100%. *, p < 0.05 versus BSA, and #, p < 0.05 versus PA with scrambled siRNA.*

This result indicate that calpain1 might be involved in triggering the lysosomal dysfunction which my lead to a dysfunctional autophagy and hence will hinder tha autophagic fulx. This inhibition of autophagic flux maybe responsible for the cells entering into necroptosis but this data need further evaluation.

3.10 Induction of autophagy is the basic trigger for necroptosis but not the lysosomal dysfunction

The interrelation between autophagy and lysosomal dysfunction that trigger PA-induced endothelial cell death was further assessed by inhibiting autophagy (wortmannin) simultaneously to the induction of lysosomal dysfunction (bafilomycin A1). In the presence of both wortmannin and bafilomycin A1 PA-induced cell death was efficiently prevented (Fig. 3-31). This is in contrast to bafilomycin A1 alone where PA-induced cell death was remarkably enhanced (Figure 3-27).

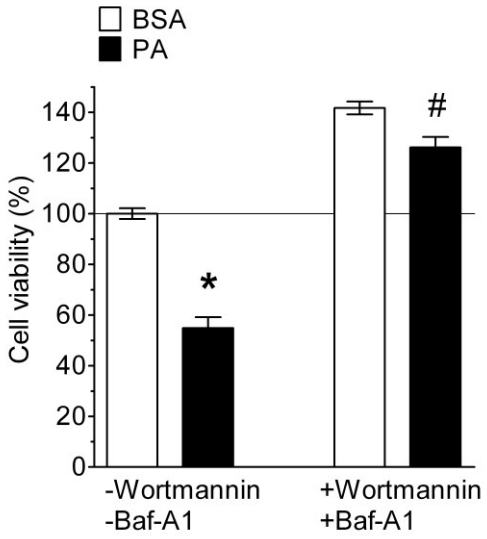

Figure 3-31: *Cells were treated with 10 µM wortmannin and 100 nM Baf-A1 simultaneously 20 minutes before incubation with BSA and 0.5 mM PA for another 24 h. Cell viability was measured with MTT assay and presented graphically as mean viability in percentage (n=3 for all conditions). The mean viability of cells treated with BSA alone was defined as 100 %.*P < 0.05 vs. BSA without wortmannin and Baf-A1, and #P < 0.05 vs. PA without wortmannin and Baf-A1.*

This data indicate that PA acid induce both autophagy and lysosomal dysfunction simultaneously which leads to a dysfunctional autophagic flux. The inhibition of an autophagic flux ultimately leads to the induction of necroptosis.

4. DISCUSSION

Endothelial cells are among the first targets of the elevated fatty acids levels in plasma and hence are more prone to the fatty acid mediated cell damage. There are a wide variety of ways in which endothelial cells are affected by the elevated fatty acid levels and different outcomes of the effect have been reported over many years. Molecular mechanisms of cell death and dysfunction have been studied extensively in different tissue and cell types and different players have been reported to be involved in lipotoxic related physiology and pathology.

Herein we provide evidence that exposure of endothelial cells to pathological PA concentrations generates a lipotoxic response that finally leads to autophagy dependent necroptotic cell death. The lethal effect of PA was initially triggered by the development of ER Ca^{2+} leakage, leading to elevated basal cytosolic Ca^{2+}. As a second messenger Ca^{2+} has the potential to activate or inhibit a variety of cellular signaling process [Scharenberg, 2007]. As shown in this data and reported by others, cytosolic Ca^{2+} is important for the induction of autophagy which could be inhibited by chelating cytosolic Ca^{2+} with BAPTA-2am (124,149). Simultaneously PA induced lysosomal dysfunction resulting in an incomplete autophagy leading to an energy crisis reflected in the form of a tremendous depletion of cellular ATP levels. Energetically these conditions are not suitable for the induction of apoptosis (138) thus leading the cells to RIPK3- and CYLD-dependent necroptotic cell death. These data unveil a novel pathway of lipotoxicity and point to PA dependent ER Ca^{2+} leakage, Ca^{2+}-dependent autophagy and a parallel induction of lysosomal dysfunction and programmed necrosis as a hallmark of lipotoxicity in endothelial cells. As a possible link between cytosolic Ca^{2+} elevation and lysosomal dysfunction the involvement of calapin 1 was evaluated and it was found as a key player in the process of cell death. In the following sections these results have been discussed in details.

4.1 PA induces programmed necrosis of endothelial cells

So far apoptosis has been reported as a predominant mood of cell death under conditions of substrate over-load [Yuan, 2013][Kuo, 2012][Artwohl, 2004] and autophagy has been shown to counteract the process and inhibiting autophagy was shown to accelerate PA induced cell death [Choi, 2009]. To reproduce the same when autophagy was inhibited by wortmannin

in endothelial cells the cell death was completely inhibited. The same was also true for 3-methyleadenine another specific inhibitor of autophagy. These findings provided the basis to question the existing dogma of PA induced cell death. Looking into the mode of cell death data contradict previously reported mode of cell death, apoptosis being the major executer of cell death under conditions of substrate overload (155). The data clearly indicate that an overload of endothelial cells with PA causes necroptosis. Z-VAD-fmk, a specific inhibitor of pan-caspases (136) was used to rule out the contribution of apoptosis in the execution of PA-induced cell death. Z-VAD-fmk experiments might also point to a possible caspase-independent apoptosis or cell might chose necrosis or necroptosis as an alternate mode of cell death under the conditions of zVAD-fmk treatment. The finding that necrosis is the major mode of cell death was further supported by annexin/PI staining. Cells treated with PA were found to be positive for both annexin V and PI which turned down apoptosis being the major mode of cell death. Further, looking into the nuclear morphology the cells stained with PI were having round and intact nuclei while the cells going through apoptosis are known to have fragmented nuclei as apoptosis results in the activation of endonucleases (156) which cut the DNA in a specific and regulated pattern leading to DNA laddering. This property of DNA laddering is used as a marker to detect apoptosis. The data here clearly indicate that no DNA laddering was observed in the cells treated with PA (Fig. 3-7). Activation of caspases is a hallmark for apoptosis (157). To further validate the mode of cell death caspase activity was measured and the data showed that there was no caspase activity. A lack of the caspase activity strengthens a non-apoptotic cell death. Also energetically the conditions were not favorable for the cells to go through apoptosis as there was early depletion of ATP upon PA treatment as apoptosis being an ATP dependent process least favored. Necrosis is already been reported to be the favored mode of cell death under conditions of ATP depletion and energy crisis (138)

Although necrosis was found as a major mode of cell death, a small fraction (11.6%) of cells treated with PA showed DNA hypoploidy, indicating that some portion of the whole cell population is going through apoptosis as well but still necrosis remains the predominant mode of cell death. An obvious explanation to this contradiction is that the hypoploidy experiments were performed with the whole cell population (i.e. attached and floating cells), while all the experiments through microscopy were performed with the attached cells only. So DNA

hypoploidy points to a mixture of apoptosis and necrosis but still necrosis is the predominant mode of cell death while apoptosis only contribute to a small proportion. There might be an initial induction of apoptosis but as cells were found to lose ATP with time the process was no more favorable and cells changed the mode of cell death to necroptosis instead. The data is in accordance with previously reported findings correlating the cellular ATP levels to the mode of cell death (138)

Necrosis has been considered as a random non-programmable process for a long time but recently it has been established that it can be programmed as well, a process often known as necroptosis or programmed necrosis (142). As a further verification of necrosis and to determine its molecular basis known players of necroptosis were knocked down and the effect was investigated on PA induced cell death. As the data indicate RIPK3 and CYLD (143), rescued the cells from PA-induced cell death. A major hurdle during these experiments was not being able to validate the siRNA against RIPK3 as mRNA levels could not be detected in control cells and cells treated with PA for 16 h. This might be because of very low levels of RIPK3 in this cell model. Therefore, a previously reported siRNA against RIPK3 was (127) used and cell death was successfully inhibited. The rescuing effect of a siRNA-mediated knockdown of RIPK3 was less pronounced compared to that of a CYLD knockdown, but reproducible and statistically significant in each set of experiment performed on four different days. The possible reasons for not being able to detect the levels of RIPK3 are the low levels of RIPK3 mRNA because it wasn't possible to detect the RIPK3 with a number of different sequence specific primers for the polymerase chain reaction. Another explanation for not being able to detect mRNA levels coding for RIPK3 can be less stability of the respective mRNA in the preparations used. Although any off target effects of the validated siRNA used to knockdown RIPK3 cannot be excluded in endothelial cells, the functional tests clearly suggested an involvement of this kinase in the toxic signaling of PA. Another hallmark finding is that PA triggers the expression of CYLD after 16h of incubation. So far we could not figure out the signaling cascade as how PA induced the up regulation of CYLD and needs further investigation. Looking into the effect of siRNA mediated knock down of RIPK3 and CYLD, the finding supports the assumption that a necrotic pathway is induced by PA in endothelial cells which is regulated and controlled by RIPK3 and CYLD. RIPK1, another player of the necroptosis cascade, was not found to be involved in the process. siRNA mediated knockdown

of RIPK1 as well as its pharmacological inhibition through necrostatin-1 shows that it is not contributing to the PA-induced necroptosis in this particular endothelial cell line. The finding is in line with recent reports, in which a RIPK1-independent but RIPK3- and CYLD-dependent cell death pathway has been described (39, 40). The induction of RIPK3- and CYLD-dependent necroptosis by PA described here may, however, point to novel strategies for the treatment of metabolic diseases and opens new horizons for the investigations of the up stream or down stream processes which can be involved in the regulation of lipotoxicity.

4.2 PA Induces Autophagy, Which Promotes Cell Death

Autophagy is among the hot topics investigated recently because of its involvement and modulation of a wide variety of processes. The process is considered as a life span increasing process and plays its role under the conditions of nutritional stress. The process is recently known to be involved in the mobilization of lipids and hence has gained an enormous attention in studies focusing lipotoxicity. Free fatty acid induced autophagy has been reported recently (8, 41, 42). Furthermore autophagic cell death is being considered as a target for designing the novel therapies against cancer [Rubinsztein, 2012].

In this study, PA was found to induce a genuine autophagy in the endothelial cells used. In pancreatic beta cells it was shown recently that the induction of autophagy was a pro-survival mechanism and inhibiting autophagy with pharmacological inhibitors enhanced the cell death (8). On the other hand the data presented here in this study demonstrate contradictory finding that autophagy is the main trigger of PA-induced cell death and inhibition of autophagy with either pharmacological inhibitors or genetic knockdown could rescue the cells from PA-induced cell death. At a first glance this is in line with recent reports that describe an uncontrolled autophagy as a mechanism able to induce type II programmed cell death (15, 43) or autophagic cell death as an innocent conviction by self over eating. On the other hand autophagy can contribute to cell death if the process is hampered by lysosomal dysfunction (44). The data presented here indicate that there is an early induction of autophagy followed by a late lysosomal dysfunction. PA was shown to induce lysosomal dysfunction in PC12 [Almaguel, 2010].

Lysosomes are central to the degradation of the biomolecules [Kolter, 2010]. Intact and functional lysosomes are required for the completion and maturation of autophagy as all the macromolecules packed into the autophagosomes are degraded and recycled in the lysosomes either to get rid of the unnecessary material or to provide the cells with nutrients to maintain the energetic levels in order to survive the conditions of starvation or stress [Stern, 2012]. Normal lysosomal activity is required in order to complete the autophagic process and to maintain the autophagic flux [Porter, 2013]. In line with the findings of this study fatty acids specially PA is recently reported to suppress autophagic turn over in β-cells resulting in a lower levels of protein degradation as depicted by the accumulation of p62 [Las, 2011]. Another consequence of lysosomal dysfunction is a lower level of ATP [Las, 2011] as cells fail to replenish the nutrient back to the cell leading the cell to an energy crisis. The data presented here clearly indicates that the ATP levels were gradually decreased and the timing coincide with the induction of lysosomal dysfunction as there is slight depletion of ATP after 8 hours which decreased further with time and was tremendous after 16 hours of incubation with PA. As depicted from the degradation pattern of p62 (Fig. 3-19) there was no signs of lysosomal dysfunction during the first 8 hours and p62 was degraded depending on the levels of autophagy [Watanabe, 2011]. After 16 hours p62 was found to be accumulated indicating lack of degradation activity in the lysosomes. It correlates with lower levels of ATP after 16 hours (Fig. 3-8) suggesting the importance of normal lysosomal activity under autophagy to maintain the energetic levels. Furthermore, ATP depletion after 16 hours coincides with the up-regulation of CYLD mRNA and the onset of necroptosis.

4.3 PA affects Ca^{2+} homeostasis of endothelial cell

Cytosolic Ca^{2+} being a second messenger control a wide variety of cellular signaling [Scharenberg, 2007]. Investigating effects of PA on Ca^{2+} homeostasis is of utmost importance as it is known to control apoptosis, necrosis and autophagy [Kim, 2003]. Here we found that cytosolic Ca^{2+} is important for PA induced autophagy as chelating the cytosolic Ca^{2+} was found to be rescuing the PA induced autophagy and cell death (Fig. 3-24). This is in line with the finding by the other groups as well showing the involvement of cytosolic Ca^{2+} in the induction of autophagy recently [Grotemeier, 2010]. This proves further that if autophagy is inhibited indirectly by chelating the cytosolic Ca^{2+} it could rescue the cell death. Besides Ca^{2+}

is important for induction of autophagy a rise in cytosolic Ca^{2+} maybe involved in controlling necrosis directly [Kim, 2003]. Although the detailed mechanisms controlling the ER Ca^{2+} mobilization by PA leading to a rise in cytosolic Ca^{2+} remain unclear the data indicate it is an early and central process in PA-induced cell damage. An acute effect of PA on the Ca^{2+} homeostasis was not observed, and the effect was slow and developing with time. This indicates that the ER Ca^{2+} leaks with time and accumulation of PA, its metabolism or derivates might be responsible for developing aberrant Ca^{2+} signaling in endothelial cells. The finding that cells treated with PA had a lower ER Ca^{2+} content and increased levels of $[Ca^{2+}]_{cyto}$ is in line with a recently reported study describing ER Ca^{2+} release by PA in beta cells (45). As discussed earlier a possible mechanism of slow Ca^{2+} leak might be the loss of ER membrane during the ongoing autophagosome formation and the membranes are not recycled as autophagy does not enter the completion phase because of lysosomal dysfunction. Decrease in ER Ca^{2+} content is slow and follows the induction of autophagy. Alternatively PA might cause damage to the ER directly by the incorporation of palmitic acid or its derivatives into the ER membrane or indirectly through the production of reactive oxygen species which is known to damage ER membrane. Ca^{2+} signaling is known to be involved in all types of cell death (46) and also plays a fundamental role in the induction of ER stress (47) and autophagy (35). The finding that cytosolic Ca^{2+} chelation by BAPTA protected the cells against PA-induced necroptosis is of particular relevance, because it points to a possibility to design a therapeutic intervention against lipotoxicity in endothelial cells.

4.4 Lysosomal Dysfunction and role of Calpain1

One of the key targets of Ca^{2+} regulating the cell death pathways is Ca^{2+} dependent cysteine proteases, the Calpain family [Harwood, 2005]. This data show that knocking down a member of calapin family, Calpain 1, could rescue PA induced cell death quite efficiently. It can be also a possible link between cytosolic Ca^{2+} elevation and lysosomal dysfunction. Calapin 1 is known to cause lysosomal membrane rupture by the degradation heat shock protein 70 in lysosomal membrane [Sahara, 2010]. Lysosomal membrane rupture has two consequences. Firstly, it can lead to the leak of lysosomal proteases into the cytosol which can lead to necrosis [Sahara, 2010]. secondly, a rupture in the lysosomal membrane is causing a lysosomal dysfunction and autophagy cannot be completed without functional lysosomes as all

the degradation processes take place in lysosomes and results in the a lower or inhibited autophagic flux [Bi, 2007]. This lower autophagic flux is the main initiator of the cell death as, temporally, it is followed by the over expression of CYLD leading ultimately to necroptosis. Calpain 1 maybe the key target in controlling the autophagic flux and inhibiting or knocking down calapain 1 might increase the autophagic flux to the normal levels and autophagy can go to completion providing the cells with nutrients to generate energy. This might be the possible way how the knock down of calapin 1 by siRNA or inhibiting it indirectly by chelating Ca^{2+}, can rescue the cells against PA induced necroptosis but this needs further investigation and a detailed study of involvement of calpain 1 in the regulation of autophagic flux is further suggested.

Functional lysosomes are the basis of a normal autophagic flux and inhibiting the lysosomes by Baf-A1 accelerated the PA induced cell death as compared to the controlled cells which were treating with PA alone and the lysosomes were not inhibited by Baf-A1. Interestingly in cells where autophagy was inhibited Baf-A1 could not accelerate cell death rather it was completely inhibited. This is interesting to know that a lysosomal dysfunction if toxic to the cells only when autophagy is also induced. A possible explanation for the process is that when autophagy is induced the cell loses its content with time which is packaged into autophagosomes for degradation and the biomolecules cannot be recycled. This might lead the cell into an energy crisis and scarcity of the essential biomolecules to maintain the organelles like ER in its shape. Origin of autophagosomes is one of the dogma still need to be solved but there are different reports suggestion that autophagosomes are originated from endoplasmic reticulum, mitochondria or plasma membrane by different groups under different conditions [Tooze, 2010]. Based on these studies it is postulated here that with the ongoing generation of autophagosome cells lose its ER membranes which cannot be recycled back if the autophagy doesn't enter into completion. A consequence of the loss of ER membrane can be a gradual leak of ER Ca^{2+} into the cytosolic thus elevation the cytosolic Ca^{2+} which can accelerate the whole process. In this way the whole process works in a cyclic manner and each preceding step can accelerate the next step leading to a major crisis of biomolecules and energy leading to necroptosis (Fig. 5-1).

In summary this study describes that PA overload of endothelial cells results in a Ca^{2+}-dependent development of autophagy and lysosomal dysfunction which finally leads to programmed necrotic cell death. The molecular mechanisms of lipotoxicity reported in this study enlightens a new mechanism of lipotoxic cell death in endothelial cells and might guide to the development of novel therapeutic strategies for vascular diseases that are caused by the accumulation of fatty acids in endothelial cells.

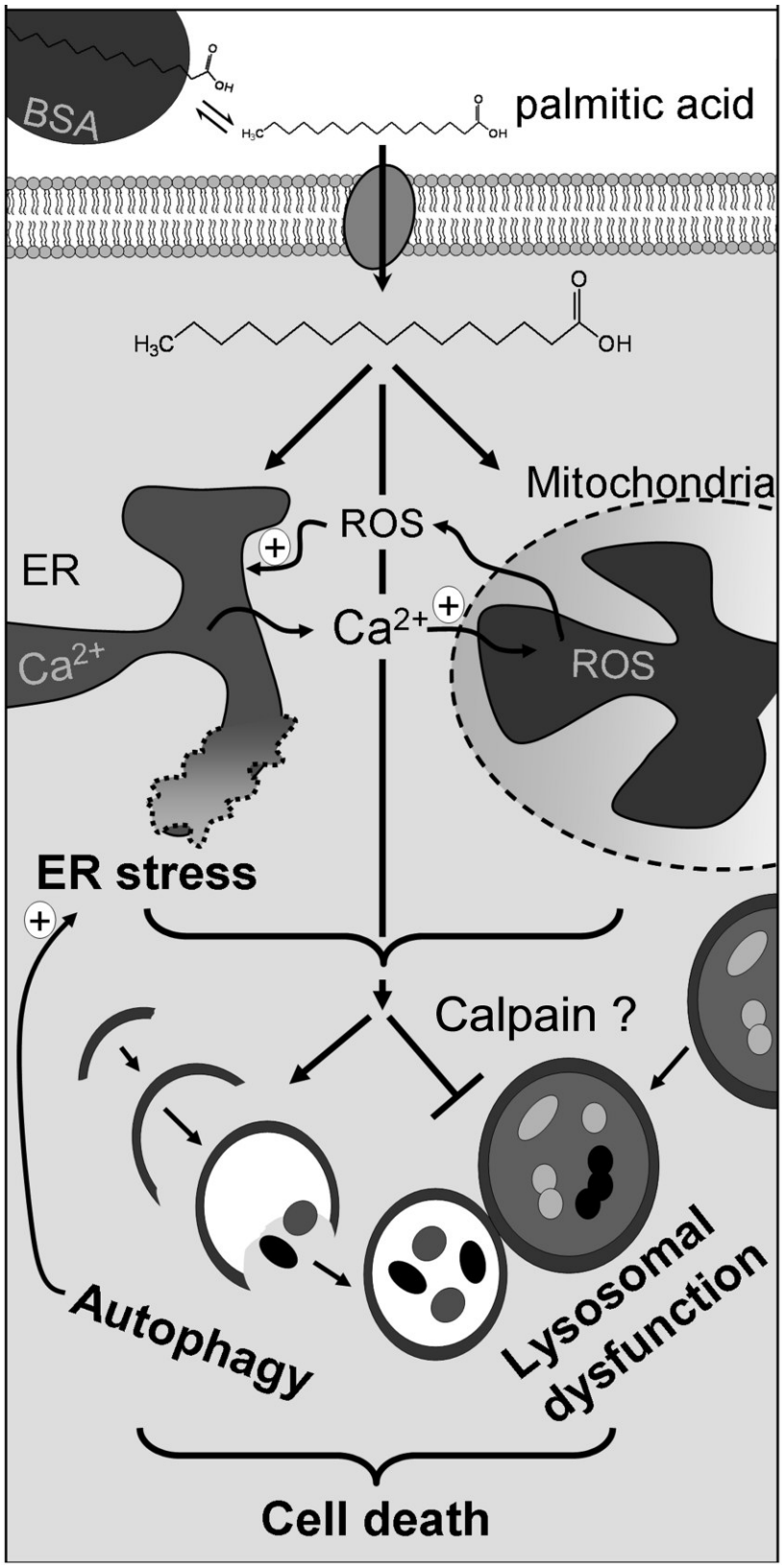

Figure 4-1: schematic presentation of PA induced necroptosis in endothelial cells

REFERENCES

1. Lee Y, Hirose H, Ohneda M, Johnson J, McGarry J, Unger R. Beta-cell lipotoxicity in the pathogenesis of non-insulin-dependent diabetes mellitus of obese rats: impairment in adipocyte-beta-cell relationships. Proc Natl Acad Sci U S A.. 1994;91(23):10878-82.

2. Postic C, Girard J. Contribution of de novo fatty acid synthesis to hepatic steatosis and insulin resistance: lessons from genetically engineered mice. J Clin Invest.. 2008;118(3):829-38.

3. Zechner R, Strauss J, Haemmerle G, Lass A, Zimmermann R. Lipolysis: pathway under construction. Curr Opin Lipidol.. 2005;16(3):333-40.

4. Jaworski K, Sarkadi-Nagy E, Duncan R, Ahmadian M, Sul H. Regulation of triglyceride metabolism. IV. Hormonal regulation of lipolysis in adipose tissue. Am J Physiol Gastrointest Liver Physiol.. 2007;293(1):G1-4.

5. Bonen A, Campbell S, Benton C, Chabowski A, Coort S, Han X et al. Regulation of fatty acid transport by fatty acid translocase/CD36. Proc Nutr Soc.. 2004;63(2):245-9.

6. Kamp F, Hamilton J, Westerhoff H. Movement of fatty acids, fatty acid analogues, and bile acids across phospholipid bilayers. Biochemistry.. 1993;32(41):11074-86.

7. Glatz J, Luiken J, Bonen A. Membrane fatty acid transporters as regulators of lipid metabolism: implications for metabolic disease. Physiol Rev.. 2010;90(1):367-417.

8. Lykidis A, Jackowski S. Regulation of mammalian cell membrane biosynthesis. Prog Nucleic Acid Res Mol Biol.. 2001;65:361-93.

9. Grynberg A, Demaison L. Fatty acid oxidation in the heart. J Cardiovasc Pharmacol.. 1996;1:S11-7.

10. Fernandis A, Wenk M. Membrane lipids as signaling molecules. Curr Opin Lipidol.. 2007;18(2):121-8.

11. Muszbek L, Rácz E, Laposata M. Posttranslational modification of proteins with fatty acids in platelets. Prostaglandins Leukot Essent Fatty Acids.. 1997;57(4-5):359-66.

12. Jump D. Fatty acid regulation of gene transcription. Crit Rev Clin Lab Sci.. 2004;41(1):41-78.

13. Kühnlein R. Thematic review series: Lipid droplet synthesis and metabolism: from yeast to man. Lipid droplet-based storage fat metabolism in Drosophila. J. Lipid. Res.. 2012;53(8):1430-6.

14. Ducharme N, Bickel P. Lipid droplets in lipogenesis and lipolysis. Endocrinology.. 2008;149(3):942-9.

15. Haemmerle G, Zimmermann R, Hayn M, Theussl C, Waeg G, Wagner E et al. Hormone-sensitive lipase deficiency in mice causes diglyceride accumulation in adipose tissue, muscle, and testis. J Biol Chem.. 2002;277(7):4806-15.

16. Haemmerle G, Lass A, Zimmermann R, Gorkiewicz G, Meyer C, Rozman J et al. Defective lipolysis and altered energy metabolism in mice lacking adipose triglyceride lipase. Science.. 2006;312(5774):734-7.

17. Boden G. Obesity and free fatty acids. Endocrinol Metab Clin North Am.. 2008;37(3):635-46.

18. Boden G. Free fatty acids, insulin resistance, and type 2 diabetes mellitus. Proc Assoc Am Physicians.. 1999;111(3):241-8.

19. Pilz S, März W. Free fatty acids as a cardiovascular risk factor. Clin Chem Lab Med.. 2008;46(4):429-34.

20. Smith S, Wilson P. Free fatty acids and atherosclerosis--guilty or innocent? J Clin Endocrinol Metab.. 2006;91(7):2506-8.

21. Boden G, Shulman G. Free fatty acids in obesity and type 2 diabetes: defining their role in the development of insulin resistance and beta-cell dysfunction. Eur J Clin Invest.. 2002;3:14-23.

22. van D, Schrauwen-Hinderling V, Schrauwen P. Lipotoxicity in type 2 diabetic cardiomyopathy. Cardiovasc Res.. 2011;92(1):10-8.

23. Eckert G, Lipka U, Muller W. Omega-3 fatty acids in neurodegenerative diseases: focus on mitochondria. Prostaglandins Leukot Essent Fatty Acids.. 2013;88(1):105-14.

24. Bobulescu I. Renal lipid metabolism and lipotoxicity. Curr Opin Nephrol Hypertens.. 2010;19(4):393-402.

25. Winzell M, Svensson H, Enerbäck S, Ravnskjaer K, Mandrup S, Esser V et al. Pancreatic beta-cell lipotoxicity induced by overexpression of hormone-sensitive lipase. Diabetes.. 2003;52(8):2057-65.

26. Trauner M, Arrese M, Wagner M. Fatty liver and lipotoxicity. Biochim Biophys Acta.. 2010;1801(3):299-310.

27. Wende A, Abel E. Lipotoxicity in the heart. Biochim Biophys Acta.. 2010;1801(3):311-9.

28. Osorio J, Stanley W, Linke A, Castellari M, Diep Q, Panchal A et al. Impaired myocardial fatty acid oxidation and reduced protein expression of retinoid X receptor-alpha in pacing-induced heart failure. Circulation.. 2002;106(5):606-12.

29. Schulze P. Myocardial lipid accumulation and lipotoxicity in heart failure. J Lipid Res.. 2009;50(11):2137-8.

30. Exil V, Roberts R, Sims H, McLaughlin J, Malkin R, Gardner C et al. Very-long-chain acyl-coenzyme a dehydrogenase deficiency in mice. Circ Res.. 2003;93(5):448-55.

31. Yue T, Bao W, Gu J, Cui J, Tao L, Ma X et al. Rosiglitazone treatment in Zucker diabetic Fatty rats is associated with ameliorated cardiac insulin resistance and protection from ischemia/reperfusion-induced myocardial injury. Diabetes.. 2005;54(2):554-62.

32. Karlsson H, Ahlsén M, Zierath J, Wallberg-Henriksson H, Koistinen H. Insulin signaling and glucose transport in skeletal muscle from first-degree relatives of type 2 diabetic patients. Diabetes.. 2006;55(5):1283-8.

33. Nolan C, Madiraju M, Delghingaro-Augusto V, Peyot M, Prentki M. Fatty acid signaling in the beta-cell and insulin secretion. Diabetes.. 2006;2:S16-23.

34. Fon T, Rozman D. Nonalcoholic Fatty liver disease: focus on lipoprotein and lipid deregulation. J Lipids. 2011;2011:783976.

35. Thomas ME, Harris KPG, Walls J, Furness PN, Brunskill NJ. Fatty acids exacerbate tubulointerstitial injury in protein-overload proteinuria. Am J Physiol Renal Physiol. 2002;283(4):F640-7.

36. Martínez D, Varela L, Fernø J, Nogueiras R, Diéguez C, López M. Hypothalamic lipotoxicity and the metabolic syndrome. Biochim Biophys Acta.. 2010;1801(3):350-61.

37. Garbarino J, Sturley S. Saturated with fat: new perspectives on lipotoxicity. Curr Opin Clin Nutr Metab Care.. 2009;12(2):110-6.

38. Verheul H, Pinedo H. Possible molecular mechanisms involved in the toxicity of angiogenesis inhibition. Nat Rev Cancer.. 2007;7(6):475-85.

39. Verheul HMW, Pinedo HM. Possible molecular mechanisms involved in the toxicity of angiogenesis inhibition. Nat Rev Cancer. 2007;7(6):475-85.

40. Caterson I, Hubbard V, Bray G, Grunstein R, Hansen B, Hong Y et al. Prevention Conference VII: Obesity, a worldwide epidemic related to heart disease and stroke: Group III: worldwide comorbidities of obesity. Circulation.. 2004;110(18):e476-83.

41. Jones J, Blecher m. On the mechanism of beta-oxidation of long chain fatty acids by liver mitochondria from normal and alloxan-diabetic rats. J Biol Chem.. 1965;240:68-70.

42. Kim J, Wei Y, Sowers J. Role of mitochondrial dysfunction in insulin resistance. Circ Res.. 2008;102(4):401-14.

43. Brookheart RT, Michel CI, Schaffer JE. As a matter of fat. Cell Metab. 2009;10(1):9-12.

44. Bugger H, Abel ED. Molecular mechanisms for myocardial mitochondrial dysfunction in the metabolic syndrome. Clin Sci (Lond). 2008;114(3):195-210.

45. Boudina S, Sena S, O'Neill BT, Tathireddy P, Young ME, Abel ED. Reduced mitochondrial oxidative capacity and increased mitochondrial uncoupling impair myocardial energetics in obesity. Circulation. 2005;112(17):2686-95.

46. Boudina S, Sena S, Theobald H, Sheng X, Wright JJ, Hu XX et al. Mitochondrial energetics in the heart in obesity-related diabetes: direct evidence for increased uncoupled respiration and activation of uncoupling proteins. Diabetes. 2007;56(10):2457-66.

47. Maestre I, Jordán J, Calvo S, Reig J, Ceña V, Soria B et al. Mitochondrial dysfunction is involved in apoptosis induced by serum withdrawal and fatty acids in the beta-cell line INS-1. Endocrinology.. 2003;144(1):335-45.

48. Chicco A, Sparagna G. Role of cardiolipin alterations in mitochondrial dysfunction and disease. Am J Physiol Cell Physiol.. 2007;292(1):C33-44.

49. Kroemer G, Galluzzi L, Brenner C. Mitochondrial membrane permeabilization in cell death. Physiol Rev.. 2007;87(1):99-163.

50. Fagone P, Jackowski S. Membrane phospholipid synthesis and endoplasmic reticulum function. J Lipid Res.. 2009;:S311-6.

51. Fu S, Yang L, Li P, Hofmann O, Dicker L, Hide W et al. Aberrant lipid metabolism disrupts calcium homeostasis causing liver endoplasmic reticulum stress in obesity. Nature.. 2011;473(7348):528-31.

52. Volmer R, van D, Ron D. Membrane lipid saturation activates endoplasmic reticulum unfolded protein response transducers through their transmembrane domains. Proc Natl Acad Sci U S A.. 2013;

53. Borradaile N, Han X, Harp J, Gale S, Ory D, Schaffer J. Disruption of endoplasmic reticulum structure and integrity in lipotoxic cell death. J Lipid Res.. 2006;47(12):2726-37.

54. Moffitt J, Fielding B, Evershed R, Berstan R, Currie J, Clark A. Adverse physicochemical properties of tripalmitin in beta cells lead to morphological changes and lipotoxicity in vitro. Diabetologia.. 2005;48(9):1819-29.

55. Zhu Q, Zhong J, Jin J, Yin X, Miao H. Tauroursodeoxycholate, a chemical chaperone, prevents palmitate-induced apoptosis in pancreatic β-cells by reducing ER stress. Exp Clin Endocrinol Diabetes.. 2013;121(1):43-7.

56. Choi S, Lee Y, Jang H, Lee K, Kim Y, Jun H et al. A chemical chaperone 4-PBA ameliorates palmitate-induced inhibition of glucose-stimulated insulin secretion (GSIS). Arch Biochem Biophys.. 2008;475(2):109-14.

57. Thannickal V, Fanburg B. Reactive oxygen species in cell signaling. Am J Physiol Lung Cell Mol Physiol.. 2000;279(6):L1005-28.

58. Almagor M, Kahane I, Gilon C, Yatziv S. Protective effects of the glutathione redox cycle and vitamin E on cultured fibroblasts infected by Mycoplasma pneumoniae. Infect Immun.. 1986;52(1):240-4.

59. Silva J, Coutinho O. Free radicals in the regulation of damage and cell death - basic mechanisms and prevention. Drug Discov Ther.. 2010;4(3):144-67.

60. Kruman I, Guo Q, Mattson M. Calcium and reactive oxygen species mediate staurosporine-induced mitochondrial dysfunction and apoptosis in PC12 cells. J Neurosci Res.. 1998;51(3):293-308.

61. Brookes P, Yoon Y, Robotham J, Anders M, Sheu S. Calcium, ATP, and ROS: a mitochondrial love-hate triangle. Am J Physiol Cell Physiol.. 2004;287(4):C817-33.

62. Ding W, Yang L, Zhang M, Gu Y. Reactive oxygen species-mediated endoplasmic reticulum stress contributes to aldosterone-induced apoptosis in tubular epithelial cells. Biochem Biophys Res Commun.. 2012;418(3):451-6.

63. Anstee Q, Goldin R. Mouse models in non-alcoholic fatty liver disease and steatohepatitis research. Int J Exp Pathol.. 2006;87(1):1-6.

64. West J, Marnett L. Endogenous reactive intermediates as modulators of cell signaling and cell death. Chem Res Toxicol.. 2006;19(2):173-94.

65. Gutierrez J, Ballinger S, Darley-Usmar V, Landar A. Free radicals, mitochondria, and oxidized lipids: the emerging role in signal transduction in vascular cells. Circ Res.. 2006;99(9):924-32.

66. Schönfeld P, Wojtczak L. Fatty acids decrease mitochondrial generation of reactive oxygen species at the reverse electron transport but increase it at the forward transport. Biochim Biophys Acta.. 2007;1767(8):1032-40.

67. Ye G, Metreveli N, Donthi R, Xia S, Xu M, Carlson E et al. Catalase protects cardiomyocyte function in models of type 1 and type 2 diabetes. Diabetes.. 2004;53(5):1336-43.

68. Kolesnick R, Fuks Z. Radiation and ceramide-induced apoptosis. Oncogene. 2003;22(37):5897-906.

69. Plesofsky N, Levery S, Castle S, Brambl R. Stress-induced cell death is mediated by ceramide synthesis in Neurospora crassa. Eukaryot Cell. 2008;7(12):2147-59.

70. Park T, Hu Y, Noh H, Drosatos K, Okajima K, Buchanan J et al. Ceramide is a cardiotoxin in lipotoxic cardiomyopathy. J Lipid Res.. 2008;49(10):2101-12.

71. Kitatani K, Idkowiak-Baldys J, Hannun Y. The sphingolipid salvage pathway in ceramide metabolism and signaling. Cell Signal.. 2008;20(6):1010-8.

72. Listenberger L, Ory D, Schaffer J. Palmitate-induced apoptosis can occur through a ceramide-independent pathway. J Biol Chem.. 2001;276(18):14890-5.

73. Shimabukuro M, Zhou Y, Levi M, Unger R. Fatty acid-induced beta cell apoptosis: a link between obesity and diabetes. Proc Natl Acad Sci U S A.. 1998;95(5):2498-502.

74. Suzuki J, Akahane K, Nakamura J, Naruse K, Kamiya H, Himeno T et al. Palmitate induces apoptosis in Schwann cells via both ceramide-dependent and independent pathways. Neuroscience.. 2011;176:188-98.

75. Cary S, Winger J, Derbyshire E, Marletta M. Nitric oxide signaling: no longer simply on or off. Trends Biochem Sci.. 2006;31(4):231-9.

76. Bauer V, Sotníková R. Nitric oxide--the endothelium-derived relaxing factor and its role in endothelial functions. Gen Physiol Biophys.. 2010;29(4):319-40.

77. Kim F, Tysseling K, Rice J, Pham M, Haji L, Gallis B et al. Free fatty acid impairment of nitric oxide production in endothelial cells is mediated by IKKbeta. Arterioscler Thromb Vasc Biol.. 2005;25(5):989-94.

78. Imrie H, Abbas A, Kearney M. Insulin resistance, lipotoxicity and endothelial dysfunction. Biochim Biophys Acta.. 2010;1801(3):320-6.

79. Low C, Shui G, Liew L, Buttner S, Madeo F, Dawes I et al. Caspase-dependent and -independent lipotoxic cell-death pathways in fission yeast. J Cell Sci.. 2008;121(Pt 16):2671-84.

80. Liu Q, Hengartner M. The molecular mechanism of programmed cell death in C. elegans. Ann N Y Acad Sci.. 1999;887:92-104.

81. Andón F, Fadeel B. Programmed Cell Death: Molecular Mechanisms and Implications for Safety Assessment of Nanomaterials. Acc Chem Res.. 2012;

82. Yuan Q, Zhao S, Wang F, Zhang H, Chen Z, Wang J et al. Palmitic acid increases apoptosis of neural stem cells via activating c-Jun N-terminal kinase. Stem Cell Res.. 2013;10(2):257-66.

83. Kuo T, Tatsukawa H, Matsuura T, Nagatsuma K, Hirose S, Kojima S. Free fatty acids induce transglutaminase 2-dependent apoptosis in hepatocytes via ER stress-stimulated PERK pathways. J Cell Physiol.. 2012;227(3):1130-7.

84. Artwohl M, Roden M, Waldhäusl W, Freudenthaler A, Baumgartner-Parzer S. Free fatty acids trigger apoptosis and inhibit cell cycle progression in human vascular endothelial cells. FASEB J.. 2004;18(1):146-8.

85. Kharroubi I, Ladrière L, Cardozo A, Dogusan Z, Cnop M, Eizirik D. Free fatty acids and cytokines induce pancreatic beta-cell apoptosis by different mechanisms: role of nuclear factor-kappaB and endoplasmic reticulum stress. Endocrinology.. 2004;145(11):5087-96.

86. Giorgi C, Baldassari F, Bononi A, Bonora M, De M, Marchi S et al. Mitochondrial Ca(2+) and apoptosis. Cell Calcium.. 2012;52(1):36-43.

87. Iturralde M, Gamen S, Pardo J, Bosque A, Piñeiro A, Alava M et al. Saturated free fatty acid release and intracellular ceramide generation during apoptosis induction are closely related processes. Biochim Biophys Acta.. 2003;1634(1-2):40-51.

88. Brüne B. Nitric oxide: NO apoptosis or turning it ON? Cell Death Differ.. 2003;10(8):864-9.

89. Edinger A, Thompson C. Death by design: apoptosis, necrosis and autophagy. Curr Opin Cell Biol.. 2004;16(6):663-9.

90. Fiers W, Beyaert R, Declercq W, Vandenabeele P. More than one way to die: apoptosis, necrosis and reactive oxygen damage. Oncogene.. 1999;18(54):7719-30.

91. Golstein P, Kroemer G. Cell death by necrosis: towards a molecular definition. Trends Biochem Sci.. 2007;32(1):37-43.

92. Li J, McQuade T, Siemer A, Napetschnig J, Moriwaki K, Hsiao Y et al. The RIP1/RIP3 necrosome forms a functional amyloid signaling complex required for programmed necrosis. Cell.. 2012;150(2):339-50.

93. O'Donnell M, Perez-Jimenez E, Oberst A, Ng A, Massoumi R, Xavier R et al. Caspase 8 inhibits programmed necrosis by processing CYLD. Nat Cell Biol.. 2011;13(12):1437-42.

94. Bozym R, Patel K, White C, Cheung K, Bergelson J, Morosky S et al. Calcium signals and calpain-dependent necrosis are essential for release of coxsackievirus B from polarized intestinal epithelial cells. Mol Biol Cell.. 2011;22(17):3010-21.

95. Karantza-Wadsworth V, Patel S, Kravchuk O, Chen G, Mathew R, Jin S et al. Autophagy mitigates metabolic stress and genome damage in mammary tumorigenesis. Genes Dev.. 2007;21(13):1621-35.

96. Kroemer G, Mariño G, Levine B. Autophagy and the integrated stress response. Mol Cell.. 2010;40(2):280-93.

97. Zhou J, Ng S, Huang Q, Wu Y, Li Z, Yao S et al. AMPK mediates a pro-survival autophagy downstream of PARP-1 activation in response to DNA alkylating agents. FEBS Lett.. 2013;587(2):170-7.

98. Vanhorebeek I, Gunst J, Derde S, Derese I, Boussemaere M, Güiza F et al. Insufficient activation of autophagy allows cellular damage to accumulate in critically ill patients. J Clin Endocrinol Metab.. 2011;96(4):E633-45.

99. Wang C, Klionsky D. The molecular mechanism of autophagy. Mol Med.. 2003;9(3-4):65-76.

100. Sly W. Receptor-mediated transport of acid hydrolases to lysosomes. Curr Top Cell Regul.. 1985;26:27-38.

101. Zschenker O, Jung N, Rethmeier J, Trautwein S, Hertel S, Zeigler M et al. Characterization of lysosomal acid lipase mutations in the signal peptide and mature polypeptide region causing Wolman disease. J Lipid Res.. 2001;42(7):1033-40.

102. Shang L, Chen S, Du F, Li S, Zhao L, Wang X. Nutrient starvation elicits an acute autophagic response mediated by Ulk1 dephosphorylation and its subsequent dissociation from AMPK. Proc Natl Acad Sci U S A.. 2011;108(12):4788-93.

103. Taguwa S, Kambara H, Fujita N, Noda T, Yoshimori T, Koike K et al. Dysfunction of autophagy participates in vacuole formation and cell death in cells replicating hepatitis C virus. J Virol.. 2011;85(24):13185-94.

104. Okamoto K, Sakimoto Y, Imai K, Senoo H, Shidoji Y. Induction of an incomplete autophagic response by cancer-preventive geranylgeranoic acid (GGA) in a human hepatoma-derived cell line. Biochem J.. 2011;440(1):63-71.

105. Shi R, Weng J, Zhao L, Li X, Gao T, Kong J. Excessive autophagy contributes to neuron death in cerebral ischemia. CNS Neurosci Ther.. 2012;18(3):250-60.

106. Kroemer G, Levine B. Autophagic cell death: the story of a misnomer. Nat Rev Mol Cell Biol.. 2008;9(12):1004-10.

107. Singh B, Kumar D, Shankar S, Srivastava R. Rottlerin induces autophagy which leads to apoptotic cell death through inhibition of PI3K/Akt/mTOR pathway in human pancreatic cancer stem cells. Biochem Pharmacol.. 2012;84(9):1154-63.

108. Samara C, Syntichaki P, Tavernarakis N. Autophagy is required for necrotic cell death in Caenorhabditis elegans. Cell Death Differ.. 2008;15(1):105-12.

109. Singh R, Kaushik S, Wang Y, Xiang Y, Novak I, Komatsu M et al. Autophagy regulates lipid metabolism. Nature.. 2009;458(7242):1131-5.

110. Choi S, Lee S, Lee Y, Li L, Lee S, Lee J et al. Protective role of autophagy in palmitate-induced INS-1 beta-cell death. Endocrinology.. 2009;150(1):126-34.

111. Almaguel F, Liu J, Pacheco F, De L, Casiano C. Lipotoxicity-mediated cell dysfunction and death involve lysosomal membrane permeabilization and cathepsin L activity. Brain Res.. 2010;1318:133-43.

112. Las G, Serada S, Wikstrom J, Twig G, Shirihai O. Fatty acids suppress autophagic turnover in β-cells. J Biol Chem.. 2011;286(49):42534-44.

113. Tan S, Shui G, Zhou J, Li J, Bay B, Wenk M et al. Induction of autophagy by palmitic acid via protein kinase C-mediated signaling pathway independent of mTOR (mammalian target of rapamycin). J Biol Chem.. 2012;287(18):14364-76.

114. Edgell C, McDonald C, Graham J. Permanent cell line expressing human factor VIII-related antigen established by hybridization. Proc Natl Acad Sci U S A.. 1983;80(12):3734-7.

115. Shui Y, Sasaki H, Pan J, Hata I, Kojima M, Yamada Y et al. Morphological observation on cell death and phagocytosis induced by ultraviolet irradiation in a cultured human lens epithelial cell line. Exp Eye Res.. 2000;71(6):609-18.

116. Schutte B, Nuydens R, Geerts H, Ramaekers F. Annexin V binding assay as a tool to measure apoptosis in differentiated neuronal cells. J Neurosci Methods.. 1998;86(1):63-9.

117. Zhang J, Xu M. DNA fragmentation in apoptosis. Cell Res.. 2000;10(3):205-11.

118. Zhang JH, Xu M. DNA fragmentation in apoptosis. Cell Res. 2000;10(3):205-11.

119. Evans D, Bishop G, Jaso-Friedmann L. Methods for cell cycle analysis and detection of apoptosis of teleost cells. MethodsCell Sci.. 2000;22(2-3):225-31.

120. Fuchs Y, Steller H. Programmed cell death in animal development and disease. Cell.. 2011;147(4):742-58.

121. McManus M. Small RNAs and immunity. Immunity.. 2004;21(6):747-56.

122. Fire A, Xu S, Montgomery MK, Kostas SA, Driver SE, Mello CC. Potent and specific genetic interference by double-stranded RNA in Caenorhabditis elegans. Nature. 1998;391(6669):806-11.

123. Kurreck J. siRNA efficiency: structure or sequence-that is the question. J Biomed Biotechnol.. 2006;2006(4):83757.

124. Høyer-Hansen M, Bastholm L, Szyniarowski P, Campanella M, Szabadkai G, Farkas T et al. Control of macroautophagy by calcium, calmodulin-dependent kinase kinase-beta, and Bcl-2. Mol Cell.. 2007;25(2):193-205.

125. Gao P, Bauvy C, Souquère S, Tonelli G, Liu L, Zhu Y et al. The Bcl-2 homology domain 3 mimetic gossypol induces both Beclin 1-dependent and Beclin 1-independent cytoprotective autophagy in cancer cells. J Biol Chem.. 2010;285(33):25570-81.

126. Stegmeier F, Sowa ME, Nalepa G, Gygi SP, Harper JW, Elledge SJ. The tumor suppressor CYLD regulates entry into mitosis. Proc Natl Acad Sci U S A. 2007;104(21):8869-74.

127. Cho YS, Challa S, Moquin D, Genga R, Ray TD, Guildford M et al. Phosphorylation-driven assembly of the RIP1-RIP3 complex regulates programmed necrosis and virus-induced inflammation. Cell. 2009;137(6):1112-23.

128. Waldeck-Weiermair M, Jean-Quartier C, Rost R, Khan M, Vishnu N, Bondarenko A et al. Leucine zipper EF hand-containing transmembrane protein 1 (Letm1) and uncoupling

proteins 2 and 3 (UCP2/3) contribute to two distinct mitochondrial Ca2+ uptake pathways. J Biol Chem.. 2011;286(32):28444-55.

129. Gehrmann W, Elsner M, Lenzen S. Role of metabolically generated reactive oxygen species for lipotoxicity in pancreatic β-cells. Diabetes Obes Metab.. 2010;2:149-58.

130. Wu L, Dunning K, Yang X, Russell D, Lane M, Norman R et al. High-fat diet causes lipotoxicity responses in cumulus-oocyte complexes and decreased fertilization rates. Endocrinology.. 2010;151(11):5438-45.

131. Prieur X, Roszer T, Ricote M. Lipotoxicity in macrophages: evidence from diseasesassociated with the metabolicsyndrome. Biochim Biophys Acta.. 2010;1801(3):327-37.

132. Pfaffenbach K, Gentile C, Nivala A, Wang D, Wei Y, Pagliassotti M. Linking endoplasmic reticulum stress to cell death in hepatocytes: roles of C/EBP homologous protein and chemical chaperones in palmitate-mediated cell death. Am J Physiol Endocrinol Metab.. 2010;298(5):E1027-35.

133. Borradaile N, Schaffer J. Lipotoxicity in the heart. Curr Hypertens Rep.. 2005;7(6):412-7.

134. Unger R, Zhou Y. Lipotoxicity of beta-cells in obesity and in other causes of fatty acid spillover. Diabetes.. 2001;1:S118-21.

135. Ortiz A, Sanchez-Niño MD. The human plasma lipidome. N Engl J Med. 2012;366(7):668; author reply 668-9.

136. Ilangovan R, Marshall W, Hua Y, Zhou J. Inhibition of apoptosis by Z-VAD-fmk in SMN-depletedS2cells. J Biol Chem.. 2003;278(33):30993-9.

137. Shcherbo D, Souslova EA, Goedhart J, Chepurnykh TV, Gaintzeva A, Shemiakina II et al. Practical and reliable FRET/FLIM pair of fluorescent proteins. BMC Biotechnol. 2009;9:24.

138. Tsujimoto Y. Apoptosis and necrosis: intracellular ATP level as a determinant for cell death modes. Cell Death Differ.. 1997;4(6):429-34.

139. Rockenfeller P, Ring J, Muschett V, Beranek A, Buettner S, Carmona-Gutierrez D et al. Fatty acids trigger mitochondrion-dependent necrosis. Cell Cycle.. 2010;9(14):2836-42.

140. Majno G, Joris I. Apoptosis, oncosis, and necrosis. An overview of cell death. Am J Pathol.. 1995;146(1):3-15.

141. Galluzzi L, Kroemer G. Necroptosis: a specialized pathway of programmed necrosis. Cell. 2008;135(7):1161-3.

142. Vandenabeele P, Galluzzi L, Vanden Berghe T, Kroemer G. Molecular mechanisms of necroptosis: an ordered cellular explosion. Nat Rev Mol Cell Biol. 2010;11(10):700-14.

143. O'Donnell MA, Perez-Jimenez E, Oberst A, Ng A, Massoumi R, Xavier R et al. Caspase 8 inhibits programmed necrosis by processing CYLD. Nat Cell Biol. 2011;13(12):1437-42.

144. Choi SE, Lee SM, Lee YJ, Li LJ, Lee SJ, Lee JH et al. Protective role of autophagy in palmitate-induced INS-1 beta-cell death. Endocrinology. 2009;150(1):126-34.

145. Kabeya Y, Mizushima N, Ueno T, Yamamoto A, Kirisako T, Noda T et al. LC3, a mammalianhomologue of yeastApg8p, is localized in autophagosomemembranesafterprocessing. EMBO J.. 2000;19(21):5720-8.

146. Klionsky DJ, Abeliovich H, Agostinis P, Agrawal DK, Aliev G, Askew DS et al. Guidelines for the use and interpretation of assays for monitoring autophagy in higher eukaryotes. Autophagy. 2008;4(2):151-75.

147. Almaguel FG, Liu JW, Pacheco FJ, De Leon D, Casiano CA, De Leon M. Lipotoxicity-mediated cell dysfunction and death involve lysosomal membrane permeabilization and cathepsin L activity. Brain Res. 2010;1318:133-43.

148. Las G, Sereda S, Wikstrom JD, Twig G, Shirihai OS. Fatty acids suppress autophagic turnover in β-cells. J Biol Chem. 2011;

149. Grotemeier A, Alers S, Pfisterer SG, Paasch F, Daubrawa M, Dieterle A et al. AMPK-independent induction of autophagy by cytosolic Ca2+ increase. Cell Signal. 2010;22(6):914-25.

150. Kroemer G, Jäättelä M. Lysosomes and autophagy in cell death control. Nat Rev Cancer.. 2005;5(11):886-97.

151. Shacka J, Klocke B, Roth K. Autophagy, bafilomycin and cell death: the "a-B-cs" of plecomacrolide-induced neuroprotection. Autophagy.. 2006;2(3):228-30.

152. Krolenko S, Adamyan S, Belyaeva T, Mozhenok T. Acridineorangeaccumulation in acidorganelles of normal and vacuolatedfrogskeletalmusclefibres. Cell Biol Int.. 2006;30(11):933-9.

153. Smith M, Schnellmann R. Calpains, mitochondria, and apoptosis. Cardiovasc Res.. 2012;

154. Yamashima T. Hsp70.1 and related lysosomal factors for necrotic neuronal death. J Neurochem.. 2012;120(4):477-94.

155. Ricchi M, Odoardi M, Carulli L, Anzivino C, Ballestri S, Pinetti A et al. Differential effect of oleic and palmitic acid on lipid accumulation and apoptosis in cultured hepatocytes. J Gastroenterol Hepatol.. 2009;24(5):830-40.

156. Johnson VL, Ko SC, Holmstrom TH, Eriksson JE, Chow SC. Effector caspases are dispensable for the early nuclear morphological changes during chemical-induced apoptosis. J Cell Sci. 2000;113 (Pt 17):2941-53.

157. Budihardjo I, Oliver H, Lutter M, Luo X, Wang X. Biochemical pathways of caspase activation during apoptosis. Annu Rev Cell Dev Biol.. 1999;15:269-90.

PUBLICATIONS

Khan, MJ, Alam Rizwan, M Waldeck-Weiermair, F Karsten, L Groschner, M Riederer, S Hallström, P Rockenfeller, V Konya, A Heinemann, F Madeo, WF Graier and R Malli. 2012. "Inhibition of autophagy rescues palmitic acid-induced necroptosis of endothelial cells." J Biol Chem. 287(25):21110-21120.

Waldeck-Weiermair, M, MR Alam, **MJ Khan**, AT Deak, N Vishnu, F Karsten, H Imamura, WF Graier and R Malli. 2012. "Spatiotemporal correlations between cytosolic and mitochondrial Ca(2+) signals using a novel red-shifted mitochondrial targeted cameleon." PLoS One. 7(9):10.

Waldeck-Weiermair, M, X Duan, S Naghdi, **MJ Khan**, M Trenker, R Malli and WF Graier. 2010. "Uncoupling protein 3 adjusts mitochondrial Ca(2+) uptake to high and low Ca(2+) signals." Cell Calcium. 48(5):288-301.

Waldeck-Weiermair, M, C Jean-Quartier, R Rost, **MJ Khan**, N Vishnu, AI Bondarenko, H Imamura, R Malli and WF Graier. 2011. "Leucine zipper EF hand-containing transmembrane protein 1 (Letm1) and uncoupling proteins 2 and 3 (UCP2/3) contribute to two distinct mitochondrial Ca2+ uptake pathways." J Biol Chem. 286(32):28444-28455.

Waldeck-Weiermair, M, R Malli, S Naghdi, M Trenker, **MJ Kahn** and WF Graier. 2010. "The contribution of UCP2 and UCP3 to mitochondrial Ca(2+) uptake is differentially determined by the source of supplied Ca(2+)." Cell Calcium. 47(5):433-440.